

Analytical profiling of plant cell wall polysaccharides

Yvonne Westphal

Thesis committee**Thesis supervisors**

Prof. dr. ir. H. Gruppen
Professor of Food Chemistry
Wageningen University

Prof. dr. ir. A.G.J. Voragen
Emeritus Professor of Food Chemistry
Wageningen University

Thesis co-supervisor

Dr. H.A. Schols
Associate professor, Food Chemistry Group

Other members

Prof. dr. M.W.F. Nielen, Wageningen University
Prof. dr. R.G.F. Visser, Wageningen University
Dr. M.-C. Ralet, INRA Nantes, France
Dr. P. Dupree, University of Cambridge, United Kingdom

This research was conducted under the auspices of the Graduate School VLAG (Voeding, Levensmiddelentechnologie, Agrobiotechnologie en Gezondheid).

Analytical profiling of plant cell wall polysaccharides

Yvonne Westphal

Thesis

submitted in fulfilment of the requirements for the degree of doctor
at Wageningen University
by the authority of the Rector Magnificus
Prof. dr. M.J. Kropff,
in the presence of the
Thesis Committee appointed by the Academic Board
to be defended in public
on Wednesday 8 September 2010
at 1:30 p.m. in the Aula.

Yvonne Westphal

Analytical profiling of plant cell wall polysaccharides,
176 pages

Thesis, Wageningen University, Wageningen, NL (2010)

With references, with summaries in Dutch, German and English

ISBN: 978-90-8585-706-8

Abstract

Westphal, Y. Analytical profiling of plant cell wall polysaccharides
Ph.D thesis Wageningen University, Wageningen, The Netherlands, 2010
Keywords: High performance liquid chromatography, capillary electrophoresis, MALDI-TOF mass spectrometry, NMR, cell wall oligosaccharides, arabinan, *Arabidopsis thaliana*, cell wall degrading enzymes, profiling

The plant cell wall polysaccharides cellulose, hemicelluloses and pectins are very heterogeneous and complex structures consisting of at least 20 different sugars and 30 different linkage types. Additionally, hemicelluloses and pectins might be acetylated and/or feruloylated. Furthermore, pectins carry methyl esters. The degree and distribution of these modifications may vary significantly depending on source and developmental stage. In this research several analytical tools were developed for the analysis of complex mixtures of cell wall derived oligomers.

The combination of 1) the use of pure and well-defined cellulases, hemicellulases and pectinases, and 2) the detection of the oligosaccharides released by MALDI-TOF MS and CE-LIF resulted in a screening method for *Arabidopsis* cell wall mutants, which addresses all enzyme-accessible polysaccharides in the cell wall.

Porous graphitized carbon (PGC)-HPLC with evaporative light scattering and mass detection was introduced to a broad range of neutral and acidic cell wall polysaccharide derived oligosaccharides and separation of almost all oligosaccharides under investigation was achieved. The used gradient ensured 1) a sufficient separation of many oligosaccharides and 2) a sequential elution of first the neutral and then the acidic oligosaccharides. This elution behavior in combination with online-recorded MSⁿ analysis facilitates the identification of (unknown) peaks.

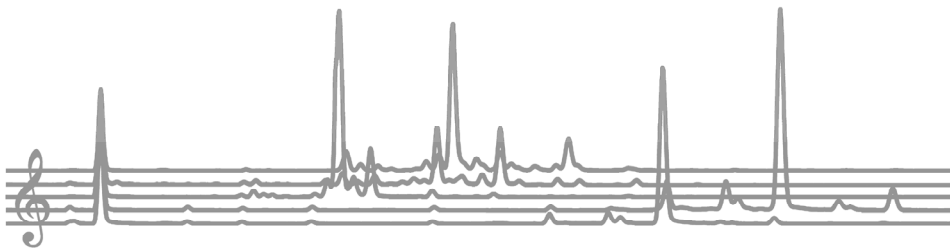
A wide range of branched arabino-oligosaccharides was isolated from sugar beet arabinan and characterized with NMR. HPAEC was demonstrated to have insufficient resolution to separate all linear and branched arabino-oligosaccharides. Therefore, PGC-HPLC-ELSD/MS and CE-LIF-MS were explored for the separation and detection of isomeric arabino-oligomers and were demonstrated to perform well. The combination of the controlled enzyme treatment, the predictive retention behavior on PGC-material, and the LC/CE-MS² fragmentation patterns led to the prediction of the structures of unknown branched arabino-oligosaccharides in a complex mixture.

Table of contents

Abstract		
Chapter 1	General introduction	1
Chapter 2	MALDI-TOF MS and CE-LIF fingerprinting of plant cell wall polysaccharide digests as screening tool for <i>Arabidopsis</i> cell wall mutants	25
Chapter 3	Introducing porous graphitized carbon liquid chromatography with evaporative light scattering and mass spectrometry detection into cell wall oligosaccharide analysis	49
Chapter 4	Branched arabino-oligosaccharides isolated from sugar beet arabinan	65
Chapter 5	LC/CE-MS tools for the analysis of complex arabino-oligosaccharides	85
Chapter 6	Mode of action of <i>Chrysosporium lucknowense</i> C1 arabinohydrolases	113
Chapter 7	Concluding remarks	133
Summary		147
Samenvatting		151
Zusammenfassung		155
Acknowledgement, Dankwoord, Danksagung		159
About the author		163

Chapter 1

General introduction



The project

Despite extensive research and steady progress, the complete elucidation of the biosynthesis of plant cell wall polysaccharides remains a big challenge. For pectin biosynthesis, for example, about 70 different glycosyltransferases, methyltransferases and acetyltransferases are required, indicating the complexity of the cell wall polysaccharides and their biosynthesis¹. Therefore, the European Marie-Curie framework 6 project “WallNet” aimed at the identification of new mutant *Arabidopsis thaliana* plants differing in cell wall polysaccharide structures. The “WallNet” project combined research from various scientific fields including genetics, molecular biology and carbohydrate chemistry. Comparative analysis of both mutant and wild-type plants can support the identification of unknown biosynthetic pathways within the complex cell wall polysaccharide biosynthesis.

The present PhD research was part of the “WallNet” EU project and focused on the development of analytical tools, which enable the (detailed) analysis of oligosaccharides derived from cell walls of (transgenic) plants, and contribute to a better characterization of the polysaccharides making up the cell walls.

Arabidopsis thaliana

Arabidopsis thaliana, a small flowering plant belonging to the *Brassicaceae* family, is used as model plant in plant sciences, genetics and molecular biology. The unraveling of the *Arabidopsis* genome sequence in 2000² has added an invaluable tool for the efficient identification and systematic functional analysis of genes encoding enzymes having different functions in the plant, for example, cell wall polysaccharide biosynthetic enzymes. Additionally, the small size, short life cycle and prodigious seed production makes *A. thaliana* an easy and inexpensive organism to propagate in the laboratory^{3,4}.

Plant cell wall

The plant cell walls are responsible for the stability and rigidity of the plant as well as for its flexibility. Furthermore, the cell wall is crucial for the protection against bacterial and fungal attacks, for repairing wounds and infections by thickening, lignification or suberization of the cell^{5,6}. Especially during plant growth the cell wall needs to adapt

continuously to allow these functions. The cell wall of dicotyledonous plants predominantly consists of polysaccharides with small amounts of structural proteins, phenolic compounds, minerals and enzymes.

Plant cell wall polysaccharides

The main cell wall polysaccharides are cellulose, hemicelluloses and pectin, which together form a complex network. The structural elements of the cell wall polysaccharides and possible structural variations within these polysaccharides are listed in **Table 1**.




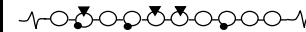


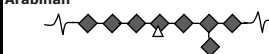
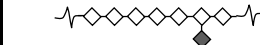

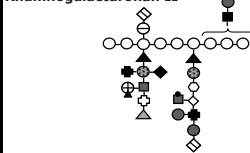
Cellulose

Cellulose is composed of β -(1,4)-linked D-glucose units, which form a linear polymer (**Table 1**). These polymers aggregate and form microfibrils via hydrogen bonds. In cell walls of higher plants cellulose chains have degrees of polymerization of 2000-6000⁷. In the native form the glucan chains are present in the cellulose I conformation, in which the molecules are oriented parallel. These crystalline regions are diversified by amorphous regions. By mercerization or regeneration cellulose is converted to the anti-parallel cellulose II form⁸.

Hemicelluloses

Xyloglucans are the main hemicellulosic structures in dicotyls^{9,10}, while only present in minor quantities in grasses¹¹. Xyloglucans consist of a backbone of β -(1,4)-linked D-glucose units, which are heavily branched, usually in a quite organized way. They can be classified in XXXG-type, XXGG-type (typical for *Solanaceae*) and XXXGG-type structures^{12,13}. In xyloglucans of the XXXG type, as present in e.g. *Arabidopsis thaliana*¹⁴, three out of four glucoses are substituted with α -D-xylose at the O-6 position. The xyloses can be further substituted with galactose, galactose and fucose, or arabinose^{9,15,16}. The galactose and/or the glucose units can be acetylated^{9,17} (**Table 1**). Within the xyloglucan-cellulose network three known elements of xyloglucan are described: 1) xyloglucan present in free loops or in cross links, which can be degraded by xyloglucan specific enzymes, 2) xyloglucan, which is bound via hydrogen toward cellulose and can be solubilized by

Table 1 Schematic structures of plant cell wall polysaccharides and possible variation of each structural element (adapted from Schols and Voragen¹⁸).

	Structural element	Diversity within the structural elements
(Hemi)celluloses	Xyloglucan 	Distribution of side chains over the β -(1,4)-glucose backbone Sugars in the side chains Degree of acetylation Hydrogen bonds to cellulose Present as free loops, trains or in crosslinks? Entrapped in amorphous cellulose?
	(Glucurono)-arabinoxylan 	Degree of arabinose and (OMe)-glucuronic acid substitution Distribution of substituents Degree of methyl esterification and acetylation Degree and distribution of ferulic acid Presence of xylose, galactose, rhamnose and galA at the reducing end Entrapped in amorphous cellulose?
	Cellulose 	Amorphous or crystalline structure (Non)-covalent linkages towards pectic elements?
Pectic structural elements	Homogalacturonan 	Length of homogalacturonan segments in between two RG-I units Degree of methyl esterification Degree of acetylation Degree of blockiness Connection to other structural elements
	Xylogalacturonan 	Degree and substitution of xylose Length of xylose side chains Degree of methyl esterification Other sugars than xylose present in side chains (e.g. fucose) Presence and level of acetylation Location of xylogalacturonan within pectic macromolecule
	Rhamnogalacturonan I 	Length of RG-I backbone Length of arabinan and arabinogalactan side chains Distribution of the side chains over the RG-I backbone Degree and localization of acetylation Presence of methyl esters Connection to other structural elements
	Arabinan 	Branching of the side chains Level and localization of ferulic acid Presence of terminal arabinose-pyranose
	Arabinogalactan I 	Size, linkages present, degree and type of branching Distribution of branching of the side chains over the galactan backbone Ratio of arabinose to galactactose Level and localization of ferulic acid Distribution of the side chains over the galactan backbone Presence of arabinofuranosyl residues in galactan backbone Ratio of the β -(1,3)-linked galactose in the β -(1,4)-galactan backbone Presence of terminal arabinopyranosyl residues
	Arabinogalactan II 	Size, linkages present, degree and type of branching Ratio of arabinose to galactactose Degree and localization of ferulic acid Terminal arabinopyranosyl-, glucuronopyranosyl and/or rhamnosyl residues present? Distribution of the side chains over the galactan backbone Attachment to other pectin structural elements
	Rhamnogalacturonan II 	Small differences in structure Level of borate crosslinking Distribution of RG-II chains over the pectic molecule
<div><div><div></div><div>α-L-AcefA</div></div><div><div></div><div>α-L-Arap</div></div><div><div></div><div>β-D-Galp</div></div><div><div></div><div>α-D-GlcpA</div></div><div><div></div><div>β-L-Rhap</div></div><div><div></div><div>Ferulic acid</div></div><div><div></div><div>β-D-Apif</div></div><div><div></div><div>β-D-Dhap</div></div><div><div></div><div>α-D-GalpA</div></div><div><div></div><div>α-D-Xylp</div></div><div><div></div><div>O-acetyl</div></div><div><div></div><div>α-L-Araf</div></div><div><div></div><div>α-L-Fucp</div></div><div><div></div><div>β-D-GalpA</div></div><div><div></div><div>α-D-Kdop</div></div><div><div></div><div>β-D-Xylp</div></div><div><div></div><div>β-L-Araf</div></div><div><div></div><div>α-D-Galp</div></div><div><div></div><div>β-D-Glcp</div></div><div><div></div><div>α-L-Rhap</div></div><div><div></div><div>O-methyl</div></div></div>		

concentrated alkali treatment, and 3) xyloglucan, which is incorporated in the amorphous cellulose microfibrils and is only accessible after removal of cellulose¹⁹.

Xylans include arabinoxylans (AX), glucuronoxylans (GX), glucuronoarabinoxylans (GAX) and linear xylans depending on origin and location. All xylans consist of a backbone of β -(1,4)-*p*-D-xylose, which can be substituted with L-arabinosyl residues (AX), (4-O-methyl)-glucuronic acid (GX) or both (GAX). Furthermore, xylans can be acetylated at O-2 and/or O-3. The attachment of ferulic acid to arabinoxylans has also been described²⁰. Due to the complex xylan structure, a one-letter nomenclature for xylans has been established recently²¹ following the example of xyloglucans¹⁶, which will facilitate the communication in xylan research.

Pectins

Pectins represent a heterogeneous group of cell wall polysaccharides. The main structural elements are homogalacturonan, rhamnogalacturonan-I, rhamnogalacturonan-II and xylogalacturonan²² (**Table 1**).

Homogalacturonan (HG) is a linear polymer composed of a backbone of α -(1,4)-linked D-galacturonic acid units. HG can be substituted with methyl esters at C-6 and/or acetyl groups at O-2 and/or O-3^{18,23,24} (**Table 1**). The degree of methyl esterification (DM), the degree of acetylation (DA) and the distribution of the esters over the backbone varies significantly depending on source and developmental stages^{18,23,24}. HG segments are rather conserved in length, containing 72-100 galacturonic acid residues as investigated for citrus, apple, sugar beet and *Arabidopsis thaliana*^{25,26}.

Xylogalacturonan (XGA) consists of an HG backbone, which is substituted by one or more β -(1,3)-linked D-xylose units^{18,27} (**Table 1**). Xylogalacturonan (XGA) could mostly be identified in reproductive tissues such as watermelon, apple and soy bean²⁸⁻³⁰ as well as in both *Arabidopsis* leaves and stems³¹. The degree of xylose substitution can vary between 25% for watermelon and 75% for apple^{30,28,32}. In *Arabidopsis*, a rather unbranched xylogalacturonan is present³¹. Furthermore, XGA may carry methyl esters at unsubstituted and substituted galacturonic acid units³⁰.

Rhamnogalacturonan-I (RG-I) consists of a backbone of alternating α -(1,2)-linked L-rhamnose units and α -(1,4)-linked D-galacturonic acid units (**Table 1**). At the O-4 position of rhamnose arabinan and/or arabinogalactan side chains are linked^{18,33}. The

proportion of branched rhamnose residues varies from 20% to 80% depending on the source, developmental stage and plant tissue³⁴. For example, RG-I from *Arabidopsis* seed mucilage is largely unbranched^{35,36}, while RG-I from sycamore cells is branched at about half of the rhamnosyl residues³⁷. The galacturonic acid residues may be acetylated at O-2 and/or O-3^{38,39,40}. Recently, in okra pectin the acetylation of the rhamnosyl residues as well as the substitution of α -linked galactosyl groups at O-4 of the rhamnose units was described⁴¹. Furthermore, in flax seed mucilage, L-galactosyl residues could be identified being attached to O-3 of the rhamnose residues⁴².

Arabinans are branched molecules with molecular masses up to 10 kDa. The linear backbone of α -(1,5)-linked L-arabinosyl residues may be substituted with one or more α -arabinofuranosyl residues at the O-2 and/or O-3 position (**Table 1**). These arabinosyl side chains might again be branched by arabinosyl residues at the O-2 and/or O-3 position⁴³. The arabinosyl residues might be feruloylated at O-2 and/or O-5⁴⁴.

Arabinogalactans type I consist of a linear backbone of β -(1,4)-D-galactosyl residues, which might be lowly branched (e.g. potato) or branched with short chains of α -(1,5)-linked L-arabinofuranosyl residues at O-3 position. The presence of an arabinopyranosyl residue at the non-reducing end and an internal α -(1,5)-linked arabinofuranosyl residue in the backbone interspersing the β -(1,4)-D-galactan backbone has been demonstrated in soy²⁹. Furthermore, the β -(1,4)-D-galactan backbone was found to be interrupted with a β -(1,3)-linked galactosyl residue with a frequency ranging from approximately 1 in 160 residues for potato, soy and citrus to 1 in 250 residues for onion⁴⁵.

Arabinogalactans type II (AG-II) are highly branched polysaccharides with a backbone of β -(1,3)-D-galactosyl residues, which can be substituted with side chains of β -(1,6)-D-galactosyl residues with 1-3 residues in length. Some β -(1,3)-D-galactan backbones are substituted with single arabinopyranosyl residues, while also rhamnose and glucuronic acid may be present in the side chains. AG-II is often reported to be linked to proteins forming the so-called arabinogalactan proteins⁴⁶.

Rhamnogalacturonan-II (RG-II) has been found in many plant tissues and seems to have a rather conserved structure. The RG-II molecule consists of 7-9 α -(1,4)-linked D-galacturonic acid residues, which carry four well-defined side chains⁴⁷. An additional side-chain composed of a single L-arabinose residue has also been reported^{48,49}. The highly complex structures includes 12 different monosaccharides including some rare ones (**Table 1**), such as 2-O-methyl xylose, 2-O-methyl fucose, aceric acid, 3-deoxy-D-manno-2-octulosonic acid (DHA) and 3-deoxy-D-lyxo-2-heptulosaric acid (KDO), which are

interlinked by 20 different linkages⁵⁰. RG-II is able to form dimers via a borate diester⁵¹, which results in a cross-link of two pectin molecules within the cell wall^{47,52,53}.

In addition to the variation of the chemical fine structures of the cell wall polysaccharides as described above and summarized in **Table 1**, also the abundance of these cell wall polysaccharide structures may vary depending on the plant origin and developmental stage. In **Table 2** the abundance of pectic structural elements for selected plants is depicted. For example, in black currant and bilberry homogalacturonan represents about 65% of the pectic substances, while in soybean no HG could be identified. The proportion of RG-I, including the neutral sugar chains, can be as low as 23% for *Arabidopsis thaliana*⁵⁴ or as high as 75% for soy bean⁵⁵ (**Table 2**). The amount of XGA can be as high as about 21% in soybean⁵⁵, most likely compensating for the absence of HG, and nearly absent in sugar beet pulp (< 1%).

Table 2 Proportion of the various structural elements (% on total pectin) in a number of plant species.

	HG	XGA	RG-I backbone	RG-I side chains	RG-II
Black currant ^a	68	0	5	24	3
Bilberry ^a	65	0	6	27	2
Soybean ^b	0	21	15	60	4
Sugar beet ^b	29	0.3	4	48	4
Apple ^b	36	4	1	47	10
<i>Arabidopsis</i> leaves ^c	48	13	$\Sigma = 23$		17

^a from Hilz et al.⁵⁶, ^b from Voragen et al.⁵⁵, ^c recalculated from Zablackis et al.⁵⁴ HG = homogalacturonan, XGA = xylogalacturonan, RG-I = rhamnogalacturonan-I, RG-II = rhamnogalacturonan-II.

Architecture of plant cell wall polysaccharides

Even though much research dedicated to the elucidation of the architecture of cell wall polysaccharides has been performed, the precise structure of the complex network of the polysaccharides described remains still unknown. Different models of the plant cell wall coexist and are continuously adapted to new findings^{38,57-59}. The most used model nowadays is the “tethered network” model⁵⁸, which is mostly based on the model of McCann and Roberts⁵⁷. The cellulose microfibrils are interlinked with xyloglucans via hydrogen bonds forming a stiff network^{38,60}. Within this network, pectin and structural proteins are assumed to act as a co-extensive network, which is physically entangled with the cellulose-hemicellulose network^{15,58,61}.

The presence of covalent linkages between the pectic structural elements has been hypothesized already for a long time based on co-extraction and co-elution. Mainly two models dealing with the pectic network have been established. The first model, the smooth and hairy regions model, was established by De Vries *et al.*⁶² and later updated by Schols and Voragen⁶³ and Thibault *et al.*⁶⁴. The so-called hairy regions consisting of RG-I (with neutral side chains attached) and XGA are interspersed with so-called smooth (HG) regions (**Figure 1**). The second model, the so-called rhamnogalacturonan backbone model, was proposed by Vincken *et al.*⁶⁵, which locates HG as a side chain of RG-I (**Figure 1**). RG-II is proposed to be attached to the homogalacturonan segments as RG-II is liberated from the pectic macromolecule by endo-polygalacturonase treatment⁶⁶.

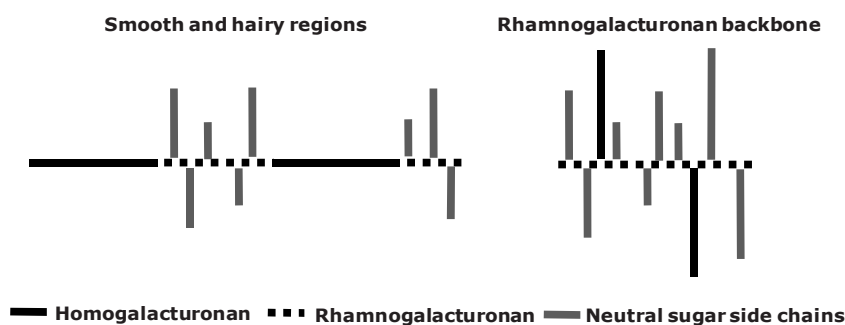


Figure 1 Schematic representation of two different models describing the hypothetical pectin structure, adapted from Vincken *et al.*⁶⁵.

Recently, key oligomeric fragments were identified, which proved a covalent linkage between HG/XGA and RG-I. The connection between HG/XGA and RGI segments was identified to be linear⁶⁷. This data supported partly the smooth and hairy region model, even though an excess of HG remains unexplainable with the ‘smooth and hairy region’-model⁶⁷. Therefore, a new model for the pectic network was hypothesized⁶⁸ as presented in **Figure 2**.

Cross-links between pectin and hemicelluloses have been hypothesized by many researchers, mainly based on co-extraction and co-elution⁶⁹. Rather recently, a possible cross-link between pectins and cellulose has been suggested⁷⁰⁻⁷⁴.

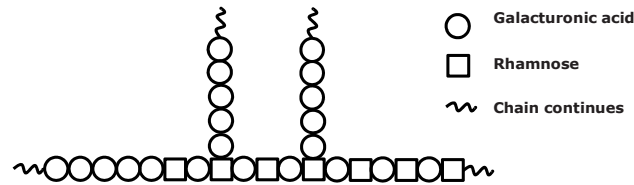


Figure 2 Putative pectin backbone model based on the observed excess of galacturonan segments and the identification of a linear connection between HG/XGA and RGI segments as presented by Coenen⁶⁸. RG-I with HG side chains, connected to rhamnose residues, in addition HG is in line attached to the non-reducing end of RG-I.

Cell wall degrading enzymes

In the following paragraphs a selection of cell wall degrading enzymes will be briefly discussed and the main family numbers of the most important enzymes will be mentioned according to the Carbohydrate-Active enZymes database (<http://www.cazy.org>).

Cellulose degrading enzymes

Within cellulases three enzyme classes are known: Endo-glucanases, cellobiohydrolases and β -glucosidases, which work synergistically. While endo-glucanases (glycoside hydrolase family 7 (GH 7)) are endo-acting enzymes, cellobiohydrolases (GH 7) and β -glucosidases (GH 3), are exo-acting enzymes⁷⁵. Cellobiohydrolase releases cellobiose, whereas β -glucosidases release single glucose units.

Xyloglucan backbone degrading enzymes

The mostly used xyloglucan backbone degrading enzyme is the xyloglucan specific endo-glucanase (XEG; GH 5), which only cleaves xyloglucan⁷⁶. XEG cleaves the bond between the non-substituted glucose (G) and the neighboring substituted glucose unit (X) as indicated in **Figure 3**, resulting in specific oligosaccharide building blocks of xyloglucan^{13,76,77}.

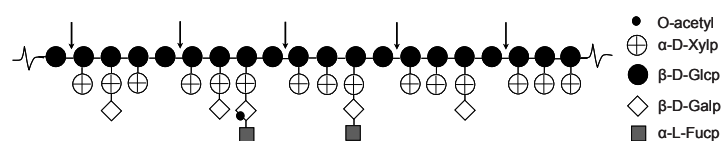


Figure 3 Schematic representation of the mode of action of xyloglucan specific endo-glucanase (adapted from Pauly et al.⁷⁶).

Xylan degrading enzymes

Endo- β -(1,4)-xylanases (GH 10 and 11) cleave the β -(1,4)-linked xylan backbone in a random manner releasing linear and branched xylo-oligosaccharides with a low degree of polymerization depending on the mode of action of the enzyme^{78,79}. β -(1,4)-Xylosidases (GH 3) attack short xylo-oligosaccharides releasing xylopyranose. Furthermore, accessory enzymes are required for the degradation of (glucurono-)arabino-xylan, such as α -glucuronidases, α -L-arabinofuranosidases, acetyl xylan esterases and ferulic acid esterases⁷⁸.

Pectin degrading enzymes

Pectinases can be divided into mainly three groups depending on their substrate: homogalacturonan specific enzymes, rhamnogalacturonan-I specific enzymes and xylogalacturonan specific enzymes. No enzymes enabling the efficient degradation of rhamnogalacturonan-II have been identified yet⁸⁰. A selection of these pectinases including enzymes degrading the arabinan and galactan side chains of RG-I will be described briefly in the paragraphs below.

HG degrading enzymes

Polygalacturonan hydrolases (endo-PG; GH 28) are endo-acting enzymes cleaving the linkages between non-substituted α -(1,4)-linked D-galacturonic acid units (**Figure 4**). With increasing degree of methyl esterification, the enzyme activity decreases⁸¹.

Pectin lyases (PL; polysaccharide lyase family 1 (PL1)) are endo-acting enzymes cleaving the linkages between two methyl esterified α -(1,4)-linked D-galacturonic acid units (**Figure 4**) releasing unsaturated galacturonic acid oligosaccharides⁸².

Pectin methyl esterases (PME; carbohydrate esterase family 8 (CE 8)) remove methyl esters from the α -(1,4)-linked D-galacturonic acid residues of the HG backbone (**Figure 4**). PME action on (highly) methyl esterified pectins does not result in complete de-esterification⁸³. The mode of action of PMEs originating from plants or fungi varies significantly. Plant PMEs act in a blockwise manner, whereas fungal PMEs remove methyl esters randomly⁸². Possible activities of both PMEs on methyl esters of the α -(1,4)-linked D-galacturonic acid residues of XGA remains to be unknown.

Pectin acetyl esterases (PAE; CE 12 and 13) remove acetyl groups from the O-2 and/or O-3 position of the α -(1,4)-linked D-galacturonic acid residues of the HG backbone⁸⁴ (Figure 4).

Xylogalacturonan specific enzymes

Xylogalacturonan hydrolase (XGH; GH 28) hydrolyzes the α -(1,4)-D-linkages of xylose substituted galacturonan moieties in xylogalacturonan^{27,85,86}. The presence of β -(1,3)-linked xylosyl side chains is important for XGH to degrade the substrate, although the precise level of xylosidation recognized by the enzyme is not known²⁷ (Figure 4).

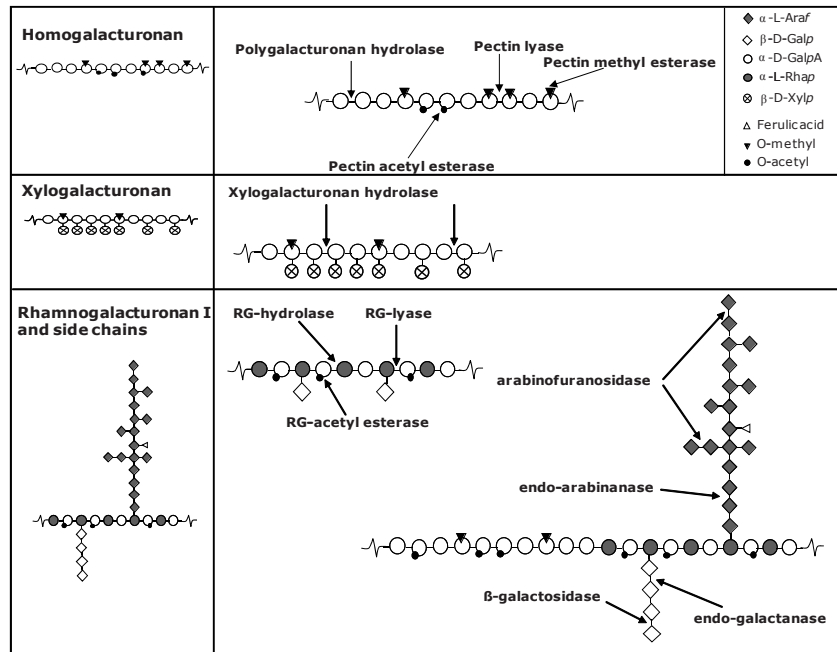


Figure 4 Schematic representation of the mode of action of pectinolytic enzymes^{27,43,82}.

RG-I degrading enzymes

Rhamnogalacturonan hydrolase (RGH; GH 28) and rhamnogalacturonan lyase (RGL; PL 4 and 11) are two very well described enzymes degrading the RG-I-backbone. Detailed structural characterization of the reaction products has shown that RGH and RGL cleave the RG-I backbone at different positions^{87,88} (Figure 4). RGH treatment results in oligomers with the rhamnosyl residues at the non-reducing end and the galacturonic acid at

the reducing end, while for the RGL treatment it is the other way around resulting in oligomers with an unsaturated galacturonic acid at the non-reducing end and a rhamnose at the reducing end^{87,89,90}. Both enzymes are hindered by acetyl groups.

Rhamnogalacturonan acetyl esterase (RGAE; CE 12) removes the acetyl groups from the galacturonic acid residues in RG-I^{84,91}, but does not remove acetyl groups attached to rhamnose residues⁴¹. Recently, it was demonstrated that RGAEs are not only restricted to the deacetylation of RG-I but remove as well acetyl groups from homogalacturonan⁹².

Arabinan and galactan degrading enzymes

Endo-arabinanases (GH 43) are endo-acting enzymes degrading the linear backbone of α -(1,5)-linked L-arabinosyl residues. Arabinofuranosidases (GH 43, 51 and 54) are described to cleave the α -(1,2) and α -(1,3)-linked side chains in an exo-manner releasing single arabinosyl residues⁴³ (**Figure 4**).

Galactan degrading enzymes belong to the glycoside hydrolase families 2, 27, 36, 42 and 53. β -(1,4)-Galactanases are endo and/or exo-acting enzymes degrading β -(1,4)-linked galactan releasing galacto-oligosaccharides with a degree of polymerization of 1 to 4 depending on the origin of the enzyme⁹³⁻⁹⁵ (**Figure 4**). β -Galactosidases are exo-acting enzymes degrading either β -(1,3)-, β -(1,4)- or β -(1,6)-linked galactan releasing exclusively single galactose units⁹⁶.

Analytical tools for cell wall derived mono-, oligo- and polysaccharides

Cell wall polysaccharides are complex macromolecules as described earlier. Nowadays, there are many different analytical tools for the analysis of these complex cell wall polysaccharides. Not every analytical tool provides data on the same information level and not every tool is suitable for all cell wall polysaccharides present in the plant cell wall. An overview of commonly used methods within cell wall analysis is given in **Table 3**. It should be mentioned that the overview presented is giving examples rather than trying to be complete.

Polysaccharides

The analysis of intact soluble cell wall polysaccharides is limited to the determination of the molecular weight⁹⁷ (High Performance Size Exclusion Chromatography (HPSEC)), and the “overall”-structure on polymeric level (FTIR⁹⁸⁻¹⁰⁰ and NMR analysis¹⁰¹) (**Table 3**). The degree of non-sugar substituents can be analyzed after saponification (e.g., methyl esterification, acetylation and feruloylation¹⁰²⁻¹⁰⁶). Sugar composition analysis of the cell wall polysaccharides providing information of the monosaccharide units present in the polysaccharide(s) includes the hydrolysis or methanolysis of the polysaccharide(s). Three different degradation techniques are used: Hydrolysis with sulfuric acid, hydrolysis with trifluoroacetic acid (TFA), and methanolysis. Neutral monosaccharides are either analyzed as alditol acetates by GC-FID^{97,107}, as trimethylsilyl glycoside derivatives by GC-FID/MS¹⁰⁸ or as underivatized monosaccharides by HPAEC-PAD¹⁰⁹ (**Table 3**). The total sugar content can alternatively be analyzed by the orcinol/sulfuric acid assay¹¹⁰ or the phenol/sulfuric acid assay¹¹¹, the total uronic acid content is analyzed with the automated *m*-hydroxybiphenyl assay¹¹². To distinguish underivatized galacturonic and glucuronic acid, HPAEC-PAD analysis after e.g. methanolysis is required^{109,113}. Linkage analysis of the sugar units present in the cell wall polysaccharide(s) can be determined by GC-FID/MS of the monosaccharides after permethylation, hydrolysis and subsequent conversion to alditol acetates^{97,114} or by NMR of the intact polymer.

All these tools deliver information of the *average* structure of the cell wall polysaccharide(s), whereas detailed information of the distribution of the various monosaccharides and non-sugar substituents within the polysaccharide(s) is not obtained. Therefore, most of the cell wall polysaccharide research aiming at the elucidation of the chemical fine structure is performed after fractionation of the polysaccharides (e.g., anion exchange or size exclusion chromatography^{113,115}) toward homogeneity and degradation of these polysaccharides into characteristic oligosaccharides.

Oligosaccharides

In addition to chemical treatments using mild and strong acids reagents⁶⁷, cell wall polysaccharide degrading enzymes, as described earlier in this chapter, are frequently used to create characteristic oligosaccharides^{63,116}. These oligosaccharides can be analyzed by

Table 3 Overview of selected analytical tools for cell wall derived mono-, oligo- and polysaccharides

METHODS	REFERENCES	MONOSACCHARIDES		OLIGOSACCHARIDES		POLYSACCHARIDES	
		neutral	acidic	non-esterified neutral	esterified acidic	neutral	acidic
Total sugar content (orcinol/sulfuric acid assay or phenol/sulfuric acid)	110,111	X	X	X	X	X	X
Sugar composition (after hydrolysis)							
Determination as aldiose acetates (GC-FID)	97,107	X		X		X	X
Determination as trimethylsilyl (TMS) derivatives (GC-MS)	108	X	X	X	X	X	X
Total uronic acid content (<i>m</i> -hydroxydiphenyl assay)	112		X	X	X	X	X
Determination of underivatized monosaccharides (HPAEC, post-column)	109,113	X	X	X	X		
Determination of non-sugar substituents							
<i>Degree of acetylation (DA)</i>							
HPLC	102,104						X
<i>Degree of methyl esterification (DM)</i>							
HPLC	102,104						X
GC	103						X
<i>Degree of feruloylation</i>	105,106						
Analysis of the average structure of intact polysaccharides							
NMR	101,117,118	X	X	X		X	X
FTIR	98-100			X		X	X
HPSEC-(RI/UV)	97			X		X	X
Determination of the glycosidic linkages							
GC-FID/MS	97,114			X		X	X
NMR	101,117,118			X		X	X
Analysis of individual oligosaccharides							
HPAEC-PAD, pH 12	119,121,122,123	(X)	X	X			
HPAEC-PAD, pH 5	128		X	X			
MALDI-TOF MS	17,41,45			X		X	X
RP-HPLC-ELSD/MS	124			X		X	
CE-LIF	126,127	X		X		X	
CE-MS	126,127			X		X	
PACE	125,129,130	X	X	X		X	X

various techniques (**Table 3**). The unambiguous identification of any oligosaccharide is achieved with NMR analysis (**Table 3**). However, this usually requires a time-consuming purification to obtain sufficient material of the oligosaccharide of interest^{117,118}.

Neutral oligosaccharides

A commonly used technique for the analysis of neutral oligosaccharides is high performance anion exchange chromatography with pulsed amperometric detection (HPAEC-PAD, pH 12) enabling the separation and detection of DP 3-15 of many different neutral oligosaccharides¹¹⁹⁻¹²¹. Offline-MS as well as online-MS-coupling of HPAEC is possible^{122,123}. Furthermore, matrix-assisted laser desorption ionization time-of-flight mass spectrometry (MALDI-TOF MS) can be used for a fast and simple overview of the oligosaccharides (DP 3-15) present in a sample^{17,45}. Reversed phase (RP) high performance liquid chromatography with evaporative light scattering and mass detection (RP-HPLC-ELSD/MS) and polysaccharide analysis using carbohydrate gel electrophoresis (PACE) were shown to enable the separation of neutral oligosaccharides^{124,125}. Capillary electrophoresis with laser-induced-fluorescence detection (CE-LIF) is a powerful method to study cell wall derived oligosaccharides in a very short time (15 min). CE-MS analysis facilitates the annotation of the peaks in the CE-LIF electropherogram¹²⁶.

Due to the use of high pH eluents during HPAEC (pH 12) methyl esters and acetyl groups attached to the oligosaccharides are eliminated during analysis. Thus, HPAEC cannot be used for the analysis of esterified oligosaccharides (**Table 3**). The analysis of esterified neutral oligosaccharides by CE-LIF and RP-HPLC seems to be very powerful as has been shown for e.g. acetylated xylans^{124,126}.

Acidic oligosaccharides

For the analysis of non-esterified acidic oligosaccharides, all analytical tools as described for non-esterified neutral oligosaccharides can be used, even though some adaptations might be required^{41,121,127}. An exception is RP-HPLC as acidic oligosaccharides are not retained on RP-material (**Table 3**).

The analysis of esterified acidic oligosaccharides is mainly limited to MALDI-TOF MS, HPAEC (pH 5) and PACE^{41,128-130} (**Table 3**).

To summarize, many analytical techniques are available for the analysis of cell wall derived oligosaccharides (**Table 3**). However, there are hardly universal methods, which

allow the separation and detection of neutral and acidic oligosaccharides including methyl esterification and acetylation within a complex mixture. Furthermore, online-MS analysis of these structures is rather difficult. With increasing size of the oligosaccharides released the information about the polysaccharides improves, but the difficulty of the separation and detection increases.

Promising HPLC column materials such as porous graphitized carbon (PGC) or hydrophilic interaction liquid chromatography (HILIC) enabling the retention of both neutral and acidic components have not yet been investigated for a broad range of cell wall oligosaccharides^{131,132}.

Thesis Outline

The analysis of the chemical fine structure of cell wall polysaccharides requires the chemical or enzymatic degradation toward diagnostic oligosaccharides. The aim of the present PhD thesis is to explore various techniques to be used as screening, fingerprinting and/or structure prediction tool for neutral *and* charged cell wall derived oligosaccharides. Furthermore, these techniques are aimed to be used in further in-depth analysis.

Chapter 2 describes a multi-enzyme assisted screening method with MALDI-TOF MS and CE-LIF detection aiming at a fingerprint of neutral *and* charged oligosaccharides derived from the whole enzyme-accessible plant cell wall in a single MALDI-TOF mass spectrum or CE-LIF electropherogram. This fingerprint allows the screening for *Arabidopsis thaliana* cell wall mutants.

In Chapter 3 PGC-HPLC with ELS- and MSⁿ detection was explored for the analysis of a broad range of cell wall derived oligosaccharides. Opposite to RP-material, on PGC-material both neutral *and* acidic oligosaccharides have retention enabling the development of an universal method for oligosaccharides based on PGC-HPLC. Online recorded MSⁿ data is shown to allow the analysis of complex cell wall derived oligosaccharide mixtures.

Chapter 4 describes the isolation and characterization of two unique series of branched arabino-oligosaccharides from sugar beet arabinan after incubation with pure and well-defined arabino-hydrolases from *Chrysosporium lucknowense*. HPAEC-PAD, PGC-HPLC-ELSD/MS and CE-LIF-MS were explored to enable the separation and characterization of all arabino-oligosaccharides under investigation. Additionally, LC/CE-MS² fragmentation

patterns derived from linear and branched arabino-oligosaccharides were evaluated for their potential to predict the presence of different linkages within the oligosaccharide (Chapter 5). The knowledge of the elution behavior of arabino-oligosaccharides on PGC-HPLC-ELSD/MS as well as the use of the branched arabino-oligosaccharides isolated allowed the detailed characterization of the mode of action of four arabino-hydrolases from *Chrysosporium lucknowense* (Chapter 6).

In Chapter 7 the results of the different chapters are summarized and discussed including further possible adjustments or extensions of the methods developed. In addition, expected developments, especially MSⁿ based methods, are discussed for cell wall oligosaccharide analysis in general.

References

1. Mohnen, D. *Current Opinion in Plant Biology*, **2008**, *11*, 266-277.
2. *Arabidopsis* Genome Initiative *Nature*, **2000**, *408*, 796-815.
3. Reiter, W.D. *Plant Physiol. Biochem.*, **1998**, *36*, 167-176.
4. Foreman, J.; Dolan, L. *Annals of Botany*, **2001**, *88*, 1-7.
5. Bacic, A.; Harris, P.; Stone, B. *The Biochemistry of Plants*, **1988**, *14*, 297-369.
6. McNeil, M.; Darvill, A.G.; Fry, S.C.; Albersheim, P. *Annu. Rev. Biochem.*, **1984**, *53*, 625-663.
7. Delmer, D.P. *Tappi J.*, **1987**, *70*, 141-143.
8. Kroon-Batenburg, L.M.J.; Kroon, J. *Glycoconjugate J.*, **1997**, *14*, 677-690.
9. Vierhuis, E.; York, W.S.; Kolli, V.S.K.; Vincken, J.P.; Schols, H.A.; Van Alebeek, G.; Voragen, A.G.J. *Carbohydr. Res.*, **2001**, *332*, 285-297.
10. Caffall, K.H.; Mohnen, D. *Carbohydr. Res.*, **2009**, *344*, 1879-1900.
11. Popper, Z.A.; Fry, S.C. *Annals of Botany*, **2005**, *96*, 91-99.
12. Buckeridge, M.S.; Crombie, H.J.; Mendes, C.J.M.; Reid, J.S.G.; Gidley, M.J.; Vieira, C.C.J. *Carbohydr. Res.*, **1997**, *303*, 233-237.
13. Vincken, J.P.; York, W.S.; Beldman, G.; Voragen, A.G.J. *Plant Physiology*, **1997**, *114*, 9-13.
14. Lerouxel, O.; Choo, T.S.; Seveno, M.; Usadel, B.; Faye, L.; Lerouge, P.; Pauly, M. *Plant Physiology*, **2002**, *130*, 1754-1763.
15. Bauer, W.D.; Talmadge, K.W.; Keegstra, K.; Albersheim, P. *Plant Physiology*, **1973**, *51*, 174-187.

16. Fry, S.C.; York, W.S.; Albersheim, P.; Darvill, A.; Hayashi, T.; Joseleau, J.P.; Kato, Y.; Lorences, E.P.; Maclachlan, G.A.; McNeil, M.; Mort, A.J.; Reid, J.S.G.; Seitz, H.U.; Selvendran, R.R.; Voragen, A.G.J.; White, A.R. *Physiol. Plant.*, **1993**, *89*, 1-3.
17. Hilz, H.; de Jong, L.E.; Kabel, M.A.; Schols, H.A.; Voragen, A.G.J. *J. Chromatogr. A*, **2006**, *1133*, 275-286.
18. Schols, H.A.; Voragen, A.G.J., in: Seymour, G.B.; Knox, J.P. (Editors), *Pectins and their manipulation*, Blackwell Publishing, Oxford, United Kingdom, **2002**, p. 1-29.
19. Pauly, M.; Albersheim, P.; Darvill, A.; York, W.S. *Plant Journal*, **1999**, *20*, 629-639.
20. Ishii, T.; Hiroi, T. *Carbohydr. Res.*, **1990**, *196*, 175-183.
21. Fauré, R.; Courtin, C.M.; Delcour, J.A.; Dumon, C.; Faulds, C.B.; Fincher, G.B.; Fort, S.; Fry, S.C.; Halila, S.; Kabel, M.A.; Pouvreau, L.; Quemener, B.; Rivet, A.; Saulnier, L.; Schols, H.A.; Driguez, H.; O'Donohue, M.J. *Aust. J. Chem.*, **2009**, *62*, 533-537.
22. Ridley, B.L.; O'Neill, M.A.; Mohnen, D.A. *Phytochemistry*, **2001**, *57*, 929-967.
23. Ralet, M.C.; Cabrera, J.C.; Bonnin, E.; Quémener, B.; Hellin, P.; Thibault, J.F. *Phytochemistry*, **2005**, *66*, 1832-1843.
24. Ralet, M.C.; Crépeau, M.J.; Bonnin, E. *Phytochemistry*, **2008**, *69*, 1903-1909.
25. Ralet, M.C.; Crépeau, M.J.; Lefebvre, J.; Mouille, G.; Hofte, H.; Thibault, J.F. *Biomacromolecules*, **2008**, *9*, 1454-1460.
26. Thibault, J.-F.; Renard, C.M.G.C.; Axelos, M.A.V.; Roger, P.; Crépeau, M.J. *Carbohydr. Res.*, **1993**, *238*, 271-286.
27. Beldman, G.; Vincken, J.P.; Schols, H.A.; Meeuwssen, P.J.A.; Herweijer, M.; Voragen, A.G.J. *Biocatal. Biotransform.*, **2003**, *21*, 189-198.
28. Yu, L.; Mort, A.J., in: Visser, J., Voragen, A.G.J. (eds), *Progress in Biotechnology 14: Pectins and pectinases*, proceedings of an Int. Symp., Elsevier, Amsterdam, The Netherlands, **1996**, p. 79-88.
29. Huisman, M.M.H.; Fransen, C.T.M.; Kamerling, J.P.; Vliegthart, J.F.G.; Schols, H.A.; Voragen, A.G.J. *Biopolymers*, **2001**, *58*, 279-294.
30. Schols, H.A.; Bakx, E.J.; Schipper, D.; Voragen, A.G.J. *Carbohydr. Res.*, **1995**, *279*, 265-279.
31. Zandleven, J.; Sorensen, S.O.; Harholt, J.; Beldman, G.; Schols, H.A.; Scheller, H.V.; Voragen, A.J. *Phytochemistry*, **2007**, *68*, 1219-1226.
32. Le Goff, A.; Renard, C.M.G.C.; Bonnin, E.; Thibault, J.F. *Carbohydr. Polym.*, **2001**, *45*, 325-334.
33. Talmadge, K.W.; Keegstra, K.; Bauer, W.D.; Albersheim, P. *Plant Physiology*, **1973**, *51*, 158-173.
34. Albersheim, P.; Darvill, A.G.; O'Neill, M.A.; Schols, H.A.; Voragen, A.G.J., in: Visser, J., Voragen, A.G.J. (eds), *Progress in Biotechnology 14: Pectins and pectinases*, proceedings of an Int. Symp., Elsevier, Amsterdam, The Netherlands, **1996**, p. 47-55.

35. Penfield, S.; Meissner, R.C.; Shoue, D.A.; Carpita, N.C.; Bevan, M.W. *Plant Cell*, **2001**, *13*, 2777-2791.
36. Western, T.L.; Young, D.S.; Dean, G.H.; Tan, W.L.; Samuels, A.L.; Haughn, G.W. *Plant Physiology*, **2004**, *134*, 296-306.
37. Lau, J.M.; McNeil, M.; Darvill, A.G.; Albersheim, P. *Carbohydr. Res.*, **1985**, *137*, 111-125.
38. Carpita, N.C.; Gibeaut, D.M. *Plant Journal*, **1993**, *3*, 1-30.
39. Schols, H.A.; Posthumus, M.A.; Voragen, A.G.J. *Carbohydr. Res.*, **1990**, *206*, 117-129.
40. Schols, H.A.; Voragen, A.G.J. *Carbohydr. Res.*, **1994**, *256*, 83-95.
41. Sengkhamparn, N.; Bakx, E.J.; Verhoef, R.; Schols, H.A.; Sajjaanantakul, T.; Voragen, A.G.J. *Carbohydr. Res.*, **2009**, *344*, 1842-1851.
42. Naran, R.; Chen, G.; Carpita, N.C. *Plant Physiology*, **2008**, *148*, 132-141.
43. Beldman, G.; Schols, H.A.; Pitson, S.M.; Searle-van Leeuwen, M.F.; Voragen, A.G.J., in: Sturgeon, R.G. (editor), *Advances in Macromolecular Carbohydrate Research*, Vol. 1, JAI Press Inc., Greenwich, United Kingdom, **1997**, p. 1-64.
44. Levigne, S.V.; Ralet, M.C.J.; Quemener, B.C.; Pollet, B.N.L.; Lapierre, C.; Thibault, J.F.J. *Plant Physiology*, **2004**, *134*, 1173-1180.
45. Hinz, S.W.A.; Verhoef, R.P.; Schols, H.A.; Voragen, A.G.J. *Carbohydr. Res.*, **2005**, *340*, 2135-2143.
46. Gaspar, Y.; Johnson, K.L.; McKenna, J.A.; Bacic, A.; Schultz, C.J. *Plant Molecular Biology*, **2001**, *47*, 161-176.
47. O'Neill, M.A.; Eberhard, S.; Albersheim, P.; Darvill, A.G. *Science*, **2001**, *294*, 846-849.
48. Pérez, S.; Rodríguez-Carvajal, M.A.; Doco, T. *Biochimie*, **2003**, *85*, 109-121.
49. Rodríguez-Carvajal, M.A.; Hervé Du Penhoat, C.; Mazeau, K.; Doco, T.; Pérez, S. *Carbohydr. Res.*, **2003**, *338*, 651-671.
50. O'Neill, M.A.; Warrenfelz, D.; Kates, K.; Pellerin, P.; Doco, T.; Darvill, A.G.; Albersheim, P. *J. Biol. Chem.*, **1997**, *272*, 3869-3869.
51. O'Neill, M.A.; Ishii, T.; Albersheim, P.; Darvill, A.G. *Annual Review Of Plant Biology*, **2004**, *55*, 109-139.
52. Pellerin, P.; Doco, T.; Vidal, S.; Williams, P.; Brillouet, J.M.; O'Neill, M.A. *Carbohydr. Res.*, **1996**, *290*, 183-197.
53. Vidal, S.; Doco, T.; Williams, P.; Pellerin, P.; York, W.S.; O'Neill, M.A.; Glushka, J.; Darvill, A.G.; Albersheim, P. *Carbohydr. Res.*, **2000**, *326*, 277-294.
54. Zablackis, E.; Huang, J.; Muller, B.; Darvill, A.G.; Albersheim, P. *Plant Physiology*, **1995**, *107*, 1129-1138.
55. Voragen, A.G.J.; Beldman, G.; Schols, H.A., in: Barry V. McCleary, Leon Prosky (eds.) *Advanced Dietary Fiber Technology*, Blackwell Science Ltd., Oxford, United Kingdom, **2001**, p. 379-398.
56. Hilz, H. *PhD thesis*, Wageningen University, Wageningen, The Netherlands, **2007**.

57. McCann, M.C.; Roberts, K., in: Lloyd, C.W. (editor), The cytoskeletal basis of plant growth and form, Academic Press, London, United Kingdom, **1991**, p. 109-129.
58. Cosgrove, D.J. *Plant Physiology*, **2001**, *125*, 131-134.
59. Talbott, L.D.; Ray, P.M. *Plant Physiology*, **1992**, *98*, 357-368.
60. Keegstra, K.; Talmadge, K.W.; Bauer, W.D.; Albersheim, P. *Plant Physiology*, **1973**, *51*, 188-196.
61. Hayashi, T.; Marsden, M.P.F.; Delmer, D.P. *Plant Physiology*, **1987**, *83*, 384-389.
62. De Vries, J.A.; Voragen, A.G.J.; Rombouts, F.M.; Pilnik, W. *Carbohydr. Polym.*, **1981**, *1*, 117-127.
63. Schols, H.A.; Voragen, A.G.J., in: Visser, J., Voragen, A.G.J. (eds), Progress in Biotechnology 14: Pectins and pectinases, proceedings of an Int. Symp., Elsevier, Amsterdam, The Netherlands, **1996**, p. 3-19.
64. Thibault, J.F.; Renard, C.M.C.G. *J. Cell. Biochem.*, **1993**, 31.
65. Vincken, J.P.; Schols, H.A.; Oomen, R.; McCann, M.C.; Ulvskov, P.; Voragen, A.G.J.; Visser, R.G.F. *Plant Physiology*, **2003**, *132*, 1781-1789.
66. Ishii, T.; Matsunaga, T. *Phytochemistry*, **2001**, *57*, 969-974.
67. Coenen, G.J.; Bakx, E.J.; Verhoef, R.P.; Schols, H.A.; Voragen, A.G.J. *Carbohydr. Polym.*, **2007**, *70*, 224-235.
68. Coenen, G.J. *PhD thesis*, Wageningen University, Wageningen, The Netherlands, **2007**.
69. Mort, A.J. in: Seymour, G.B., Knox, J.P. (eds.) Pectins and their Manipulation, Oxford, United Kingdom, **2002**, p. 30-51.
70. Zykwinska, A.; Gaillard, C.; Buléon, A.; Pontoire, B.; Garnier, C.; Thibault, J.F.; Ralet, M.C. *Biomacromolecules*, **2007**, *8*, 223-232.
71. Zykwinska, A.; Thibault, J.F.; Ralet, M.C. *J. Exp. Bot.*, **2007**, *58*, 1795-1802.
72. Zykwinska, A.; Thibault, J.F.; Ralet, M.C. *Carbohydr. Polym.*, **2008**, *74*, 23-30.
73. Zykwinska, A.; Thibault, J.F.; Ralet, M.C. *Carbohydr. Polym.*, **2008**, *74*, 957-961.
74. Zykwinska, A.W.; Ralet, M.C.J.; Garnier, C.D.; Thibault, J.F.J. *Plant Physiology*, **2005**, *139*, 397-407.
75. Beldman, G.; Searle-Van Leeuwen, M.F.; Rombouts, F.M.; Voragen, F.G. *Eur. J. Biochem.*, **1985**, *146*, 301-308.
76. Pauly, M.; Andersen, L.N.; Kauppinen, S.; Kofod, L.V.; York, W.S.; Albersheim, P.; Darvill, A. *Glycobiology*, **1999**, *9*, 93-100.
77. Fry, S.C.; York, W.S.; Albersheim, P.; Darvill, A.; Hayashi, T.; Joseleau, J.-P.; Kato, Y.; Lorences, E.P.; Maclachlan, G.A.; McNeil, M.; Mort, A.J.; Reid, J.S.G.; Seitz, H.-U.; R.R. Selvendran; Voragen, A.G.J.; White., A.R. *Physiologia Plantarum*, **1993**, *89*, 1-3.
78. Kormelink, F.J.M. *PhD thesis*, Wageningen Agricultural University, Wageningen, The Netherlands, **1992**.
79. Kormelink, F.J.M.; Searle-Van Leeuwen, M.J.E.; Wood, T.M.; Voragen, A.G.J. *J. Biotechnol.*, **1993**, *27*, 249-265.

80. Séveno, M.; Voxeur, A.; Rihouey, C.; Wu, A.M.; Ishii, T.; Chevalier, C.; Ralet, M.C.; Driouich, A.; Marchant, A.; Lerouge, P. *Planta*, **2009**, *230*, 947-957.
81. Pařenicova, L.; Kester, H.C.M.; Benen, J.A.E.; Visser, J. *FEBS Lett.*, **2000**, *467*, 333-336.
82. Benen, J.A.E.; Vincken, J.-P.; Alebeek, G.-J.W.M.v. in: Seymour, G.B., Knox, J.P. (eds.) *Pectins and their Manipulation*, Oxford, United Kingdom, **2002**, p. 174-221.
83. Versteeg, C.; Rombouts, F.M.; Pilnik, W. *Lebensm. Wiss. Technol.*, **1978**, *11*, 267-274.
84. Searle-van Leeuwen, M.J.F.; Vincken, J.P.; Schipper, D.; Voragen, A.G.J.; Beldman, G. in: Visser, J., Voragen, A.G.J. (eds), *Progress in Biotechnology 14: Pectins and pectinases, proceedings of an Int. Symp.*, Elsevier, Amsterdam, The Netherlands, **1996**, p. 793-798.
85. Vlugt-Bergmans, v.d. C.J.B.; Meeuwsen, P.J.A.; Voragen, A.G.J. *Appl. Environ. Microbiol.*, **2000**, *66*, 36-41.
86. Herweijer, M.A.; Vincken, J.-P.; Meeuwsen, P.J.A.; Vlugt-Bergmans, v.d.C.J.B.; Beldman, G.; Ooyen, A.J.J.; Voragen, A.G.J. Benen, J.A.E.; Vincken, J.-P.; Alebeek, G.-J.W.M.v. in: Seymour, G.B., Knox, J.P. (eds.) *Pectins and their Manipulation*, Oxford, United Kingdom, **2002**, p.257-266.
87. Colquhoun, I.J.; De Ruiter, G.A.; Schols, H.A.; Voragen, A.G.J. *Carbohydr. Res.*, **1990**, *206*, 131-144.
88. Mutter, M.; Renard, C.M.C.G.; Beldman, G.; Schols, H.A.; Voragen, A.G.J. *Carbohydr. Res.*, **1998**, *311*, 155-164.
89. Mutter, M.; Colquhoun, I.J.; Beldman, G.; Schols, H.A.; Bakx, E.J.; Voragen, A.G.J. *Plant Physiology*, **1998**, *117*, 141-152.
90. Mutter, M.; Colquhoun, I.J.; Schols, H.A.; Beldman, G.; Voragen, A.G.J. *Plant Physiology*, **1996**, *110*, 73-77.
91. Searle-Van Leeuwen, M.J.F.; Van Den Broek, L.A.M.; Schols, H.A.; Beldman, G.; Voragen, A.G.J. *Appl. Microbiol. Biotechnol.*, **1992**, *38*, 347-349.
92. Bonnin, E.; Clavurier, K.; Daniel, S.; Kauppinen, S.; Mikkelsen, J.D.M.; Thibault, J.F. *Carbohydr. Polym.*, **2008**, *74*, 411-418.
93. van de Vis, J.W.; Searle-van Leeuwen, M.J.F.; Siliha, H.A.; Kormelink, F.J.M.; Voragen, A.G.J. *Carbohydr. Polym.*, **1991**, *16*, 167-187.
94. Labavitch, J.M.; Freeman, L.E.; Albersheim, P. *J. Biol. Chem.*, **1976**, *251*, 5904-5910.
95. Lahaye, M.; Vigouroux, J.; Thibault, J.F. *Carbohydr. Polym.*, **1991**, *15*, 431-444.
96. van de Vis, J.W. *PhD thesis*, Wageningen Agricultural University, Wageningen, The Netherlands, **1994**.
97. Hilz, H.; Bakx, E.J.; Schols, H.A.; Voragen, A.G.J. *Carbohydr. Polym.*, **2005**, *59*, 477-488.
98. Verhoef, R.P.; Schols, H.A.; Blanco, A.; Siika-aho, M.; Ratto, M.; Buchert, J.; Lenon, G.; Voragen, A.G.J. *Biotechnol. Bioeng.*, **2005**, *91*, 91-105.
99. Chen, L.M.; Carpita, N.C.; Reiter, W.D.; Wilson, R.H.; Jeffries, C.; McCann, M.C. *Plant Journal*, **1998**, *16*, 385-392.

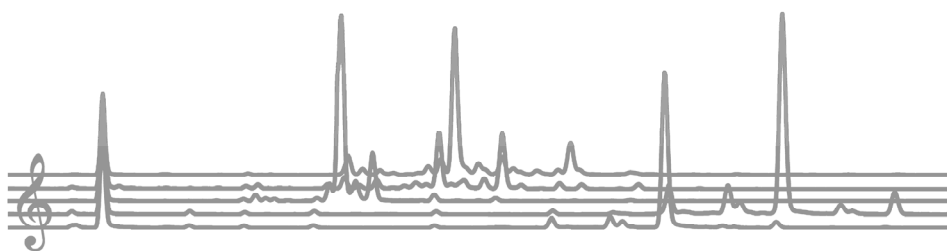
100. Mouille, G.; Robin, S.; Lecomte, M.; Pagant, S.; Hofte, H. *Plant Journal*, **2003**, *35*, 393-404.
101. Capek, P.; Toman, R.; Kardosova, A.; Rosik, J. *Carbohydr. Res.*, **1983**, *117*, 133-140.
102. Voragen, A.G.J.; Schols, H.A.; Pilnik, W. *Food Hydrocolloids*, **1986**, *1*, 65-70.
103. Huisman, M.M.H.; Oosterveld, A.; Schols, H.A. *Food Hydrocolloids*, **2004**, *18*, 665-668.
104. Levigne, S.; Thomas, M.; Ralet, M.C.; Quemener, B.; Thibault, J.F. *Food Hydrocolloids*, **2002**, *16*, 547-550.
105. Ralph, J.; Quideau, S.; Grabber, J.H.; Hatfield, R.D. *J. Chem. Soc. Perkin Trans.*, **1994**, *1*, 3485-3498.
106. Oosterveld, A.; Beldman, G.; Schols, H.A. *Carbohydr. Res.*, **1996**, *288*, 143-153.
107. Englyst, H.N.; Cummings, J.H. *Analyst*, **1984**, *109*, 937-942.
108. Doco, T.; O'Neill, M.A.; Pellerin, P. *Carbohydr. Polym.*, **2001**, *46*, 249-259.
109. De Ruiter, G.A.; Schols, H.A.; Voragen, A.G.J.; Rombouts, F.M. *Anal. Biochem.*, **1992**, *207*, 176-185.
110. Tollier, M.T.; Robin, J.P. *Ann. Technol. Agric.*, **1979**, *28*, 1-15.
111. Dubois, M.; Gilles, K.A.; Hamilton, J.K.; Rebers, P.A.; Smith, F. *Anal. Chem.*, **1956**, *28*, 350-356.
112. Thibault, J.F. *Lebensm. Wiss. Technol.*, **1979**, *12*, 247-251.
113. Sengkhamparn, N.; Verhoef, R.; Schols, H.A.; Sajjaanantakul, T.; Voragen, A.G.J. *Carbohydr. Res.*, **2009**, *344*, 1824-1832.
114. Verhoef, R.; de Waard, P.; Schols, H.A.; Ratto, M.; Siika-aho, M.; Voragen, A.G.J. *Carbohydr. Res.*, **2002**, *337*, 1821-1831.
115. Oosterveld, A.; Beldman, G.; Schols, H.A.; Voragen, A.G.J. *Carbohydr. Res.*, **2000**, *328*, 185-197.
116. Vierhuis, E.; Korver, M.; Schols, H.A.; Voragen, A.G.J. *Carbohydr. Polym.*, **2003**, *51*, 135-148.
117. Colquhoun, I.J.; Ralet, M.C.; Thibault, J.F.; Faulds, C.B.; Williamson, G. *Carbohydr. Res.*, **1994**, *263*, 243-256.
118. Ishii, T.; Ono, H.; Maeda, I. *J. Wood Sci.*, **2005**, *51*, 295-302.
119. Vincken, J.P.; Beldman, G.; Niessen, W.M.A.; Voragen, A.G.J. *Carbohydr. Polym.*, **1996**, *29*, 75-85.
120. Lee, Y.C. *Anal. Biochem.*, **1990**, *189*, 151-162.
121. Zalyalieva, S.V.; Kabulov, B.D.; Akhundzhanov, K.A.; Rashidova, S.S. *Chem. Nat. Compd.*, **1999**, *35*, 1-13.
122. Kabel, M.A.; Schols, H.A.; Voragen, A.G.J. *Carbohydr. Polym.*, **2001**, *44*, 161-165.
123. Bruggink, C.; Maurer, R.; Herrmann, H.; Cavalli, S.; Hoefler, F. *J. Chromatogr. A*, **2005**, *1085*, 104-109.
124. Kabel, M.A.; de Waard, P.; Schols, H.A.; Voragen, A.G.J. *Carbohydr. Res.*, **2003**, *338*, 69-77.

- 125. Goubet, F.; Jackson, P.; Deery, M.J.; Dupree, P. *Anal. Biochem.*, **2002**, *300*, 53-68.
- 126. Kabel, M.A.; Heijnis, W.H.; Bakx, E.J.; Kuijpers, R.; Voragen, A.G.J.; Schols, H.A. *J. Chromatogr. A*, **2006**, *1137*, 119-126.
- 127. Coenen, G.J.; Kabel, M.A.; Schols, H.A.; Voragen, A.G.J. *Electrophoresis*, **2008**, *29*, 2101-2111.
- 128. Daas, P.J.H.; Meyer-Hansen, K.; Schols, H.A.; De Ruiter, G.A.; Voragen, A.G.J. *Carbohydr. Res.*, **1999**, *318*, 135-145.
- 129. Goubet, F.; Morriswood, B.; Dupree, P. *Anal. Biochem.*, **2003**, *321*, 174-182.
- 130. Barton, C.J.; Tailford, L.E.; Welchman, H.; Zhang, Z.N.; Gilbert, H.J.; Dupree, P.; Goubet, F. *Planta*, **2006**, *224*, 163-174.
- 131. Pereira, L. *J. Liq. Chromatogr. Related Technol.*, **2008**, *31*, 1687-1731.
- 132. Hemstrom, P.; Irgum, K. *J. Sep. Sci.*, **2006**, *29*, 1784-1821.

Chapter 2

MALDI-TOF MS and CE-LIF fingerprinting of plant cell wall polysaccharide digests as screening tool for *Arabidopsis* cell wall mutants

Westphal, Y., Schols, H.A., Voragen, A.G.J., Gruppen. H.,
J. Agric. Food Chem., **2010**, 58, 4644-4652.



Abstract

Cell wall materials derived from leaves and hypocotyls of *Arabidopsis* mutant and wild type plants have been incubated with a mixture of pure and well-defined pectinases, hemicellulases, and cellulases. The resulting oligosaccharides have been subjected to MALDI-TOF MS and CE-LIF analysis. MALDI-TOF MS analysis provided a fast overview of all oligosaccharides released, whereas CE-LIF-measurements enabled the separation and characterization of many oligosaccharides under investigation. Both methods have been validated with leaf material of known mutant *Arabidopsis* plants and were shown to be able to discriminate mutant from wild type plants. Downscaling of the MALDI-TOF MS and CE-LIF approaches toward the hypocotyl level was established, and the performance of MALDI-TOF MS and CE-LIF was shown by the successful recognition of the *Arabidopsis* mutant *gaut13* as an interesting candidate for further analysis.

Introduction

Primary plant cell walls of dicotyledonous plants are mainly composed of the polysaccharides cellulose, hemicelluloses (mainly xyloglucan and (glucurono)-arabinoxylans), and pectin (homogalacturonan, rhamnogalacturonan I and II, xylogalacturonan). Knowledge of their biosynthesis is rather incomplete, especially concerning the pectin structures. The elucidation of the biosynthesis of cell wall polysaccharides is nowadays mainly based on comparable analysis of wild type and mutant plants of *Arabidopsis thaliana*¹⁻³. As its genome is known completely and many mutants can be obtained relatively easy, the dicotyledonous plant *A. thaliana* has broadly been accepted as a model plant in plant sciences. The cell wall polysaccharides of *A. thaliana* have been described quite intensively⁴⁻⁶ and are comparable to the ones identified in other dicotyledonous plants (e.g., apple). For further elucidation of the cell wall polysaccharide biosynthesis, the identification of more (new) *Arabidopsis* mutant plants, which differ specifically in the cell wall polysaccharide structure, is necessary.

Sugar composition analysis after extraction of the cell wall material has frequently been used as a screening tool for *Arabidopsis* cell wall mutants⁷. However, due to complete hydrolysis of the polymer, crucial information of the origin and linkage of the various sugars is lost. Fourier transform infrared (FTIR) microspectroscopy is a fast and nondisruptive method, which has been shown to successfully select cell wall mutant *Arabidopsis* hypocotyls⁸. However, no detailed information about the nature of the polysaccharide altered is provided. Other screening techniques are mostly based on enzymatic degradation of a specific polysaccharide followed by analysis of the oligosaccharides released. Such an approach by using matrix-assisted laser desorption/ionization time-of-flight mass spectrometry (MALDI-TOF MS) analysis after enzymatic degradation has been shown to be efficient in selecting *Arabidopsis* mutants, which differ in xyloglucan (XG) oligosaccharides released by xyloglucan specific endo-glucanase (XEG⁹). Recently, the same approach has been described for homogalacturonan (HG) oligosaccharides released by endo-polygalacturonase (PG) and pectin methyl esterase (PME²⁵). The degradation of all enzyme-accessible polysaccharide structures in the cell wall by using a mixture of various cell wall degrading enzymes prior to MALDI-TOF MS analysis to recognize changes in cell wall polysaccharides as well as cell wall architecture has, however, not yet been investigated. In this study we present a multipolysaccharide screening method by using a mixture of 10 pure and well-defined cell wall degrading enzymes followed by MALDI-TOF MS analysis of the oligosaccharides released to enable

the detection of *Arabidopsis* mutants with alterations in any polysaccharide of the whole cell wall. As MALDI-TOF MS detection is based on ionization of the molecule, which is highly dependent on the nature (especially charge) of the molecule, capillary electrophoresis with laser induced fluorescence detection (CE-LIF) has been evaluated as a complementary medium-throughput quantitative screening method. CE-LIF has been described recently to be a suitable method to analyze complex oligosaccharides, enabling the separation and mole-based detection of various cell wall oligosaccharides within 15 min¹⁰⁻¹². This makes it an outstanding method to be used as a medium-throughput quantitative screening method.

Materials and Methods

Plant material

Wild type and mutant leaves (6-12 weeks old) and hypocotyls (4 days old, dark grown) of *A. thaliana* have been kindly provided by partners of the European framework 6 project “WallNet” (Herman Höfte, INRA, Versailles, France; Markus Pauly, University of California, Berkeley, CA, USA; Henrik Scheller, JBEI, Berkeley, CA, USA). All materials have been delivered freeze-dried. An overview of all samples and the various analyses performed are listed in **Table 1**.

Table 1 Overview of the analyses performed for various leaf and hypocotyl materials.

		Background	Leaf material		sugar composition	Hypocotyl material	
			MALDI-TOF MS	CE-LIF		MALDI-TOF MS	CE-LIF
<i>Col0</i>	wild-type		x	x	x	x	x
<i>qrt</i>	wild-type		x	x			
<i>WS</i>	wild-type		x	x			
<i>mur3</i>	XG-altered	<i>Col0</i>	x	x			
<i>xgd1</i>	XGA-deficient	<i>qrt</i>	x	x			
<i>qua1</i>	HG-deficient	<i>WS</i>	x	x			
<i>irx14</i> (SALK 038212)	xylan-deficient	<i>Col0</i>			x	x	x
<i>qua1</i> (SALK 102380)	HG-deficient	<i>Col0</i>			x	x	x
<i>At4g21060</i> (SALK 033674)	not known	<i>Col0</i>			x	x	x
<i>gaut13</i> (SALK 122602)	not known	<i>Col0</i>			x	x	x

Preparation of alcohol insoluble solids (AIS) of leaf material

About 10 g of freeze-dried sample was milled and subsequently extracted with 70% (v/v) aqueous ethanol at 50 °C as described in Hilz et al.¹³. The extraction was repeated twice, and the residue (AIS) was dried after solvent exchange with acetone at ambient temperature.

Preparation of AIS of hypocotyls

Twenty hypocotyls (4 days old, dark grown) were weighed into a reaction vial (1 mL; Alltech Biotechnology, Lexington, KY, USA), and the tissue was destroyed by ball milling in liquid nitrogen (4 min, 3×1 mm stainless steel balls, RetschMillM200, Retsch, Haan, Germany). Subsequently, the material was extracted three times with 70% (v/v) aqueous ethanol at 70 °C (0.75 mL, 2 min ball-milling) followed by centrifugation (1 min, 1500 g, ambient temperature). The residue (AIS) was dried by solvent exchange using acetone at ambient temperature. The whole residue was used for further enzyme treatments.

Enzyme digestion of leaf and hypocotyl materials

Suspensions of 5 mg/mL and 0.02-0.05 mg/100 μ L AIS derived from leaf material and 20 hypocotyls, respectively, were treated with an enzyme cocktail of 10 different enzymes. As buffers, 50 and 10 mM sodium acetate buffers (pH 5.0) for leaves and hypocotyls, respectively, were used. The enzyme cocktail contained α -(1,4)-polygalacturonase (endo-PG, *Kluyveromyces fragilis marxianus*¹⁴), pectin methyl esterase (PME, *Aspergillus niger*), rhamnogalacturonan hydrolase (RGH, *Aspergillus aculeatus*¹⁵), xylogalacturonan hydrolase (XGH, *A. niger*¹⁶), β -(1,4)-galactanase (*A. niger*¹⁷), α -(1,5)-arabinanase (*A. aculeatus*), β -(1,4)-xylanase (*Aspergillus awamori*¹⁸), xyloglucan specific endo-glucanase (XEG, *A. aculeatus*¹⁹), endo-glucanase I and cellobiohydrolase (*Trichoderma viride*²⁰). Enzymes were added in an overdose to ensure that the enzyme reactions reach their end point within 6 h, and the samples were incubated for 22 h at 37 °C. The enzymes were inactivated by boiling the digests for 5 min. Subsequently, the digests were centrifuged (5 min, 1500 g, ambient temperature), and the supernatants were used for MALDI-TOF MS analysis and CE-LIF labeling.

MALDI-TOF MS analysis

The supernatants (10 and 15 μ L for leaves and hypocotyls, respectively) of the enzyme digests were desalted with AG50W-X8 resin (Bio-Rad Laboratories, Hercules, CA, USA). For leaves, one spatula spoon of AG 50W-X8 resin was added to 100 μ L of each enzyme digest and desalting was allowed for ~ 30 min²¹. For hypocotyls, the desalting step has been standardized by always incubating 15 μ L of sample with 10 mg of AG 50W-X8 resin for 60 min. Each desalted sample solution (1 μ L) was mixed on a MALDI plate (Bruker Daltonics, Bremen, Germany) with 1 μ L of matrix solution of 12 mg/mL 2,5-dihydroxybenzoic acid (Bruker Daltonics) in 30% (v/v) acetonitrile and dried under a stream of air²².

MALDI-TOF MS analysis was performed by using an Ultraflex workstation (Bruker Daltonics) equipped with a nitrogen laser of 337 nm and operated in positive mode. After a delayed extraction time of 350 ns, the ions were accelerated to a kinetic energy of 22000 V. The ions were detected using the reflector mode. The lowest laser power required to obtain good spectra was used. The mass spectrometer was calibrated with a mixture of maltodextrins (AVEBE, Foxhol, The Netherlands; average degree of polymerization = 5; mass range m/z 500-2000). Data were processed using flexAnalysis version 2.2 (Bruker Daltonics).

Oligosaccharide separation by capillary electrophoresis and laser induced fluorescence detection (CE-LIF)

To 75 and 30 μL of the non-desalted enzyme digests were added 5 and 2 nmol of maltose as internal standard for leaf and hypocotyl material, respectively. After this solution had been dried (SpeedVac concentrator; Savant ISS110, Thermo Scientific, Waltham, MA, USA), the oligomers were labeled with 9-aminopyrene-1,4,6-trisulfonate (APTS) using the ProteomeLab Carbohydrate Labeling and Analysis Kit (Beckman Coulter, Fullerton, CA, USA). This solution (4 μL) was filled to 50 μL with Millipore water and subsequently diluted with Millipore water, 20 times for the leaf enzyme digests and 10 times for the hypocotyl enzyme digests. The labeled oligosaccharides were separated on a polyvinyl alcohol (NCHO) coated capillary (50 μm ID \times 50.2 cm, detection window after 40 cm; Beckman Coulter) using a ProteomLab PA 800 capillary electrophoresis system, equipped with a laser-induced fluorescence detector (excitation, 488 nm; emission, 520 nm; Beckman Coulter). Samples were loaded hydrodynamically (7 s at 0.5 psi, representing approximately 25 nL sample solution) on the capillary. Separation was carried out in reversed polarity at 30 kV with 25 mM acetate buffer (pH 2.98) containing 0.4% polyethylene oxide and 0.3% formic acid. The capillary was kept at 25 $^{\circ}\text{C}$.

Statistical analysis of MALDI-TOF MS data

From each wild type and mutant leaf material AIS was extracted, and subsequently each AIS was incubated with the enzyme cocktail in triplicate. Every digest was subjected twice to MALDI-TOF MS and for every spot two times 200 shots were taken to exclude interferences due to different crystallization. In total, 12 MALDI-TOF mass spectra per sample were transferred to a statistical program (Grams, Thermo Scientific). Prior to principal component analysis (PCA), the MALDI-TOF mass spectra (m/z 500-2000) were

exported from the flexAnalysis 2.2 software and were preprocessed. For each data point (in total about 66000 points) the absolute logarithm was calculated to receive a normal distribution of the data set. Afterward, a normalization of the data set on the peak XXXG (m/z 1085; xyloglucan heptamer²³) was performed.

Enzyme digests of hypocotyls were obtained from three biological replicates (each 20 hypocotyls). The digests were subjected to MALDI-TOF MS (2 spots each, at least 2 times 200 shots), and the spectra obtained were subjected to PCA as has been described for leaf material.

Sugar composition analysis of hypocotyl material

Ten hypocotyls (4 days old, dark grown) were weighed into a reaction vial (1 mL; Alltech Biotechnology, Lexington, KY, USA). AIS from the hypocotyls was obtained as described earlier. The obtained AIS was incubated with 0.75 mL of 2 M trifluoroacetic acid for 1 h at 121 °C¹, followed by evaporation at ambient temperature. The material obtained was re-dissolved twice with methanol and subsequently dissolved in 0.25 mL of Millipore water. The solution was analyzed with HPAEC-PAD for its sugar composition²⁴.

Results and discussion

MALDI-TOF MS of enzyme digests of wild type *Arabidopsis* plants (*Col0*)

A mixture of 10 pure and well-defined enzymes was used to degrade all enzyme-accessible polysaccharide structures of the cell wall of leaves and hypocotyls derived from *A. thaliana* prior to MALDI-TOF MS analysis. By using such a multi-enzyme-assisted MALDI-TOF MS approach, a fingerprint of all characteristic oligosaccharides released from various enzyme-accessible cell wall polysaccharides becomes visible in a single mass spectrum. This is exemplified in **Figure 1** for wild type leaves (Columbia-0 (*Col0*)) and in **Figure 2** for 4-day-old dark-grown wild type hypocotyls (*Col0*). In **Table 2** a summary of m/z values, which could be annotated to various oligosaccharides, is given. Although some peaks are doubly annotated, for example, m/z 569 can be explained by either a galacturonic acid trimer or a pentose tetramer (**Table 2**, peaks 1 and 36), 80% of the peaks present in the mass spectra are annotated unambiguously.

The most abundant HG oligomers released are GalA₃, GalA₃Me, GalA₄Me, and GalA₅Me₂ (**Figures 1** and **2**, peaks 1, 2, 4, and 9, respectively). Furthermore, some smaller peaks corresponding to HG oligosaccharides are visible in the MALDI-TOF mass spectra (**Figures 1** and **2**, peaks 7, 10, 11, and 15). These m/z values can be annotated either as multiple methyl-esterified HG oligosaccharides or as acetylated HG oligosaccharides. In contrast to Obel and co-workers²⁵, we prefer to interpret the annotation of these peaks as oligosaccharides having one acetyl group attached (**Table 2**) rather than as multiple methyl-esterified oligosaccharides (e.g., GalA₄AcMe rather than GalA₄Me₄), because the endo-PG used is hindered in its action by methyl esters¹⁴. Comparison of the mass spectra of leaves

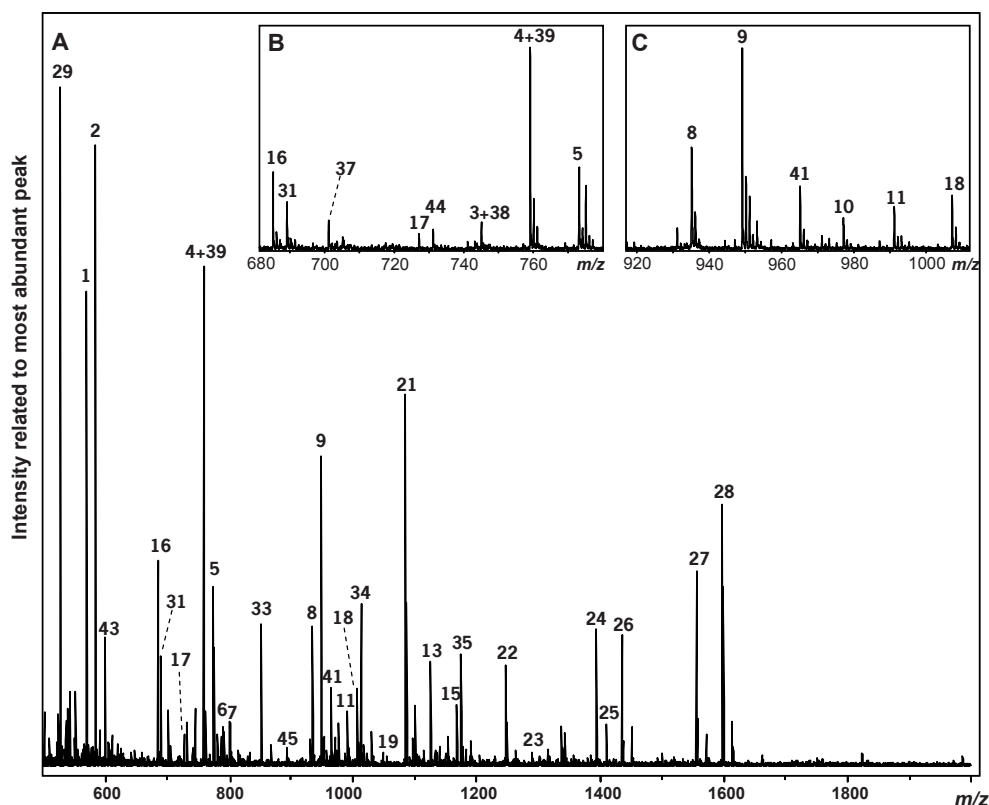


Figure 1 MALDI-TOF mass spectrum of *Col0* leaf material after digestion with the enzyme cocktail: (A) m/z 500-2000; (B) zoom of m/z 680-780; (C) zoom of m/z 920-1010. Given numbers correspond to oligosaccharides as described in **Table 2**.

Table 2 Possible degradation products after digestion with the enzyme cocktail^a

peak	m/z	annotation [M+Na] ⁺	peak	m/z	annotation [M+Na] ⁺
Oligomers released from homogalacturonan by endo-PG and PME			Oligomers released from β-(1,4)-galactan by β-(1,4)-galactanase		
1	569	GalA ₃	29	527	Gal ₃
2	583	GalA ₃ Me	30	629	Gal ₂ Ara ₂
3	745	GalA ₄	31	689	Gal ₄
4	759	GalA ₄ Me	32	791	Gal ₃ Ara ₂
5	773	GalA ₄ Me ₂	33	851	Gal ₅
6	787	GalA ₄ Me ₃ and/or GalA ₄ Ac	34	1013	Gal ₆
7	801	GalA ₄ MeAc	35	1175	Gal ₇
8	935	GalA ₅ Me	Oligomers released from β-(1,4)-xylan by β-(1,4)-xylanase and α-(1,5)-arabinan by α-(1,5)-arabinanase		
9	949	GalA ₅ Me ₂	36	569	Ara ₄ and/or Xyl ₄ and/or mixtures
10	977	GalA ₅ Me ₄ and/or GalA ₅ MeAc	37	701	Ara ₅ and/or Xyl ₅ and/or mixtures
11	991	GalA ₅ Me ₂ Ac	38	745	Xyl ₄ GlcA
12	1097	GalA ₆	39	759	Xyl ₄ GlcAME and/or Xyl ₃ RhaGalA
13	1125	GalA ₆ Me ₂	40	833	Ara ₆ and/or Xyl ₆ and/or mixtures
14	1153	GalA ₆ Me ₄ and/or GalA ₆ MeAc	41	965	Ara ₇ and/or Xyl ₇ and/or mixtures
15	1167	GalA ₆ Me ₅ and/or GalA ₆ Me ₂ Ac	42	1097	Ara ₈ and/or Xyl ₈ and/or mixtures
Oligomers released from rhamnogalacturonan by RGH			Mixed oligosaccharides (pentoses and hexoses)		
16	685	(Rha-GalA) ₂	43	599	P ₃ H ₁
17	727	(Rha-GalA) ₂ Ac	44	731	P ₄ H ₁
18	1007	(Rha-GalA) ₃	45	893	P ₄ H ₂
19	1049	(Rha-GalA) ₃ Ac	46	1055	P ₄ H ₃
Oligomers released from xylogalacturonan by XGH					
20	525	GalA ₂ Xyl			
Oligomers released from xyloglucan by XEG					
21	1085	XXXG			
22	1247	X[XL]G			
23	1289	X[XL]G + Ac			
24	1393	X[XF]G			
25	1409	XLLG or X[XF]G			
26	1435	X[XF]G + Ac			
27	1555	X[LF]G			
28	1597	X[LF]G + Ac			

^a GalA, galacturonic acid; GlcA, glucuronic acid; Rha, rhamnose; H, hexose; P, pentose; Ara, arabinose; Xyl, xylose; Ac, acetyl group; Me, methyl ester; xyloglucan nomenclature according to Fry et al.²³.

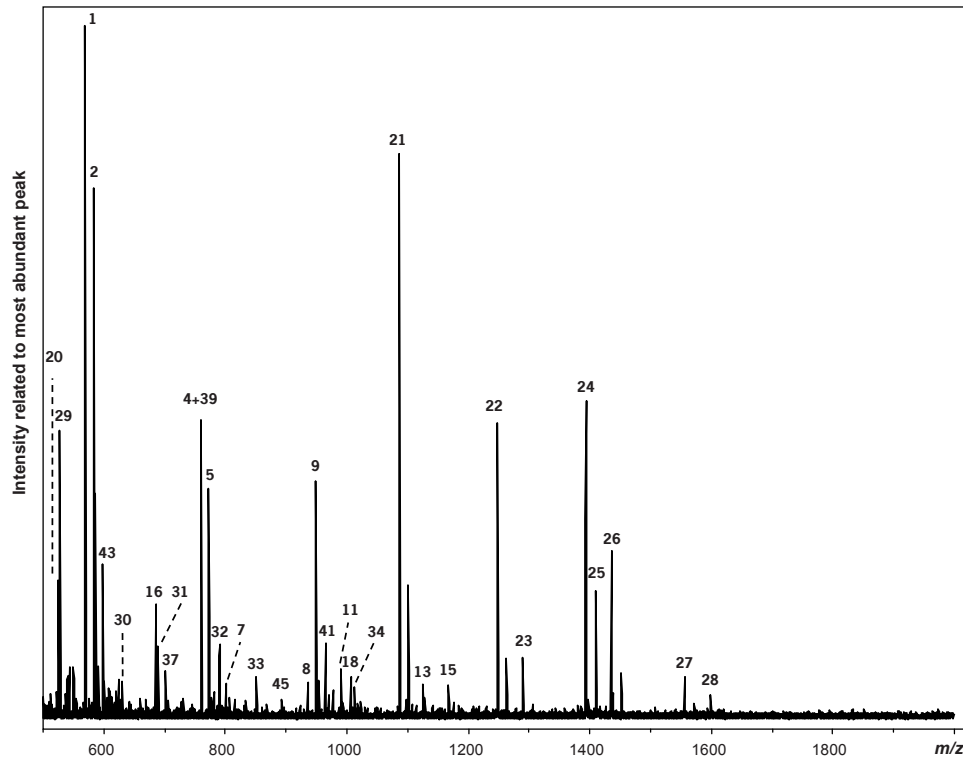


Figure 2 MALDI-TOF mass spectrum of *Col0* hypocotyls after digestion with the enzyme cocktail. Given numbers correspond to oligosaccharides as described in **Table 2**.

and hypocotyls reveals that there are clear changes within the HG oligosaccharides released (**Figures 1** and **2**). Especially the relative abundances of the low methyl-esterified oligosaccharides (peaks 2, 4, 8, and 9; normalized to GalA₃ (peak 1)) are higher in leaves compared to hypocotyls. The most abundant RG-I oligosaccharides released are (Rha-GalA)₂ and (Rha-GalA)₃ (**Figures 1** and **2**, peaks 16 and 18). Traces of acetylated RG-I oligosaccharides (**Figures 1** and **2**, peaks 17 and 19) could be detected as well. In agreement with Zandleven and co-workers no peaks corresponding to xylogalacturonan (XGA) oligosaccharides could be identified in *Col0* leaf digest, because XGH is not active on the XGA present in the AIS of *Arabidopsis* leaves⁴. In contrast to the *Col0* leaf digest, in *Col0* hypocotyls the XGA oligosaccharide GalA₂Xyl (**Figure 2**, peak 20) could be annotated, indicating a substantial difference of the XGA present in hypocotyls compared to XGA in leaves. Enzymes degrading rhamnogalacturonan II (RG-II), representing 8% of the cell wall material of *Col0* leaves^{5,26}, are not yet available. To degrade the side chains of

RG-I, α -(1,5)-arabinanase and β -(1,4)-galactanase have been added to the enzyme mixture. β -(1,4)-Xylanase has been included to enable the identification of possible xylan mutants²⁷. In **Figures 1** and **2** several m/z values, which can be annotated to either arabinan-, (arabino)-galactan or (arabino)-xylan oligosaccharides, have been identified, for example, m/z 569, 629, 701, and 791 (**Figures 1** and **2**, peaks 36, 30, 37, and 32, respectively). Due to the addition of XEG to the enzyme mixture, the XG oligosaccharides released could be recognized by MALDI-TOF MS (**Figures 1** and **2**, peaks 21-28) as described before⁹. The relative abundances of the individual XG oligosaccharides released from *Arabidopsis* leaves differ compared to data from the literature^{9,29}, which can most likely be explained by different extraction techniques as well as by the use of an enzyme cocktail within this research. It can be hypothesized that the use of pectinases and cellulases in combination with XEG liberates XG moieties, which are tightly bound to cellulose and/or pectin²⁸. By comparison of the relative abundance of the XG oligosaccharides in *Col0* hypocotyl digests to the ones in *Col0* leaf digests, clear differences can be observed. Apparently, the XLFG oligosaccharide (peak 27) is substantially less abundant, whereas the X[XL]G and XXFG oligosaccharides (peaks 22 and 24, respectively) are more abundant in *Col0* hypocotyl digests (**Figures 1** and **2**). Additionally, the level of acetylated XG oligosaccharides (XXFG and XLFG, peaks 26 and 28, respectively) appears to be lower in hypocotyls than in leaf tissue. All enzyme-accessible polysaccharides are represented by oligosaccharides in a single MALDI-TOF mass spectrum as demonstrated for *Col0* leaves and hypocotyls, respectively. Hence, this MALDI-TOF MS method after digestion of *Arabidopsis* tissue with a mixture of 10 pure and well-defined enzymes gives a good fingerprint of the complete enzyme-accessible *Arabidopsis* cell wall, which qualifies this method to be used for screening of *Arabidopsis* plants or even other dicotyledonous plants.

PCA of mass spectra of known mutant *Arabidopsis* leaf digests for method validation

The enzyme cocktail was subjected to AIS of leaves from various *Arabidopsis* wild type and known mutant plants, namely, *mur3*, *qual*, and *xgd1*, and their corresponding wild type plants as given in **Table 1**. The mutant plant *mur3* is described to have an altered XG structure²⁹, whereas *qual* and *xgd1* have altered pectic structures (*qual*, HG deficient^{2,30}; *xgd1*, XGA deficient³¹). As all of the mutant plants were grown in different wild type backgrounds (used within the EU project “WallNet”), the different wild type plants were included in the analysis resulting in the following pairs: *Col0-mur3*, quartet (*qrt*)-*xgd1*, and

Wassilewskija (*WS*)-*qual*. All MALDI-TOF mass spectra were subjected to PCA, resulting in a total variance of 65% (PC1 and PC2). This value is acceptable when taking into account that the whole MALDI-TOF mass spectra (with 66000 data points each) were used to perform PCA. The results of the PCA performed are presented in **Figure 3A** by plotting PC1 against PC2. In the lower left quadrant of the graph all wild type plants cluster (*Col0* (○), *qrt* (□), and *WS* (+)), whereas the mutants under investigation cluster either in the upper right quadrant (*mur3* (◆) and *qual* (△)) or in the lower right quadrant (*xgd1* (*)). In **Figure 3B-D** we highlighted the mutant-wild type pairs *Col0-mur3*, *qrt-xgd1*, and *WS-qual*, respectively. It can be seen that PCA results in the distinction of all mutant

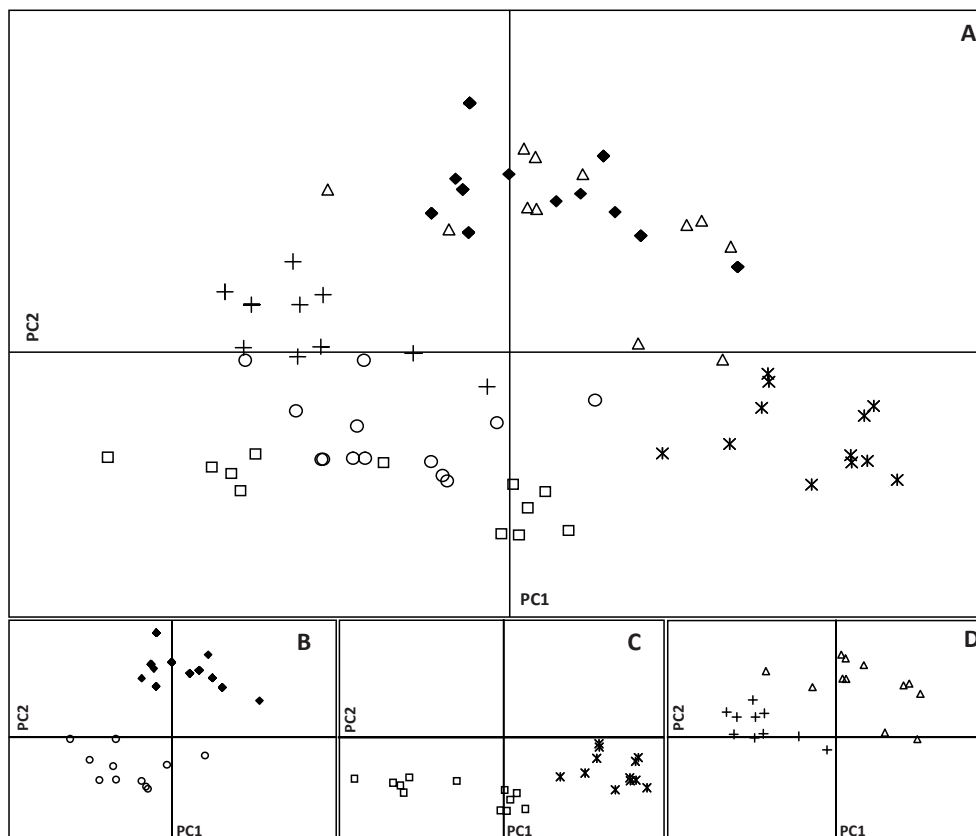


Figure 3 Principal component analysis of MALDI-TOF mass spectra of different wild type and mutant leaf materials after digestion with the enzyme cocktail: (A) all data points; (B) *Col0-mur3*; (C) *qrt-xgd1*; (D) *WS-qual*; (○) *Col0*; (◆) *mur3*; (□) *qrt*; (*) *xgd1*; (+) *WS*; (△) *qual*.

Arabidopsis plants from their corresponding wild type plants. Even the three different wild type plants (*Col0*, *qrt*, and *WS*) clustered mainly in three distinct clouds (**Figure 3A**), although a complete distinction could not be achieved. Due to this partial distinction between different wild type plants, analysis of the corresponding wild type plant in combination with the mutant plant is always required in the screening for *Arabidopsis* mutants.

PCA of mass spectra of known mutant *Arabidopsis* hypocotyl digests for method validation

Much research in plant sciences is performed with *Arabidopsis* hypocotyls because they can be obtained quickly and strongly defected mutants may not even reach the leaf state. Thus, after the successful distinction of all (known) mutant leaf materials as described above, the multienzyme-assisted MALDI-TOF MS screening method has been downscaled to hypocotyls. The use of twenty 4-day-old dark-grown hypocotyls for each enzyme digest and the analysis of three independent grown biological replicates ensure a good representation of every mutant plant²⁵. Due to much less material available when working with hypocotyls, we observed that the MALDI-TOF MS measurements became much more sensitive to external influences such as salts and matrix effects. Especially the ratio between the XG and HG oligosaccharides appeared to be very sensitive toward small differences in sample preparation. Therefore, some general requirements had to be defined for the data processing of the mass spectra obtained. First, mass spectra were excluded from further data processing when peaks, which were annotated as the potassium adduct of a component, account for > 40% of the sodium adduct as this is a sign of incorrect desalting. Second, the data processing excludes data points below m/z 568 as peaks originating from the DHB matrix ($m/z < 550$) were not reproducible and disturbed the PCA substantially. Third, all mass spectra, which were subjected to PCA, had to be analyzed parallel as inter-day differences were visible in PCA, even though a standardized desalting step within the sample preparation procedure was introduced to minimize this effect. The PCAs, which were performed on different days with the same hypocotyl material, showed independently the same distinction between the mutant and corresponding wild type hypocotyls. Therefore, the use of this modified MALDI-TOF MS method has been explored to be used as screening method for *Arabidopsis* hypocotyls. Four mutant hypocotyls have been chosen for analysis: *gaut13*³², the β -(1,4)-xylan-deficient *irx14*²⁷, the HG-deficient *qual*², and the

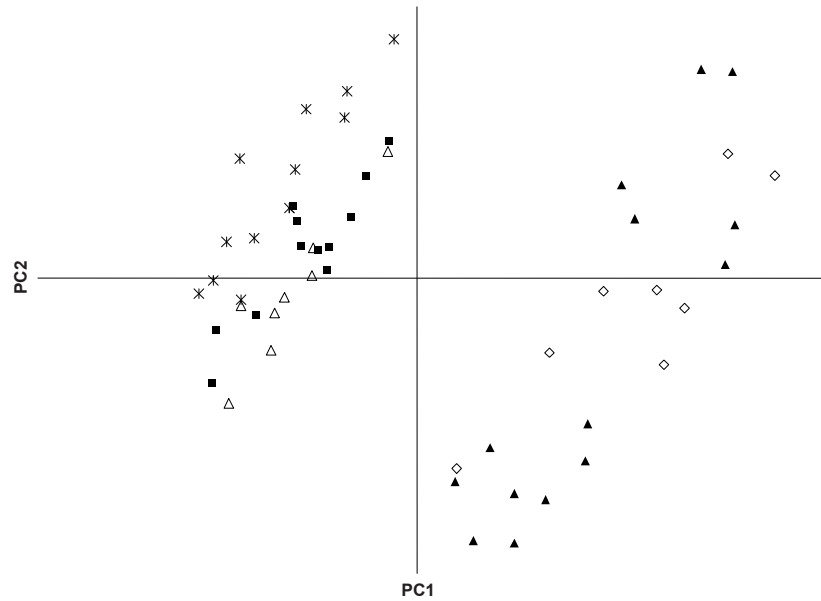


Figure 4 Principal component analysis of MALDI-TOF mass spectra of wild type (*Col0*) and mutant *Arabidopsis* hypocotyls after digestion with the enzyme cocktail: (◇) *Col0*; (■) *irx14*; (*) galactose-deficient mutant (At4g21060); (△) *gaut13*; (▲) *qual*.

mutant line SALK 033674, which lacks the gene At4g21060 (**Table 1**). Whereas the chemical composition of the mutants *irx14* and *qual* has been described earlier (at least for leaf material), no or hardly any cell wall analysis has been performed for *gaut13* and the mutant line SALK 033674 (At4g21060). In **Table 3** the results of the sugar composition analysis (mol %) of the four mutant hypocotyls is presented. The sugar composition

Table 3 Sugar composition of hypocotyls of different mutant lines after hydrolysis with TFA analyzed with HPAEC-PAD^a

	Fuc	Ara	Rha	Gal	Glc	Xyl	Man	GalA	GlcA
	[mol%]								
<i>Col0</i>	2	16	5	19	13	15	2	26	1
<i>gaut13</i> (SALK 122602)	2	14	5	18	9	15	3	32	1
<i>At4g21060</i> (SALK 033674)	2	15	5	17	13	16	3	29	1
<i>irx14</i> (SALK 038212)	2	16	6	18	11	12	2	32	1
<i>qual</i> (SALK 102380)	2	16	4	18	23	14	2	21	1

^a *Col0*, n = 7; SALK 102380 (*qual*), n = 4; SALK 122602 (*gaut13*), n = 3; SALK 038212 (*irx14*), n = 3; and SALK 033674, n = 3.

analysis of *qual* (hypocotyls from the SALK line 102380; *Col0* background) and *irx14* (SALK 038212; *Col0* background) is in good agreement with experiments performed earlier (significant decrease of galacturonic acid and xylose, respectively^{2,27}). The sugar composition of the mutant line SALK 033674 (At4g21060) shows a significant decrease of galactose without a significant change of any other monosaccharide (**Table 3**). The *gaut13* hypocotyls (SALK line 122602; *Col0* background) showed a significant increase in galacturonic acid, which was recently also found for *gaut13* inflorescences and stems³³. This is in good agreement with the literature predicting *gaut13* to be involved in pectic biosynthesis³². In **Figure 4** the PCA of the mass spectra of the mutant and wild type hypocotyl enzyme digests has been plotted, and it can be seen that *irx14* (■), *gaut13* (△), and At4g21060 (SALK 033674 (*)) are clearly separated from the corresponding wild type hypocotyls (*Col0* (◇)). The *qual* (▲) mutant clusters with the wild type *Col0*, which is in disagreement with FTIR studies, in which the *qual* mutant hypocotyls were distinguished from the wild type hypocotyls^{8,34}. A possible explanation for this deviant behavior could be that the enzyme-accessible part of HG is not (yet) affected in 4-day-old *qual* hypocotyls.

Detailed analysis of the oligosaccharides released after enzyme treatment to identify possibly altered polysaccharide(s)

After successful distinction of the wild type and mutant *Arabidopsis* leaves and hypocotyls by PCA, the mass spectra obtained by the MALDI-TOF MS screening method as well as CE-LIF analysis (see below) were evaluated to enable the identification of the altered structure(s) within the mutant tissue.

Interpretation of the mass spectra of the wild type and known mutant leaf digests

In **Figure 5** typical mass spectra of the wild type and mutant leaf materials analyzed are given. In the mass spectrum of *mur3* the peaks of (acetylated) XXFG and XLFG (**Figure 5B**, peaks 24 and 26-28, respectively) are absent, whereas the intensity of the peaks XXXG and X[XL]G (peaks 21-22) is increased compared to the wild type plant (*Col0*; **Figure 5A**).

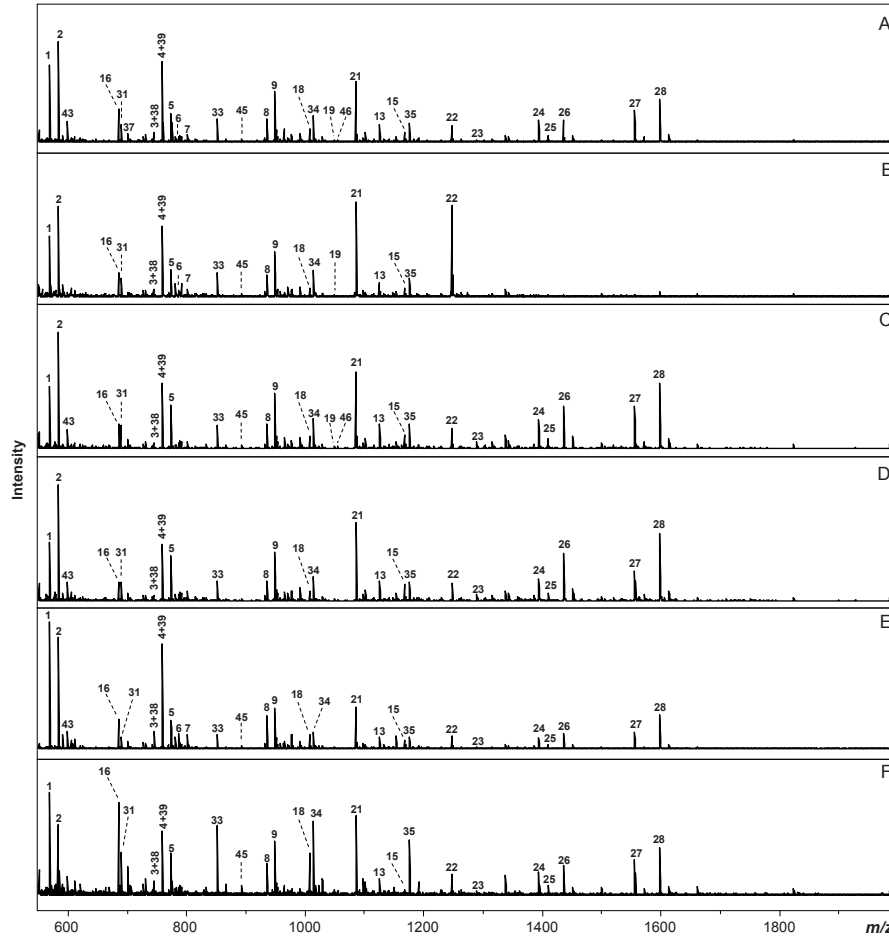


Figure 5 MALDI-TOF mass spectra of different wild type and mutant *Arabidopsis* leaf materials after AIS extraction and digestion with the enzyme cocktail: (A) *Col0*; (B) *mur3*; (C) *qrt*; (D) *xgd1*; (E) *WS*; (F) *qual*. Annotation of oligosaccharides based on m/z values; given numbers correspond to oligosaccharides as described in **Table 2**.

Both observations are in good agreement with the literature describing *mur3* to lack the fuco-galactosyl structures²⁹. Obviously, MALDI-TOF MS is not suitable to distinguish XLXG and XXLG, because these structures have the same m/z values (1247). Thus, the increase of XLXG and decrease of XXLG described before²⁹ cannot be observed by MALDI-TOF MS. Besides the XG alteration, the rest of the oligosaccharides released, including HG, RG-I, and (arabino)-galactan oligosaccharides, remain the same (**Figure 5A,B**). The *xgd1* mutant has been grown in *qrt* background, which is a *Col0* plant

differing in a gene encoding a pectin methyl esterase³⁵. By comparison of the mass spectra of the two different wild type plants *Col0* and *qrt* (**Figure 5A,C**), it can be seen that the signal intensities of the methyl-esterified HG oligosaccharides (**Figure 5A-C**, peaks 2 and 5) are increased when normalized to GalA₃ (peak 1), which is in good agreement with earlier data³⁵. The differences between the mass spectra of the mutant *xgd1* and its wild type *qrt* are minimal. These results were expected as *xgd1* is deficient in XGA and the enzyme XGH is not active on AIS of *Arabidopsis* leaf material⁴. Nevertheless, the performed PCA of the MALDI-TOF mass spectra could distinguish between *xgd1* and *qrt* (**Figure 3**), most likely on the basis of the different levels of acetylation of the XG oligosaccharides (**Figure 5C,D**; ratio of peak 26 to 24 and peak 28 to 27). In the mass spectrum of *qual* (**Figure 5F**) a clear decrease in the relative abundance of the HG oligosaccharides released can be observed compared to the corresponding wild type leaf material (**Figure 5E,F**, GalA₃-GalA₅, with and without methyl esters (peaks 2, 4, 5, 8, 9; ratios of these peaks toward peak 1)), which is in good agreement with the earlier described HG deficiency². The RG-I oligosaccharides (including side chains thereof) and XG oligosaccharides seem to remain unaffected.

Thus, this multi-enzyme-assisted MALDI-TOF MS high-throughput screening method is also capable of giving directions for further detailed analysis by pointing to specific altered polysaccharides, but, obviously, it must be kept in mind that MS is not capable of distinguishing between two different components with the same *m/z* values, as has been shown for XXLG and XLXG in the *mur3* mutant. Furthermore, the ionization in MALDI-TOF MS analysis depends on the charge of the oligosaccharides. Thus, drawing conclusions by comparing the relative abundances of different groups of oligosaccharides such as neutral and acidic oligosaccharides with each other might not result in correct data. Therefore, another sensitive method able to quantify the oligosaccharides released might be suitable for complementary analysis. Recently, CE-LIF analysis has been shown to enable the separation and mole-based quantification of complex oligosaccharide structures in a short time requiring only very low amounts of sample¹⁰⁻¹². This indicates that CE-LIF enables the measurement of leaf and hypocotyl digests, even though only very low amounts of sample might be present.

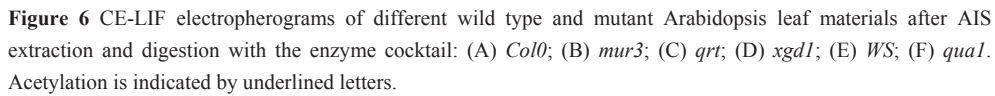
Therefore, CE-LIF analysis has been evaluated as medium-throughput screening method for *Arabidopsis* leaves and hypocotyls to provide complementary data, using the same enzyme digests, which were used for MALDI-TOF MS measurements. As we start with the same enzyme digest, the extra time for CE-LIF analysis is reduced to the labeling of the

oligosaccharides present after enzyme incubation (~ 100 samples/day) and the analysis time itself (15-20 min/sample).

CE-LIF analysis of wild type and known mutant leaf material

In **Figure 6** are given the electropherograms of the various enzyme digests of the leaf materials. Even though complete annotation of all oligosaccharides released has not been achieved, many of the main degradation products could be identified using the literature^{11,36}. Although not further described in this paper, a first exploration of CE-(LIF-) MS¹² seems to be extremely useful for further improvement of the analysis of *Arabidopsis* digests. Due to the unexpected α -amylase side activity in the enzyme cocktail (e.g., the presence of maltotriose), the added maltose could be used as a mobility marker, but proved to be an unreliable internal standard.

For *Col0* leaf material it was calculated that about 20-25% of the cell wall polysaccharides were released as oligosaccharides (degree of polymerization (DP) of 2-12). The main peak in all enzyme digests is cellobiose (4.70 min; about 30% of the identified oligosaccharides for *Col0* leaves), which results from cellulose degradation by endoglucanase I and cellobiohydrolase. HG oligosaccharides elute earlier than neutral oligosaccharides as has been indicated in **Figure 6** (GalA₁₋₃, 4.30, 4.48, and 4.86 min, respectively). For *Col0* leaves about 10% of the oligosaccharides released can be accounted for by GalA₁₋₃. RG-I and XG oligosaccharides elute significantly later (5.62 min (Rha-GalA)₂ and 6.4-7.6 min (XXXG, XXLG+XXLG, XXFG+XXFG, XLFG+XLFG; acetylation indicated by underlined letter), respectively) with nonacetylated and monoacetylated XG oligosaccharides coeluting within CE-LIF analysis³⁶. Whereas MALDI-TOF MS analysis of *Arabidopsis* leaf materials (**Figure 5A**) indicated a relatively high amount of HG oligosaccharides compared to XG oligosaccharides, CE-LIF (**Figure 6A**) analysis reveals that MALDI-TOF MS analysis is overestimating the amount of HG oligosaccharides released, especially when the mole-based detection is taken into account.



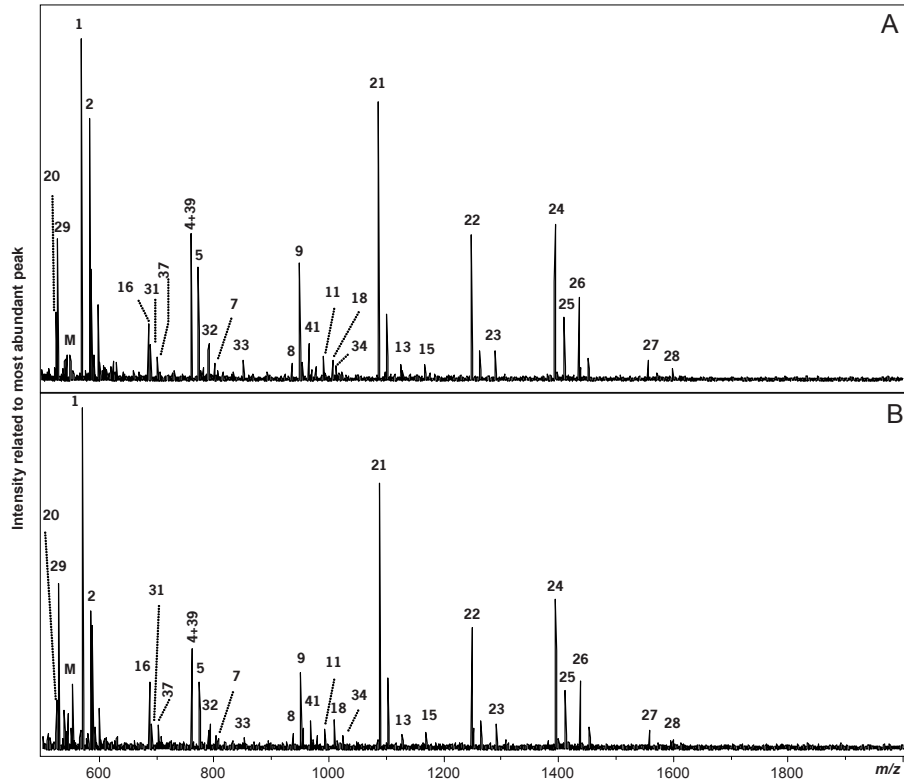


Figure 7 MALDI-TOF mass spectra of (A) *Col0* and (B) *gaut13* hypocotyls after AIS extraction and digestion with the enzyme cocktail. Annotation of oligosaccharides based on m/z values; given numbers correspond to oligosaccharides as described in **Table 2**.

CE-LIF analysis of *mur3* leaves (**Figure 6B**) shows clearly the absence of XXFG and XLFG, which confirms the MALDI-TOF MS results. Furthermore, although not visible in MALDI-TOF MS analysis, an 18-fold increase of XLXG and a 14-fold decrease of XXLG can be observed in the electropherogram of *mur3*. No variation in any other oligosaccharide was detected, as predicted by MALDI-TOF MS analysis. CE-LIF analysis of *qrt* and *xgd1* leaves did not show any significant differences between both enzyme digests (**Figure 6C,D**), besides an increase in galacturonic acid (GalA) in *xgd1* leaves, which cannot be explained yet. The differences between *WS* and *qual* leaves are obvious in the CE-LIF electropherograms (**Figure 6E,F**), and especially the amount of oligosaccharides released from the enzyme-accessible HG is reduced substantially (GalA1-4, -69%, -86%, -87%, and -85%, respectively). The RG-I and XG oligosaccharides are much less affected,

which is in good agreement with the MS results (**Figure 5E,F**). In addition, the amount of cellobiose is decreased (-37%, data not shown), indicating that the *qual* mutation affects not only the pectin moiety but as well cellulose or even the whole cell wall architecture.

MALDI-TOF MS and CE-LIF analysis of *Col0* and *gaut13* hypocotyl material

To exemplify the potential of MALDI-TOF MS and CE-LIF analysis performed for further identification of deviating structures within mutant *Arabidopsis* hypocotyls, the MALDI-TOF mass spectra and CE-LIF electropherograms of *gaut13* and its corresponding wild type *Col0*, as presented in **Figures 7** and **8**, are discussed. Both CE-LIF and MALDI-TOF MS analysis revealed that the XG oligosaccharides released by enzyme treatment are similar in *gaut13* and *Col0* hypocotyls as the ratios of these XG oligosaccharides to each other remain constant (**Figures 7** and **8**). Furthermore, MALDI-TOF MS analysis revealed that in *gaut13* hypocotyls fewer galacturonic acid oligomers of higher DP (DP 4-5) are released compared to GalA₃ (peaks 4 and 9 compared to peak 1; **Figure 7**), which was confirmed by CE-LIF analysis (**Figure 8A,B**). Opposite to the GalA₄, GalA₁₋₃ are slightly increased in *gaut13* enzyme digest as can be observed in the CE-LIF electropherograms (**Figure 8A,B**). In addition, fewer methyl-esterified HG oligosaccharides are released from *gaut13* hypocotyls compared to *Col0* hypocotyls as can be seen in MALDI-TOF-MS (peaks 2 and 5 compared to peak 1; **Figure 7**). In total, these results could indicate either a different degree of methyl esterification of the HG present and/or another distribution of these methyl esters for the *gaut13* hypocotyls. Cellobiose (4.70 min) and cellotriose (5.12 min) are more abundant in *gaut13* hypocotyls compared to *Col0* hypocotyls, whereas unknown peaks at 5.35 and 6.75 min are not (or much less) present in *gaut13* (**Figure 8**).

In conclusion, this research demonstrated the potential of a multi-enzyme-assisted MALDI-TOF MS screening method for the recognition of altered cell wall polysaccharide structures. In addition, CE-LIF analysis has been shown to be a suitable method for the detailed analysis of cell wall polysaccharide derived oligosaccharides, whereas also quantitative data on oligosaccharide levels could be obtained. Even though only a very low amount of, for example, hypocotyls was presented, CE-LIF showed to be much less affected by matrix or salt effects. The accuracy of such quantification will increase when an internal standard, other than maltose, is used.

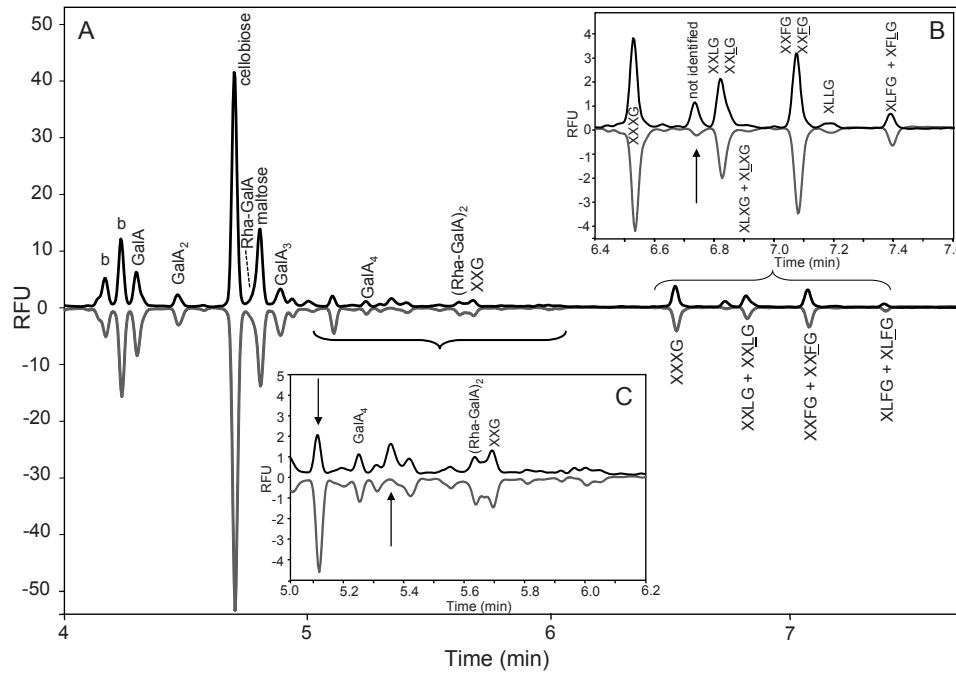


Figure 8 CE-LIF electropherograms of *Col0* and *gaut13* hypocotyls (A) after AIS extraction and digestion with the enzyme cocktail: *Col0* (upper line), *gaut13* (lower line); (B) zoom of 6.4-7.6 min, (C) zoom of 5.0-6.2 min. Acetylation is indicated by underlined letters. Arrows indicate differences between *Col0* and *gaut13*.

The combination of techniques was used to screen for *Arabidopsis* mutants, and it is anticipated that this approach could also be used to analyze (changed) cell wall polysaccharide structures in other (dicotyledonous) plant materials.

Acknowledgements

We thank Herman Höfte, Markus Pauly, and Henrik Scheller for growing various wild type and mutant *Arabidopsis* tissues as well as for the fruitful discussions during WallNet project meetings.

References

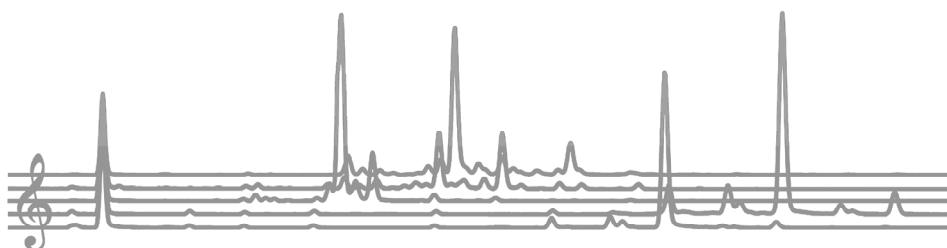
1. Harholt, J.; Jensen, J.K.; Sorensen, S.O.; Orfila, C.; Pauly, M.; Scheller, H.V. *Plant Physiology*, **2006**, *140*, 49-58.
2. Bouton, S.; Leboeuf, E.; Mouille, G.; Leydecker, M.T.; Talbotec, J.; Granier, F.; Lahaye, M.; Hofte, H.; Truong, H.N. *Plant Cell*, **2002**, *14*, 2577-2590.
3. Pauly, M.; Eberhard, S.; Albersheim, P.; Darvill, A.; York, W.S. *Planta*, **2001**, *214*, 67-74.
4. Zandleven, J.; Sorensen, S.O.; Harholt, J.; Beldman, G.; Schols, H.A.; Scheller, H.V.; Voragen, A.J. *Phytochemistry*, **2007**, *68*, 1219-1226.
5. Zablackis, E.; Huang, J.; Muller, B.; Darvill, A.G.; Albersheim, P. *Plant Physiology*, **1995**, *107*, 1129-1138.
6. Ralet, M.C.; Crépeau, M.J.; Lefebvre, J.; Mouille, G.; Hofte, H.; Thibault, J.F. *Biomacromolecules*, **2008**, *9*, 1454-1460.
7. Reiter, W.D.; Chapple, C.; Somerville, C.R. *Plant Journal*, **1997**, *12*, 335-345.
8. Mouille, G.; Robin, S.; Lecomte, M.; Pagant, S.; Hofte, H. *Plant Journal*, **2003**, *35*, 393-404.
9. Lerouxel, O.; Choo, T.S.; Seveno, M.; Usadel, B.; Faye, L.; Lerouge, P.; Pauly, M. *Plant Physiology*, **2002**, *130*, 1754-1763.
10. Kabel, M.A.; Heijnis, W.H.; Bakx, E.J.; Kuijpers, R.; Voragen, A.G.J.; Schols, H.A. *J. Chromatogr. A*, **2006**, *1137*, 119-126.
11. Coenen, G.J.; Kabel, M.A.; Schols, H.A.; Voragen, A.G.J. *Electrophoresis*, **2008**, *29*, 2101-2111.
12. Albrecht, S.; van Muiswinkel, G.C.J.; Schols, H.A.; Voragen, A.G.J.; Gruppen, H. *J. Agric. Food. Chem.*, **2009**, *57*, 3867-3876.
13. Hilz, H.; Bakx, E.J.; Schols, H.A.; Voragen, A.G.J. *Carbohydr. Polym.*, **2005**, *59*, 477-488.
14. Daas, P.J.H.; Meyer-Hansen, K.; Schols, H.A.; De Ruiter, G.A.; Voragen, A.G.J. *Carbohydr. Res.*, **1999**, *318*, 135-145.
15. Schols, H.A.; Voragen, A.G.J. *Carbohydr. Res.*, **1994**, *256*, 83-95.
16. Beldman, G.; Vincken, J.P.; Schols, H.A.; Meeuwsen, P.J.A.; Herweijer, M.; Voragen, A.G.J. *Biocatal. Biotransform.*, **2003**, *21*, 189-198.
17. van de Vis, J.W.; Searle-van Leeuwen, M.J.F.; Siliha, H.A.; Kormelink, F.J.M.; Voragen, A.G.J. *Carbohydr. Polym.*, **1991**, *16*, 167-187.
18. Kormelink, F.J.M.; Searle-van Leeuwen, M.J.E.; Wood, T.M.; Voragen, A.G.J. *J. Biotechnol.*, **1993**, *27*, 249-265.
19. Pauly, M.; Andersen, L.N.; Kauppinen, S.; Kofod, L.V.; York, W.S.; Albersheim, P.; Darvill, A. *Glycobiology*, **1999**, *9*, 93-100.
20. Beldman, G.; Searle-Van Leeuwen, M.F.; Rombouts, F.M.; Voragen, F.G. *Eur. J. Biochem.*, **1985**, *146*, 301-308.

21. Sengkhamparn, N.; Bakx, E.J.; Verhoef, R.; Schols, H.A.; Sajjaanantakul, T.; Voragen, A.G.J. *Carbohydr. Res.*, **2009**, *344*, 1842-1851.
22. Verhoef, R.; Beldman, G.; Schols, H.A.; Siika-Aho, M.; Ratto, M.; Buchert, J.; Voragen, A.G.J. *Carbohydr. Res.*, **2005**, *340*, 1780-1788.
23. Fry, S.C.; York, W.S.; Albersheim, P.; Darvill, A.; Hayashi, T.; Joseleau, J.P.; Kato, Y.; Lorences, E.P.; MacLachlan, G.A.; McNeil, M.; Mort, A.J.; Reid, J.S.G.; Seitz, H.U.; Selvendran, R.R.; Voragen, A.G.J.; White, A.R. *Physiol. Plant.*, **1993**, *89*, 1-3.
24. Sengkhamparn, N.; Verhoef, R.; Schols, H.A.; Sajjaanantakul, T.; Voragen, A.G.J. *Carbohydr. Res.*, **2009**, *344*, 1824-1832.
25. Obel, N.; Erben, V.; Schwarz, T.; Kuhnle, S.; Fodor, A.; Pauly, M. *Mol. Plant.*, **2009**, *2*, 922-932.
26. O'Neill, M.A.; Eberhard, S.; Albersheim, P.; Darvill, A.G. *Science*, **2001**, *294*, 846-849.
27. Brown, D.M.; Goubet, F.; Wong, V.W.; Goodacre, R.; Stephens, E.; Dupree, P.; Turner, S.R. *Plant Journal*, **2007**, *52*, 1154-1168.
28. Zykowska, A.W.; Ralet, M.C.J.; Garnier, C.D.; Thibault, J.F.J. *Plant Physiology*, **2005**, *139*, 397-407.
29. Madson, M.; Dunand, C.; Li, X.; Verma, R.; Vanzin, G.F.; Caplan, J.; Shoue, D.A.; Carpita, N.C.; Reiter, W.D. *Plant Cell*, **2003**, *15*, 1662-1670.
30. Leboeuf, E.; Guillon, F.; Thoirion, S.; Lahaye, M. *J. Exp. Bot.*, **2005**, *56*, 3171-3182.
31. Jensen, J.K.; Sorensen, S.O.; Harholt, J.; Geshi, N.; Sakuragi, Y.; Moller, I.; Zandleven, J.; Bernal, A.J.; Jensen, N.B.; Sorensen, C.; Pauly, M.; Beldman, G.; Willats, W.G.; Scheller, H.V. *Plant Cell*, **2008**, *20*, 1289-1302.
32. Sterling, J.D.; Atmodjo, M.A.; Inwood, S.E.; Kolli, V.S.K.; Quigley, H.F.; Hahn, M.G.; Mohnen, D. *PNAS*, **2006**, *103*, 5236-5241.
33. Caffall, K.H.; Pattathil, S.; Phillips, S.E.; Hahn, M.G.; Mohnen, D. *Mol. Plant.*, **2009**, *2*, 1000-1014.
34. Mouille, G.; Ralet, M.C.; Cavellier, C.; Eland, C.; Effroy, D.; Hematy, K.; McCartney, L.; Truong, H.N.; Gaudon, V.; Thibault, J.F.; Marchant, A.; Hofte, H. *Plant Journal*, **2007**, *50*, 605-614.
35. Francis, K.E.; Lam, S.Y.; Copenhaver, G.P. *Plant Physiology*, **2006**, *142*, 1004-1013.
36. Hilz, H.; de Jong, L.E.; Kabel, M.A.; Schols, H.A.; Voragen, A.G.J. *J. Chromatogr. A*, **2006**, *1133*, 275-286.

Chapter 3

Introducing porous graphitized carbon liquid chromatography with evaporative light scattering and mass spectrometry detection into cell wall oligosaccharide analysis

Westphal, Y., Schols, H.A., Voragen, A.G.J., Gruppen, H.,
J. Chromatogr. A, **2010**, 1217, 689–695.



Abstract

Separation and characterization of complex mixtures of oligosaccharides is quite difficult and, depending on elution conditions, structural information is often lost. Therefore, the use of a porous-graphitized carbon (PGC)-HPLC-ELSD/MSⁿ-method as analytical tool for the analysis of oligosaccharides derived from plant cell wall polysaccharides has been investigated. It is demonstrated that PGC-HPLC can be widely used for neutral and acidic oligosaccharides derived from cell wall polysaccharides. Furthermore, it is a non-modifying technique that enables the characterization of cell wall oligosaccharides carrying, e.g. acetyl groups and methyl esters. Neutral oligosaccharides are separated based on their size as well as on their type of linkage and resulting 3D-structure. Series of the planar β -(1,4)-xylo- and β -(1,4)-gluco-oligosaccharides are retained much more by the PGC material than the series of β -(1,4)-galacto-, β -(1,4)-manno- and α -(1,4)-gluco-oligosaccharides. Charged oligomers such as α -(1,4)-galacturonic acid oligosaccharides are strongly retained and are eluted only after addition of trifluoroacetic acid depending on their net charge. Online-MS-coupling using a 1:1 splitter enables quantitative detection by ELSD as well as simple identification of many oligosaccharides, even when separation of oligosaccharides within a complex mixture is not complete. Consequently, PGC-HPLC-separation in combination with MS-detection gives a powerful tool to identify a wide range of neutral and acidic oligosaccharides derived from various cell wall polysaccharides.

Introduction

Plant cell wall polysaccharides play an important role in the structure and functionality of the whole plant^{1,2}. The elucidation of their biosynthesis as well as a better understanding of their functional properties and enzymatic degradability is essential for the use of these polysaccharides by the food and non-food industry. Therefore, detailed analysis of their precise structure is essential³.

Since monomeric sugar composition analysis alone cannot deliver any structural information of the parental polysaccharide, the analysis of these polysaccharides is mostly done after partial degradation by chemical or enzymatic treatment into oligosaccharides. Nowadays, high performance anion exchange chromatography with pulsed amperometric detection (HPAEC-PAD) is frequently used for oligosaccharide analysis^{4,5}. However, the high pH eluent used for separation and detection will result in elimination of methyl esters and acetyl groups of the oligomers under investigation. In addition, HPAEC-PAD is not fully MS-compatible due to the high salt content used within the eluents. As methyl- and acetyl-substitutions are important for the function and the properties of polysaccharides, it is necessary to have analytical methods that leave the structural features intact⁶.

Recently, oligosaccharide analysis using capillary electrophoresis (CE) coupled to laser induced fluorescence (LIF) and mass spectrometry (MS) detection has been described⁷⁻⁹. This technique is very powerful and provides good separation of many oligosaccharides derived from plant cell wall polysaccharides in a short time but may not be commonly available. In addition, sample preparation includes time-consuming labeling of the oligosaccharides with a fluorescent chromophore by which non-reducing sugars are excluded from analysis. Furthermore, acidic oligosaccharides derived from pectin are being eluted rather rapidly due to the additional charges and an adequate separation is rather difficult to obtain⁹.

Another available technique for the separation and identification of neutral oligosaccharides is the gradient elution using RP-HPLC coupled to an evaporative light scattering (ELS) detector and a mass spectrometer (MS) as described by Kabel et al.¹⁰. However, due to the high polarity no retention could be achieved for acidic oligosaccharides derived from pectins. Recently, Hemström and Irgum¹¹ reviewed the use of hydrophilic interaction chromatography (HILIC) for the separation of certain classes of oligosaccharides. Although the use of HILIC within oligosaccharide analysis seems to be

promising, solubility of higher oligomers in the starting eluent (e.g. 80% organic modifier) might be a problem.

Porous graphitized carbon (PGC)-HPLC columns have been shown to be able to separate maltodextrins, fructo-oligosaccharides, human milk oligosaccharides, oligosaccharides derived from glycoproteins and even very polar sugar phosphates and glucosinolates^{12,13}. The ability of PGC material in retaining very polar components is based on the polar retention effect of graphite, which enables electron transfer between the carbon material and the acidic analytes as described by Pereira¹⁴.

As analysis of neutral and acidic oligosaccharides still lacks a rapid, versatile and widely available technique, this research aimed at the separation and identification of a broad range of neutral and acidic oligosaccharides within complex mixtures derived from plant cell wall polysaccharides. To this end, the use of PGC-HPLC in combination with ELS- and MS-detection was explored.

Materials and Methods

Materials

Neutral and acidic homoglycan oligosaccharides

The following components have been used as such: maltodextrins (α -(1,4)-gluco-oligomers) with an average degree of polymerization (DP) of 5 (AVEBE, Veendam, The Netherlands) and cellulodextrins (β -(1,4)-gluco-oligomers) with DP 2–7 (a kind gift of Dr. Vladimir Farkas, Institute of Chemistry, Slovak Academy of Sciences, Bratislava, Slovakia).

α -(1,5)-Arabino-oligomers (DP 1–8) were produced by partial enzymatic degradation of linear arabinan with α -(1,5)-arabinanase (*Aspergillus aculeatus*)¹⁵. A mixture of acetylated β -(1,4)-xylo-oligomers derived from Eucalyptus wood has been produced as described by Kabel et al.¹⁶ (fraction Euc NI A). β -(1,4)-Manno-oligomers were produced by partial enzymatic degradation of β -(1,4)-mannan derived from Ivory Nut (Megazyme, Bray, Ireland) with β -(1,4)-mannanase (*Aspergillus niger*¹⁷). β -(1,4)-galacto-oligomers were produced by partial enzymatic degradation of pectic potato galactan (Megazyme, Ireland) with β -(1,4)-galactanase (*A. niger*¹⁸).

Purified fractions of α -(1,4)-galacturonic acids (DP 2–10) as described by Van Alebeek et al.¹⁹ have been used.

Neutral and acidic heteroglycan oligosaccharides

Xyloglucan oligosaccharides derived from tamarind were obtained after digestion with xyloglucan specific endo-glucanase (XEG, *A. aculeatus*) as described by Hilz et al.⁸.

Partially esterified α -(1,4)-galacturonic acid oligosaccharides were obtained by digestion of low methyl esterified pectin (DM 30) with α -(1,4)-endo-polygalacturonase (*Kluyveromyces fragilis marxianus*²⁰).

Oligosaccharides derived from rhamnogalacturonan I were obtained by saponification of pectic modified hairy regions (MHR-B²¹) with 0.1 M sodium hydroxide followed by treatment with rhamnogalacturonan hydrolase in overdose²².

Xylogalacturonan oligomers were produced by treating xylogalacturonan from *gum tragacanth*²³ with an overdose of xylogalacturonan hydrolase (XGH²⁴).

HPLC-ELSD-MSⁿ

Liquid chromatography was performed on a Thermo Accela UHPLC system (Waltham, MA, USA) equipped with a Hypercarb column (PGC, 100 mm \times 2.1 mm; 3 μ m, Thermo Electron Corporation, San José, CA, USA) in combination with a Hypercarb guard column (10 mm \times 2.1mm; 3 μ m, Thermo Electron Corporation). Elution was performed with a flow of 0.4 mL/min and a column oven temperature of 70 °C. The injection volume was set to 10 μ L. The following eluents were used: Millipore water (A), acetonitrile (B) and 0.2% (w/v) trifluoroacetic acid (TFA) in water (C), to all eluents 25 μ M sodium acetate was added to ensure sodium adducts of all components. The following gradient was used: 0–1 min, isocratic 100% A, 1–15 min, linear from 0 to 27.5% (v/v) B, 15–28 min linear from 27.5 to 60% B and concomitant linear from 0 to 10% (v/v) C, 28–31 min linear from 60 to 80% B and from 10 to 20% C, 31–35 min isocratic 80% B and 20% C, 35–36 min from 80% B and 20% C to 100% A, 36–41 min equilibration with 100% A. The PGC-column was coupled to a 1:1-splitter (Accurate, Dionex, Sunnyvale, CA, USA) directing the eluent both to the evaporative light scattering detector (ELSD 85, Sedere, Alfortville, France) and to the ESI-MSⁿ-detector (LTQ XL MS, ion trap, Thermo Scientific, San Jose, CA, USA). The ELSD micro flow nebulizer (Sedere, Alfortville, France) had a gas pressure of 3.5 bar and a gas flow of 1.75 L/min. The drift tube temperature of the ELSD was set to 50 °C and the gain to 12. MS-detection was performed in positive mode using a spray voltage of 4.5 kV and a capillary temperature of 260 °C and auto-tuned on malto-pentaose (*m/z* 851). The MSⁿ-experiments were performed based on dependent scan

settings (Xcalibur software, Thermo Electron Corporation). The addition of sodium acetate (25 μ M) in combination with the use of TFA introduces a significant amount of noise due to the polymerization of sodium trifluoroacetate ($\Delta m/z$ 136). The m/z values originating from the sodium-TFA-complexes are excluded from the online-MS² measurements by means of Xcalibur software (Thermo Electron Corporation). The column was regenerated with 70 column volumes of tetrahydrofuran after each series of analysis²⁵.

Results and discussion

Various mixtures of oligosaccharides have been analyzed with a PGC-HPLC column in order to investigate the potential of porous graphitized carbon material in the analysis of oligosaccharides derived from a broad range of neutral and acidic oligosaccharides and to understand the mechanism involved in this separation.

Optimization of elution conditions for separation of various cell wall derived oligosaccharides

Different conditions including various compositions of organic and acidic modifiers as well as different temperatures have been investigated for their ability to elute and separate the broad range of cell wall derived neutral and acidic oligosaccharides.

Water–acetonitrile (ACN)-gradients have been described before to be effective to separate oligosaccharides of various sources^{13,26}. During this research the steepness of the water-ACN gradient has been varied and an increase of 2% (v/v) ACN/min has been selected as a suitable compromise for the separation of all neutral oligosaccharides under investigation in reasonable run times. In **Figure 1A–C** typical chromatograms of α -(1,4)-linked maltodextrins (**Figure 1A**), β -(1,4)-linked cellulodextrins (**Figure 1B**) and α -(1,5)-linked arabinan oligomers (**Figure 1C**) are presented.

α -(1,4)-Galacturonic acid oligomers are strongly retained by the PGC material and an acidic modifier is needed for elution. During this research three different acidic modifiers have been investigated, namely acetic acid, formic acid and TFA. The use of acetic acid did not result in an elution of all charged oligomers under investigation, whereas formic acid and TFA enable the elution of all oligomers. For a quick overview of all oligomers being present in a complex mixture, TFA is more suitable than formic acid due to less retention of the acidic oligomers when using TFA as acidic modifier. Nevertheless, for separation of

specific series of oligosaccharides, the use of formic acid may provide a good alternative due to reduced elution strength. In **Figure 1D** the chromatogram of α -(1,4)-galacturonic acid oligomers (DP 4, 7 and 10) by using a water–acetonitrile-gradient followed by a second gradient of trifluoroacetic acid (TFA) is presented.

Due to the fact that the addition of TFA is only started after 15 min, first neutral and afterwards acidic oligosaccharides are eluted (**Figure 1A–D**). This elution behavior simplifies the identification of unknown components because the retention time already provides an indication about the nature of the component.

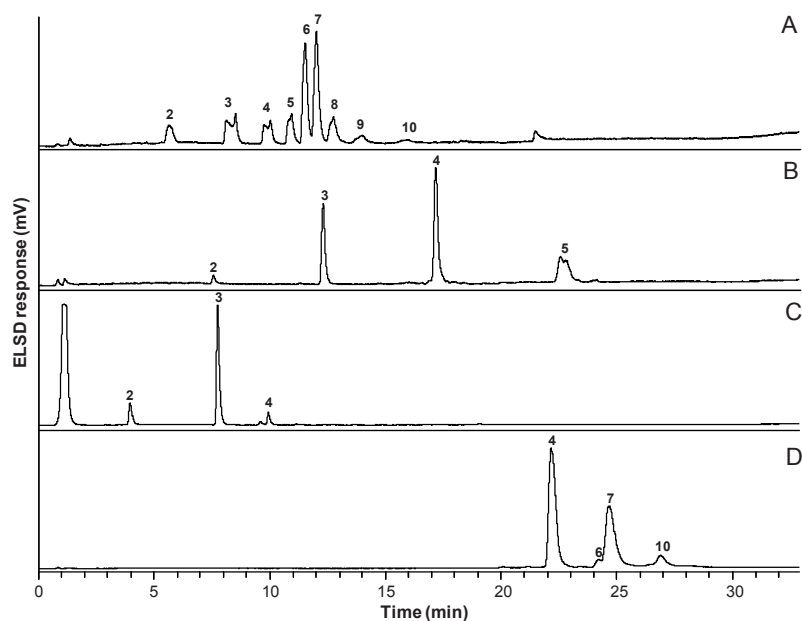


Figure 1 Elution pattern of oligosaccharides on a PGC column using ELS-detection: (A) maltodextrins, (B) cellulodextrins (DP 2–5), (C) linear arabinan after digestion with endo-arabinanase and (D) mixture of galacturonic acids (tetra-, hepta- and decamer). Numbers indicate the degree of polymerization.

The PGC-HPLC system is very versatile due to the possibility of using various organic and acidic modifiers. Thus, many adjustments can be performed, which are tailored for separating specific oligosaccharides. For strongly retained neutral oligosaccharides, such as xylo- and celULO-oligosaccharides, either the steepness of the water–ACN-gradient can be adjusted or a stronger organic modifier such as isopropanol can be used for a faster elution. The use of ammonium acetate (pH 8) for elution has been investigated as well as it has been shown to be efficient in separating oligosaccharides derived from glycoproteins²⁵. Indeed,

separation of neutral and even acidic oligosaccharides could be achieved, although MSⁿ-spectra obtained from the NH₄⁺-adducts of the oligomers did not include any structural information due to the absence of internal ring cleavages as has been described earlier²⁷.

Due to the tendency of the PGC-material to separate anomeric structures, which is not desired as this would not give any additional information, the separation has been carried out at elevated temperature (70 °C). Elevated temperatures have been described earlier to significantly reduce anomeric peak-forming for dimers²⁸. In this study this behavior was seen for oligomers as well.

Influence of the degree of polymerization on retention time

To illustrate the influence of the DP, the structural conformation and the charge of the different oligosaccharides on the retention time under the conditions used for this research, the retention time has been plotted against the DP (**Figure 2**).

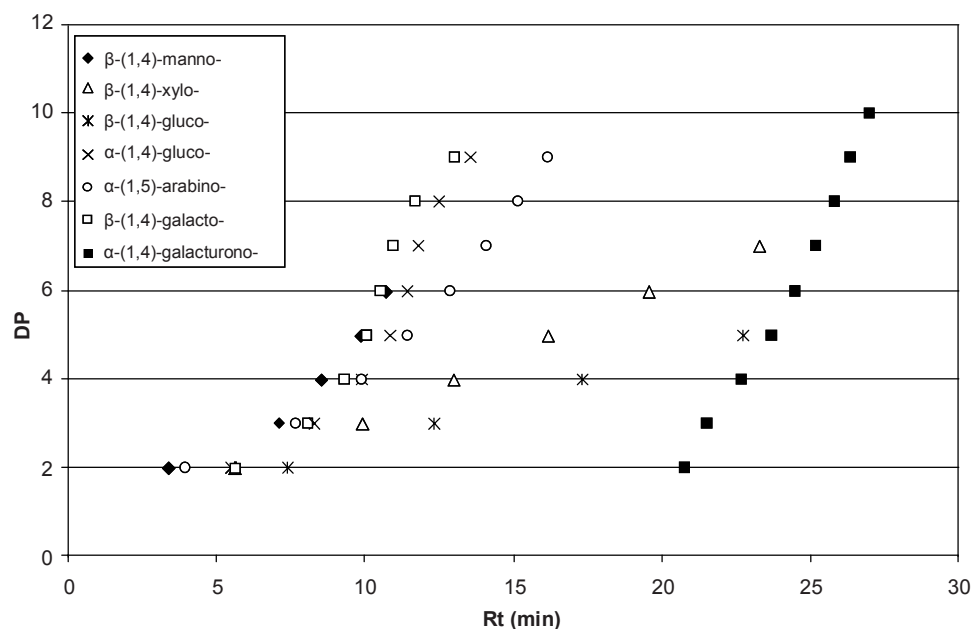


Figure 2 Retention time (min) plotted against the degree of polymerization (DP) for different neutral and acidic oligosaccharides: ◆ β-(1,4)-manno-, △ β-(1,4)-xylo-, * β-(1,4)-gluco-, × α-(1,4)-gluco-, ○ α-(1,5)-arabino-, □ β-(1,4)-galacto-, ■ α-(1,4)-galacturono-oligosaccharides.

Neutral oligosaccharide series

The series of β -(1,4)-gluco-oligosaccharides and β -(1,4)-xylo-oligosaccharides elute significantly later compared to other neutral oligosaccharide series such as β -(1,4)-galacto-, β -(1,4)-manno- and α -(1,4)-gluco-oligosaccharides. This elution behavior is in good agreement with the elution mechanism based on both hydrophobicity and planarity of the molecule¹⁴. A more planar structure will have a greater number of points of interaction with the graphite surface. While all hydroxyl-groups within the β -(1,4)-gluco- and the β -(1,4)-xylo-oligosaccharides are oriented in equatorial direction, in the β -(1,4)-manno- and β -(1,4)-galacto-oligosaccharides one hydroxyl-group is oriented in axial direction, O-2 for β -(1,4)-manno- and O-4 for α -(1,4)-galacto-oligosaccharides, respectively.

The series of α -(1,4)-gluco-oligosaccharides elutes significantly earlier in comparison to the β -(1,4)-gluco-oligosaccharides. Whereas the β -(1,4)-glucose-linkage creates a flat structure of the oligosaccharides, the α -(1,4)-glucose-linkage results in a helical structure, which has fewer points to interact with the column material resulting in earlier elution. The retention of α -(1,5)-arabino-oligosaccharides by the graphite surface is stronger when compared to β -(1,4)-manno-, β -(1,4)-galacto- and α -(1,4)-gluco-oligosaccharides.

Acidic oligosaccharide series

PGC material has been described to have a so called ‘polar retention effect on graphite’ where charge-induced interactions of the graphite surface with hydrophilic analytes determine the retention behavior¹⁴. The retention behavior of the analyzed α -(1,4)-galacturonic acid oligosaccharides supports this mechanism. By applying a gradient addition of TFA (0.002% (w/v)/min), elution of α -(1,4)-galacturonic acid oligomers with good separation can be achieved (**Figure 2**) while maintaining good peak shape as can be seen in **Figure 1**. The separation of the galacturonic acid-oligomers (DP 2-10) seems to be predominantly based on their net charge.

Retention behavior of complex neutral oligosaccharides

To investigate the influence of acetyl groups on the retention behavior of neutral oligosaccharides in more detail an *Eucalyptus* wood xylan hydrolysate¹⁶ has been subjected to the PGC column. The mass base peak chromatogram including peak annotation as based on the interpretation of automated MS¹⁻²-spectra, is presented in **Figure 3**. Highly acetylated xylo-oligosaccharides are present in the *Eucalyptus* wood xylan hydrolysate confirming the results of Kabel et al.¹⁰. With increasing number of acetyl groups attached to

the xylo-oligosaccharides of a given DP, the retention times increase significantly. Many peaks with the same m/z -values, corresponding to differently acetylated xylo-oligosaccharides, are present indicating that the PGC material is indeed able to separate different isomers.

The group of xyloglucan oligomers under investigation (XXXG, X(XL)G, XLLG, XLFG; nomenclature as described by Fry et al.²⁹) elute between DP 5 and 6 of the β -(1,4)-gluco-oligosaccharides. This elution behavior is most likely due to the fact that the

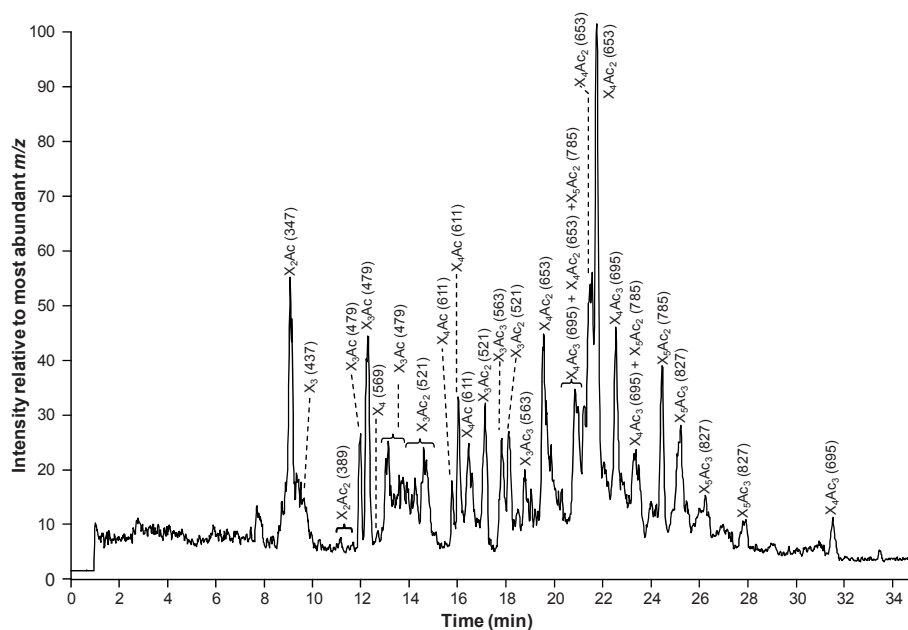


Figure 3 PGC-HPLC-elution profile of an *Eucalyptus* wood xylan hydrolysate: mass base peak chromatogram; in brackets the m/z -values of sodium adducts are given.

xyloglucan oligomers are mostly interacting with the column material through their glucan backbone. The side chains L and F are influencing the retention mechanism based on planarity that much that separation between the xyloglucans occurs. The elution order of the xyloglucan oligosaccharides (XLLG < XLFG < XXXG < X(XL)G) is predominantly based on the extension or reduction of the planar system which is present in XXXG. However, further optimization of the elution conditions has to be performed for optimal separation, possibly by using a gradient including stronger organic modifiers, such as isopropanol.

Retention behavior of complex acidic oligosaccharides

The influence of the presence of methyl esters on the elution behavior of the α -(1,4)-galacturonic acid oligomers has been investigated. In **Figure 4A-F** the selected ion chromatograms (SIC) of oligo-uronides derived from a 30% methyl-esterified pectin (DM 30) is shown, representing oligo-uronides of various degrees of polymerization (DP 2-7) with a diverse number of methyl esters attached. It can be observed that the presence of methyl esters decreases the retention time of the α -(1,4)-galacturonic acid oligosaccharides significantly due to the shielding of a charged carboxyl-group by the methyl ester. As demonstrated in **Figure 4A-C** the dimer (GalA₂) is coeluting with the trimer carrying one methyl ester (GalA₃Me) and the tetramer carrying two methyl esters (GalA₄Me₂). This behavior can be observed for every charge-level (*z*) as is demonstrated

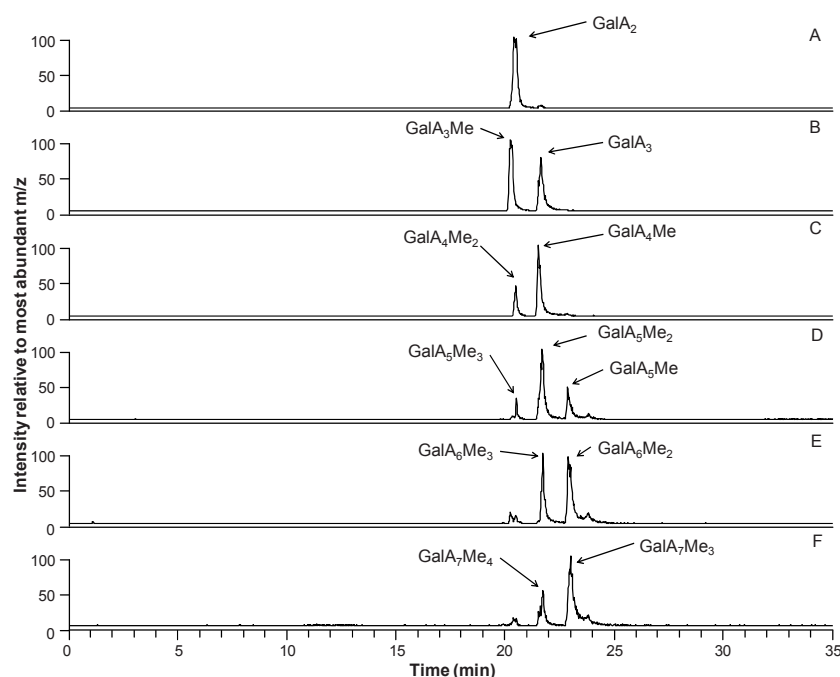


Figure 4 PGC-HPLC-elution profile of partly methylesterified galacturonic acids derived from DM 30 pectin after treatment with endo-polygalacturonase (MS detection): (A) selected ion chromatogram (SIC) of GalA₂ (393); (B) SIC of GalA₃ (569), GalA₃Me (583); (C) SIC of GalA₄ (745), GalA₄Me (759), GalA₄Me₂ (773); (D) SIC of GalA₅Me (935), GalA₅Me₂ (949), GalA₅Me₃ (963); (E) SIC of GalA₆Me₂ (1125), GalA₆Me₃ (1139), GalA₆Me₄ (1153); (F) SIC of GalA₇Me₃ (1325), GalA₇Me₄ (1339), GalA₇Me₅ (1353); in brackets the *m/z*-values of sodium adducts are given.

in **Figure 4A-F** for $z = 2-4$. From this behavior it can be concluded that the elution pattern of galacturonic acid oligomers, partly present as methyl esters, appears to be predominantly based on the net charge of the molecules.

By applying a gradient using formic acid instead of TFA, a partial separation of galacturonic acid oligosaccharides with methyl esters attached becomes possible, however, elution time will be increased significantly (data not shown).

A similar behavior is observed for rhamnogalacturonan- and xylogalacturonan-oligosaccharides. The elution patterns of these structures within the TFA gradient appear to be predominantly based on the net charge of the molecule. Only neutral sugar side chains of acidic oligomers highly influencing the planarity of the whole molecule will change the elution behavior in such a rate that separation will occur based on these differences in 3D-structure as well.

Structural information using PGC-HPLC-MSⁿ

In order to demonstrate the efficiency of our PGC-HPLC-ELSD/MS-method to elucidate complex acidic structures, a digest of xylogalacturonan derived from *gum tragacanth* after xylogalacturonan hydrolase digestion has been subjected to analysis. XGA is a pectic

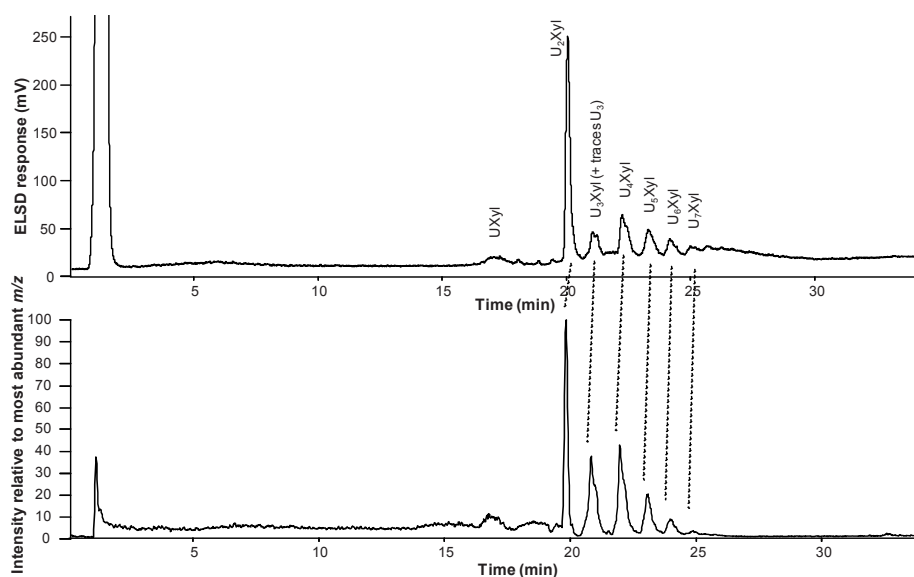
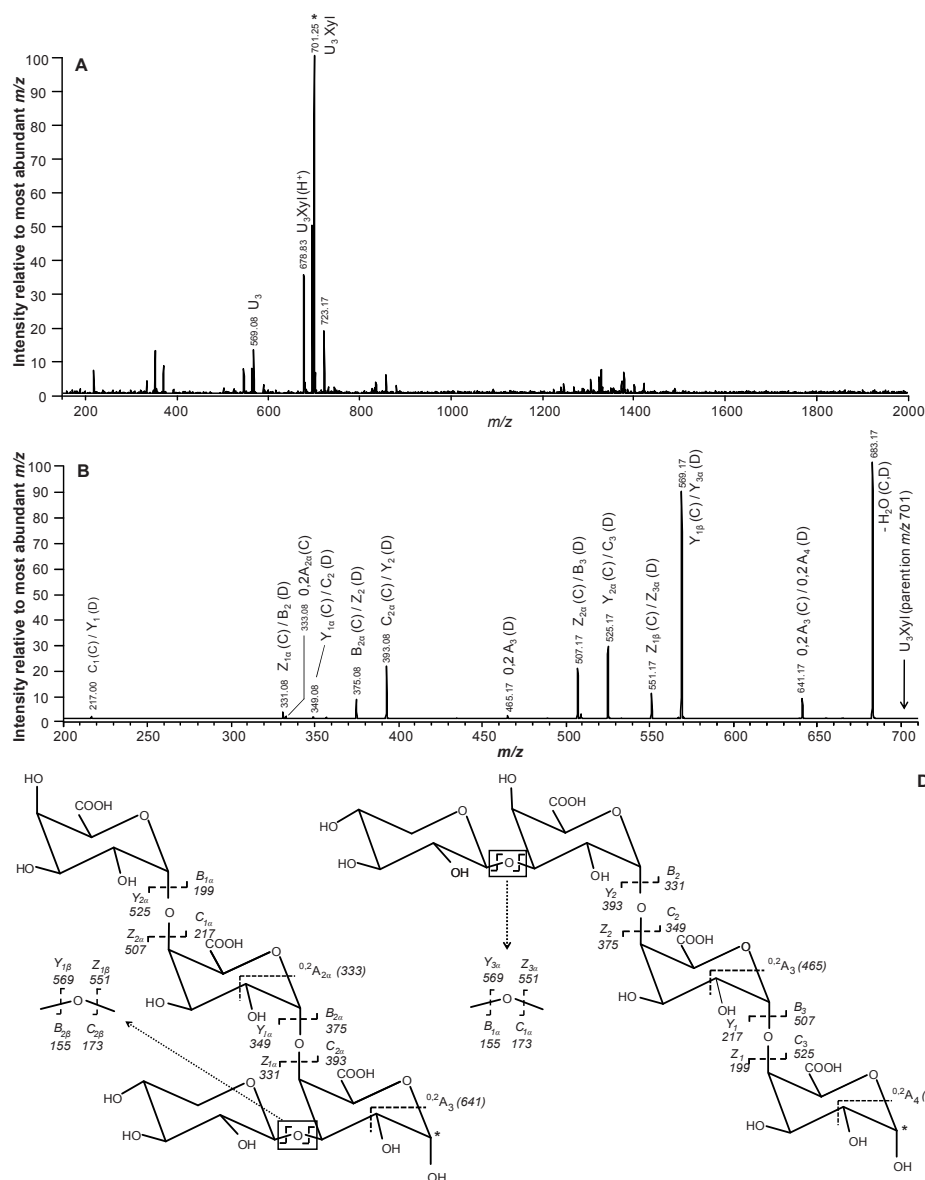


Figure 5 PGC-HPLC chromatograms of a xylogalacturonan derived from *gum tragacanth* after digestion with xylogalacturonan hydrolase with (A) ELS-detection and (B) MS (base peak)-detection; annotation of peaks according to their m/z -values.



polysaccharide having a backbone of α -(1,4)-galacturonic acids containing xylose residues attached to O-3 of the galacturonic acids³⁰. Typical XGA degradation products after XGH digestion are single xylose substituted oligo-uronides^{9,24}. In **Figure 5** an overlay of an ELSD-chromatogram (**Figure 5A**) and simultaneously recorded mass base peak chromatogram (**Figure 5B**) is presented. Good alignment for both chromatograms can be observed, which allows mass peak annotation in the ELSD chromatogram. The given annotation in **Figure 5** has been made based on the online-measured mass spectra and is in agreement with HPAEC- and CE-LIF measurements²⁴. For the peak eluted at 20.9 min in the ELSD-chromatogram and at 21.0 min in the mass base peak chromatogram the MS¹- and MS²-spectra are presented in **Figure 6** to substantiate the annotation. As can be seen in **Figure 6A** the main m/z -value present in the MS¹ spectrum is m/z 701 corresponding to GalA₃Xyl. Furthermore, some minor peaks are present: m/z 569 belongs to a trimer of galacturonic acid, which is not separated from GalA₃Xyl as explained before. m/z 679 represents the H⁺-adduct of GalA₃Xyl and m/z 723 represents GalA₃Xyl with additional sodium attached. All other peaks could be considered as background peaks.

To verify the position of the xylose attached, the online measured MS²-spectrum of m/z 701 has been evaluated. In **Figure 6B** the MS²-spectrum is shown with all fragments annotated following the nomenclature established by Domon and Costello³¹. According to the MS²-spectrum the structure with xylose attached to the second galacturonic acid within the oligomer is not very likely as the fragments m/z 331, 349, 375 and 393 indicate the presence of a dimer of galacturonic acid. The other two chemical structures are depicted in **Figure 6C** (reducing end) and **6D** (non-reducing end). As the reducing end is not labeled, the m/z -values of the fragments originating from glycosidic bond cleavage are similar in both structures. Nevertheless, the expected internal ring cleavage in the middle galacturonic acid ring is different as depicted in **Figure 6C-D** (^{0,2}A_{2α}, ^{0,2}A₃), respectively. As both fragments, in very small amounts, are present in the MS²-spectrum, it is most likely that both structures are present, although Zandleven et al.²⁴ and Coenen et al.⁹ have only supposed the xylose to be attached to the reducing end of the oligomer.

Conclusions

To our knowledge this is the first time that a PGC-HPLC-ELSD/MS method has been applied to such a broad range of neutral and acidic oligosaccharides derived from plant cell wall polysaccharides. Within a homologous oligosaccharide series separation is based on

size for neutral and on charge for galacturonic acid oligosaccharides. Between different series of neutral oligosaccharides the type of linkage and their resulting 3D-structure is responsible for separation. Acetyl groups present within neutral oligosaccharides result in a significant increase of retention.

Acknowledgements

This study is carried out with financial support from the Commission of the European Communities (WallNet: “Functional Genomics for Biogenesis of the Plant Cell Wall”, Marie Curie contract number: MRTN-CT-2004-512265). It does not necessarily reflect its views and in no way anticipates the Commission’s future policy in this area.

References

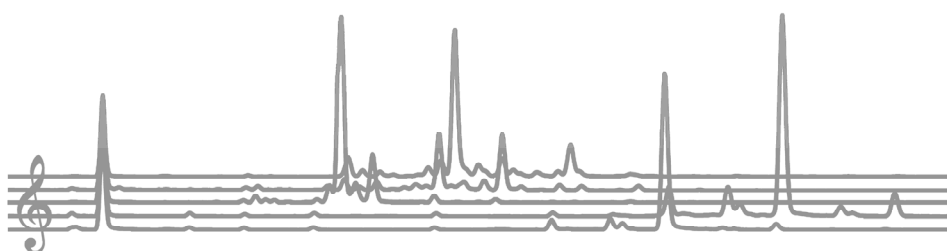
1. Bacic, A.; Harris, P.; Stone, B. *The Biochemistry of Plants*, **1988**, *14*, 297-369.
2. Albersheim, P.; Darvill, A.G.; O'Neill, M.A.; Schols, H.A.; Voragen, A.G.J. in: Visser, J., Voragen, A.G.J. (eds), *Progress in Biotechnology 14: Pectins and pectinases*, proceedings of an Int. Symp., Elsevier, Amsterdam, The Netherlands, **1996**, p. 47-55.
3. Hilz, H.; Bakx, E.J.; Schols, H.A.; Voragen, A.G.J. *Carbohydr. Polym.*, **2005**, *59*, 477-488.
4. Lee, Y.C. *J. Chromatogr. A*, **1996**, *720*, 137-149.
5. Schols, H.; Kabel, M.; Bakx, E.; Daas, P.; Van Alebeek, G.-J.; Voragen, F. in: Association Andrew van Hook, *Comptes Rendus, 7th Symposium International, Les séparations chromatographiques dans l'analyse et les process sucriers*, Reims, **2000**, p. 39-45.
6. Voragen, A.G.J.; Pilnik, W.; Thibault, J.F.; Axelos, M.A.V.; Renard, C.M.G.C., in: Stephen, A.M.(editor), *Food polysaccharides and their applications*, Marcel Dekker Inc., New York, USA, **1995**, p. 287-339.
7. Kabel, M.A.; Heijnis, W.H.; Bakx, E.J.; Kuijpers, R.; Voragen, A.G.J.; Schols, H.A. *J. Chromatogr. A*, **2006**, *1137*, 119-126.
8. Hilz, H.; de Jong, L.E.; Kabel, M.A.; Schols, H.A.; Voragen, A.G.J. *J. Chromatogr. A*, **2006**, *1133*, 275-286.
9. Coenen, G.J.; Kabel, M.A.; Schols, H.A.; Voragen, A.G.J. *Electrophoresis*, **2008**, *29*, 2101-2111.
10. Kabel, M.A.; de Waard, P.; Schols, H.A.; Voragen, A.G.J. *Carbohydr. Res.*, **2003**, *338*, 69-77.
11. Hemstrom, P.; Irgum, K. *J. Sep. Sci.*, **2006**, *29*, 1784-1821.

12. Antonio, C.; Larson, T.; Gilday, A.; Graham, I.; Bergström, E.; Thomas-Oates, J. *J. Chromatogr. A*, **2007**, *1172*, 170-178.
13. Elfakir, C.; Dreux, M. *J. Chromatogr. A*, **1996**, *727*, 71-82.
14. Pereira, L. *J. Liq. Chromatogr. Related Technol.*, **2008**, *31*, 1687-1731.
15. McCleary, B.V.; Cooper, J.M.; Williams, E.L. *Pat. Application, GB 88283809*, **1989**.
16. Kabel, M.A.; Schols, H.A.; Voragen, A.G.J. *Carbohydr. Polym.*, **2002**, *50*, 191-200.
17. Dusterhoft, E.M.; Bonte, A.W.; Voragen, A.G.J. *J. Sci. Food Agric.*, **1993**, *63*, 211-220.
18. van de Vis, J.W.; Searle-van Leeuwen, M.J.F.; Siliha, H.A.; Kormelink, F.J.M.; Voragen, A.G.J. *Carbohydr. Polym.*, **1991**, *16*, 167-187.
19. Van Alebeek, G.J.W.M.; Zabotina, O.; Beldman, G.; Schols, H.A.; Voragen, A.G.J. *Carbohydr. Polym.*, **2000**, *43*, 39-46.
20. Daas, P.J.H.; Meyer-Hansen, K.; Schols, H.A.; De Ruiter, G.A.; Voragen, A.G.J. *Carbohydr. Res.*, **1999**, *318*, 135-145.
21. Schols, H.A.; Posthumus, M.A.; Voragen, A.G.J. *Carbohydr. Res.*, **1990**, *206*, 117-129.
22. Schols, H.A.; Geraeds, C.; Searle-van Leeuwen, M.F.; Kormelink, F.J.M.; Voragen, A.F.J. *Carbohydr. Res.*, **1990**, *206*, 105-115.
23. Beldman, G.; Vincken, J.P.; Schols, H.A.; Meeuwsen, P.J.A.; Herweijer, M.; Voragen, A.G.J. *Biocatal. Biotransform.*, **2003**, *21*, 189-198.
24. Zandleven, J.; Beldman, G.; Bosveld, M.; Benen, J.; Voragen, A. *Biochem. J.*, **2005**, *387*, 719-725.
25. Thermo Electron Corporation *Method Development Guide for Hypercarb Columns*, **2004**.
26. Gnoth, M.J.; Rudloff, S.; Kunz, C.; Kinne, R.K.H. *J. Biol. Chem.*, **2001**, *276*, 34363-34370.
27. Harvey, D.J.; Bateman, R.H.; Bordoli, R.S.; Tyldesley, R. *Rapid Commun. Mass Spectrom.*, **2000**, *14*, 2135-2142.
28. Koimur, M.; Lu, B.; Westerlund, D. *Chromatographia*, **1996**, *43*, 254-260.
29. Fry, S.C.; York, W.S.; Albersheim, P.; Darvill, A.; Hayashi, T.; Joseleau, J.P.; Kato, Y.; Lorences, E.P.; MacLachlan, G.A.; McNeil, M.; Mort, A.J.; Reid, J.S.G.; Seitz, H.U.; Selvendran, R.R.; Voragen, A.G.J.; White, A.R. *Physiol. Plant.*, **1993**, *89*, 1-3.
30. Schols, H.A.; Bakx, E.J.; Schipper, D.; Voragen, A.G.J. *Carbohydr. Res.*, **1995**, *279*, 265-279.
31. Domon, B.; Costello, C.E. *Glycoconjugate J.*, **1988**, *5*, 397-409.

Chapter 4

Branched arabino-oligosaccharides isolated from sugar beet arabinan

Westphal, Y., Kühnel, S., Waard, P. de, Hinz, S.W.A,
Schols, H.A., Voragen, A.G.J., Gruppen. H.,
Carbohydrate Research, **2010**, 345, 1180-1189.



Abstract

Sugar beet arabinan consists of an α -(1,5)-linked backbone of L-arabinosyl residues, which can be either single or double substituted with α -(1,2)- and/or α -(1,3)-linked L-arabinosyl residues. Neutral branched arabino-oligosaccharides were isolated from sugar beet arabinan by enzymatic degradation with mixtures of pure and well-defined arabinohydrolases from *Chrysosporium lucknowense* followed by fractionation based on size and analysis by MALDI-TOF MS and HPAEC. Using NMR analysis, two main series of branched arabino-oligosaccharides have been identified, both having an α -(1,5)-linked backbone of L-arabinosyl residues. One series carries single substituted α -(1,3)-linked L-arabinosyl residues at the backbone, whereas the other series consists of a double substituted α -(1,2,3,5)-linked arabinan structure within the molecule. The structures of eight such branched arabino-oligosaccharides were established.

Introduction

Pectins belong to the main polysaccharides within the primary plant cell wall of dicotyls¹. Four main pectic components have been identified: homogalacturonan, rhamnogalacturonan-I (RG-I), rhamnogalacturonan-II, and xylogalacturonan, which have been described extensively²⁻⁴. RG-I consists of a backbone of repeating units of alternating α -(1,2)-linked rhamnose and α -(1,4)-linked galacturonic acids. Depending on the type of cell wall and tissue, 20–80% of the rhamnose residues are substituted with side chains composed of galactose and/or arabinose attached to O-3 and/or O-4. The length of these side chains can vary from one single sugar residue up to chains of 50 residues⁴. The RG-I arabinans are branched molecules with a linear α -(1,5)-linked arabinose backbone, which can be single or double substituted with α -(1,2)-linked and/or α -(1,3)-linked arabinose side chains, which again may be further branched^{5,6}. In addition, the arabinan of, for example, sugar beet cell walls can be feruloylated at the O-2 and/or O-5 position of one of the arabinose moieties^{7,8}.

Enzymes able to degrade arabinans of various sources have been reviewed previously⁵ and include endo-arabinanases and exo-arabinanases to degrade the linear α -(1,5)-linked arabinan. For the degradation of branched arabinan, arabinofuranosidases (Abf A and B) are necessary to debranch the arabinan and to enable the degradation of the resulting linear α -(1,5)-linked arabinan backbone by the endo- and exo-arabinanases⁵. Complete insight of the linkage specificity of the arabinofuranosidases has not yet been achieved due to a lack of well-characterized branched arabino-oligosaccharides (AOS). Recently, novel arabinohydrolases from *Chrysosporium lucknowense*, Abn1 (endo-arabinanase), Abn2 (exo-arabinanase), and Abn4 (arabinofuranosidase), have been described⁹. Together these enzymes were able to degrade 60% of the sugar beet arabinan resulting in the main degradation products arabinose and arabinobiose in the presence of significant amounts of AOS (DP 3-6). Some of these oligosaccharides were hypothesized to be branched AOS⁹. The isolation and identification of these unknown oligomeric arabinan structures would provide essential information for the detailed elucidation of the polymeric arabinan structure. In addition, the further characterization of arabinan-specific enzymes and possible exploration of these AOS for their prebiotic potential, as has been described for linear α -(1,5)-linked AOS¹⁰, are of great interest. Therefore, this research deals with the isolation of these novel oligomeric branched arabinan structures derived from sugar beet arabinan by enzymatic degradation with a mixture of arabinohydrolases from

C. lucknowense (Abn1, Abn2, and Abn4) and the characterization of purified branched AOS by NMR.

Materials and Methods

Materials

Branched sugar beet arabinan was obtained from British Sugar (Peterborough, United Kingdom, McCleary¹⁸). The arabinose content is 66% (w/w%), the remaining part consists of hairy regions (rhamnose, galacturonic acid, and galactose) and glucans (glucose)⁹.

Linear AOS (DP 2–8) have been purchased from Megazyme International Ltd (Bray, Ireland), and were denoted 2.0, 3.0, 4.0, 5.0, 6.0, 7.0, and 8.0, respectively.

Branched AOS were denoted according to the elution order during HPAEC analysis.

Enzymatic degradation of sugar beet arabinan

For fractionation and isolation of branched AOS two times 1 g of branched sugar beet arabinan was digested in 200 mL water set at pH 5 (30 °C) with the arabinohydrolases Abn1, Abn2, and Abn4 (*C. lucknowense* strain C1⁹). One arabinan batch (D-100) was incubated for 15 h with an overdose of Abn4 (1.1 U), whereas another batch (D-30) was incubated for 15 h with 0.22 U Abn4 (t = 15 h) resulting in about 30% of maximal degradation by Abn4. This enzyme dosage was calculated based on the fact that about 18% of arabinose present can be degraded by Abn4.⁹ The degradation was monitored by arabinose monomer release by HPAEC. After inactivation of the enzyme by boiling for 10 min, both incubations were followed by an end-point degradation of Abn1 and Abn2 (t = 24 h, 4.8 U and 4.4 U, respectively). After enzyme incubation, the samples were freeze-dried.

High performance anion exchange chromatography

Arabinose and AOS were determined by HPAEC with pulsed amperometric detection (PAD). A HPAEC system (ICS-3000, Dionex Corporation, Sunnyvale, CA, USA) was equipped with a CarboPac PA-1 separation column (2 mm ID × 250 mm; Dionex Corporation) and a CarboPac PA-1 guard column (2 mm ID × 25 mm; Dionex Corporation). A flow of 0.3 mL/min was used and the temperature was kept at 20 °C. AOS (injection volume 10 µL; 10–100 µg/mL) were separated using a gradient with 0.1 M

NaOH (A) and 1 M NaOAc in 0.1 M NaOH (B): 0-36 min from 0% B to 42% B, 36-42 min at 100% B, and 42-57 min at 0% B.

Fractionation based on size: Biogel P2

Freeze-dried material of both digests was each dissolved in 22.5 mL water and subsequently centrifuged. Fractionation of the supernatants was performed on an Äkta Explorer system (Amersham Biosciences, Uppsala, Sweden) equipped with a Bio-Gel P2 column (porous polyacrylamide, 1000 × 26 mm, 200-400 mesh, Bio-Rad Laboratories, Hercules, CA, USA) thermostated at 60 °C and eluted with Millipore water at 1.0 mL/min. Twenty milliliters of each sample (50 mg/mL) were injected. The column efflux was first led through a refractive index detector (Shodex RI72, Showa Denko K.K., Tokyo, Japan) and secondly collected in fractions of 3.5 mL by a fraction collector (Superfrac, GE Amersham, Uppsala, Sweden). Appropriate fractions were pooled and freeze-dried for further analysis.

Determination of neutral sugar and uronic acid content of the Biogel P2 fractions

The total neutral sugar and uronic acid content was determined with an automated colorimetric assay analyzer. The total neutral sugar content was determined by using the orcinol-sulfuric acid color assay with arabinose (25-200 µg/mL) as standard curve¹⁹. The uronic acid content was determined with the *m*-hydroxy-biphenyl assay based on a standard curve of galacturonic acid (12.5-100.0 µg/mL)²⁰.

MALDI-TOF MS

Each sample was desalted with AG 50W-X8 Resin (Bio-Rad Laboratories, Hercules, CA, USA) and 1 µL of the desalted sample solution was mixed on a MALDI-plate (Bruker Daltonics, Bremen, Germany) with 1 µL matrix solution of 12 mg/mL 2,5-dihydroxybenzoic acid (Bruker Daltonics) in 30% acetonitrile and dried under a stream of air²¹. MALDI-TOF MS analysis was performed using an Ultraflex workstation (Bruker Daltonics) equipped with a nitrogen laser of 337 nm and operated in positive mode. After a delayed extraction time of 350 ns, the ions were accelerated to a kinetic energy of 22000 V and detected using reflector mode. The lowest laser power required to obtain good spectra was used and 200 spectra were collected for each measurement. The mass spectrometer was calibrated with a mixture of maltodextrins (Avebe, Foxhol, The Netherlands; MD20; mass

range m/z 500-2000). The data were processed using Bruker Daltonics flexAnalysis version 2.2.

NMR analysis

Samples (1–6 mg) have been exchanged with D₂O (99.9 atom % D, Sigma–Aldrich, St. Louis, MO, USA) and subsequently dissolved in 0.5 mL D₂O (99.9 atom % D, Sigma–Aldrich) containing 0.75% 3-(trimethylsilyl)-propionic-2,2,3,3-d₄ acid, sodium salt (TMSP, Sigma–Aldrich). NMR spectra were recorded at a probe temperature of 300 K on a Bruker Avance-III-600 spectrometer, equipped with a cryo-probe located at Bqualys (Wageningen, The Netherlands). Chemical shifts are expressed in parts per million (ppm) relative to internal TMSP at 0.00 ppm. 1D and 2D COSY, TOCSY, HMBC, and HMQC spectra were acquired using standard pulse sequences delivered by Bruker. For the ¹H-COSY and -TOCSY spectra, 400 experiments of two scans were recorded, resulting in measuring times of 0.5 h. The mixing time for the TOCSY spectra was 100 ms. For the [¹H, ¹³C]-HMBC and -HMQC spectra 800 experiments of 32 scans and 512 experiments of 8 scans, respectively, were recorded, resulting in measuring times of 8.7 h and 2.5 h, respectively.

Results and discussion

Enzymatic preparation of AOS from sugar beet arabinan

Enzymatic degradation of sugar beet arabinan with a mixture of the arabinohydrolases Abn1, Abn2, and Abn4 (*C. lucknowense*) releases the main degradation products arabinose and arabinobiose, but as well produces various unknown AOS, which elute differently in high performance anion exchange chromatography with pulsed amperometric detection (HPAEC-PAD) compared to linear α -(1,5)-linked AOS⁹. To explore the precise structure of various unknown AOS, sugar beet arabinan was digested with two different treatments of Abn1, Abn2, and Abn4. Although sugar beet arabinan only contains 66% (w/w) arabinose in addition to significant amounts of residual rhamnogalacturonan-I, the use of pure and well-defined arabinohydrolases ensured specific degradation of the arabinan segments for this experiment. To the first digest (D-30) the arabinofuranosidase Abn4 has been added in a concentration that should ensure partial degradation of the side chains of sugar beet arabinan resulting in partly debranched backbone. HPAEC results showed that 30% of the maximal degradation by Abn4 took place. This equals the release of 6% of all arabinose

present (data not shown). To the second digest (D-100) Abn4 has been added in an overdose, thereby allowing Abn4 to cleave all possible linkages by releasing about 18% of all arabinose present. This results in a heavily debranched arabinan backbone. Both digests were subsequently treated with a mixture of endo-arabinanase Abn1 and exo-arabinanase Abn2 to ensure degradation of the linear part of the arabinan present toward mono-, di-, and oligosaccharides. The HPAEC chromatograms of both enzyme digests, D-30 and D-100, are presented in **Figure 1A** and **B**, respectively. In both digests, the main degradation products were arabinose and arabinobiose. Their levels increased with an increase of Abn4 conversion level (D-30 to D-100). This is in good agreement with previous results⁹. In addition to the monomer and dimer, several oligomeric structures were obtained as well. Most of these oligomeric structures do not co-elute with the α -(1,5)-linked AOS standards (**Figure 1**), suggesting that these peaks are branched AOS as hypothesized already earlier by Kühnel et al⁹. The peak at 19.1 min, which is present in the D-30 digest, and the peak at 22.6 min, which appears in the D-100 digest are the dominant peaks not co-eluting with linear α -(1,5)-linked AOS. Many more unknown AOS are present in minor quantities in both digests. As HPAEC analysis of both digests indicated the presence of various unknown AOS, both digests were subjected to further analysis.

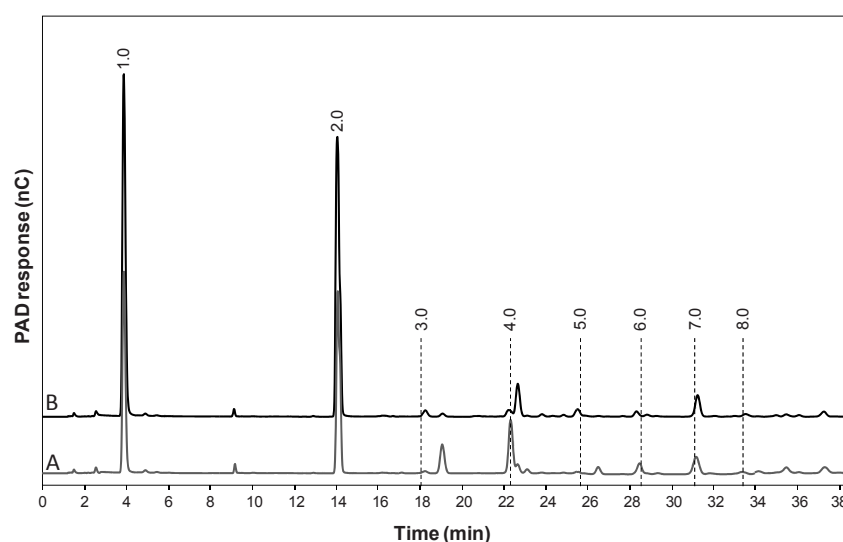


Figure 1 HPAEC elution pattern of AOS after degradation of sugar beet arabinan with different amounts of Abn4 followed by end-point-incubation with Abn1 and Abn2: D-30 (**A**), D-100 (**B**); indication of linear α -(1,5)-linked AOS (DP 1-8; denoted 1.0-8.0).

Fractionation of the AOS derived from sugar beet arabinan after enzyme digestion

For detailed structural characterization of the AOS, a preparative fractionation based on size of both digests was performed. In **Figures 2A** and **3A** the refractive index (RI) patterns of preparative Biogel P2 separations of both digests are given, including the DP as established using MALDI-TOF MS analysis (**Figures 2** and **3**, inset tables). The total sugar analysis of all fractions taken (3.5 mL each) confirmed the RI patterns of both digests. Significant amounts of uronic acid were only detected in the first 15 fractions of the Biogel P2 separations. Sugar composition of these pools (fractions 1–15) of both digests is given in **Table 1**. It supports the assumption that the main peak in the beginning of the RI patterns in both digests consists of the remaining rhamnogalacturonan-I (RG-I) core structure ('RG-I remnants' in **Figures 2A** and **3A**) due to the presence of significant amounts of rhamnose, galacturonic acid, arabinose, and galactose. The arabinose levels (35 and 21 w/w% for D-30 and D-100, respectively) represent 34 and 11 w/w% of the arabinose present in the starting material (crude sugar beet arabinan), whereas the rest is present as small molecular weight material.

Table 1 Sugar composition (w/w%) of the 'RG-I remnants' (Biogel P2 fractions 1–15) of the D-30 and D-100 sugar beet arabinan digests.

w/w%	Rha	Ara	Gal	Glc	GalA	total sugar
D-30	4	35	17	4	10	70
D-100	5	21	21	6	11	64

Fractions 18–71 from the Biogel P2 separations (3.5 mL each) have been analyzed by HPAEC and MALDI-TOF MS. The fractions have been pooled based on HPAEC analysis aiming at pools with high purity of the compounds present. The pool numbers are indicated as $I_{30-VII_{30}}$ and $I_{100-VIII_{100}}$ in **Figures 2A** and **3A** for samples D-30 and D-100, respectively.

HPAEC showed that pools I_{30} and I_{100} consisted of arabinose monomers. In the following part HPAEC, MALDI-TOF MS, and NMR results of the various pools will be discussed in more detail. Concerning the NMR results of all resolved structures it can be stated that full assignment of both proton and carbon spectra was possible combining the data of the various 2D experiments (**Table 2**). All linkages could be confirmed with HMBC cross-peaks.

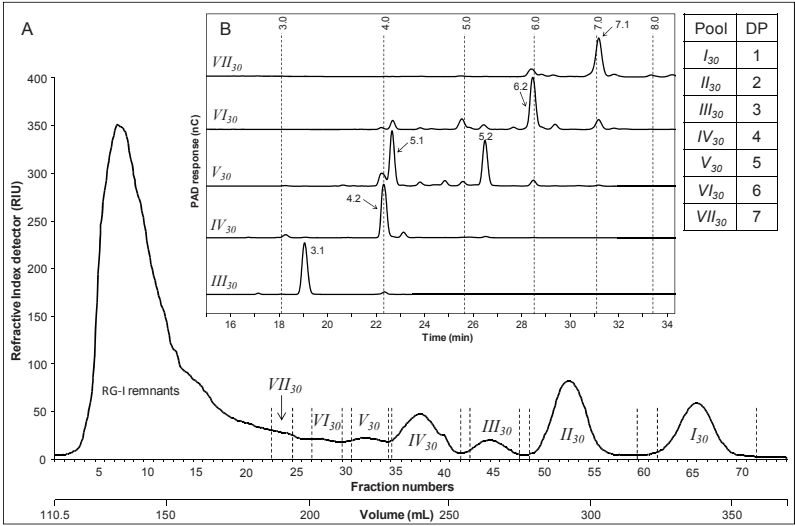


Figure 2 Biogel P2 elution pattern of the D-30 digest with indication of the pooled fractions (A); HPAEC elution pattern of pooled fractions (B; zoom) with indication of linear α -(1,5)-linked AOS (DP 3-8); inserted table represents the DP of the pools as analyzed with MALDI-TOF MS.

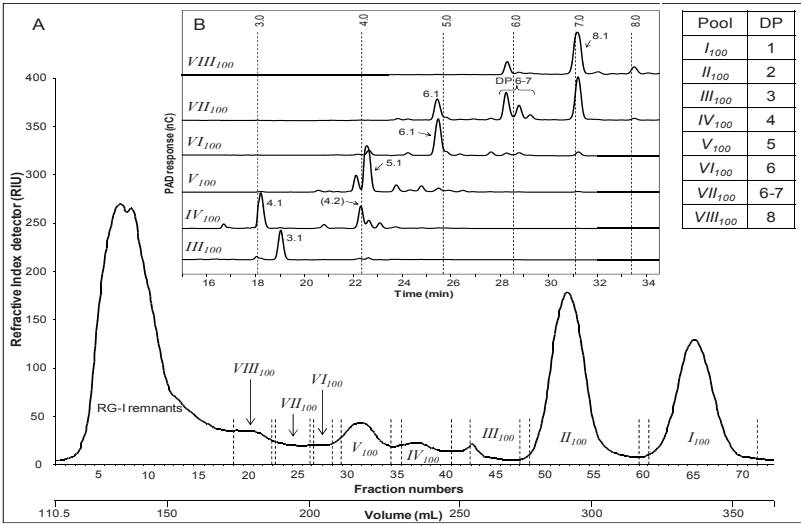


Figure 3 Biogel P2 elution pattern of the D-100 digest with indication of the pooled fractions (A); HPAEC elution pattern of pooled fractions (B; zoom) with indication of linear α -(1,5)-linked AOS (DP 3-8); inserted table represents the DP of the pools as analyzed with MALDI-TOF MS.

Table 2 ^1H and ^{13}C NMR data of arabino-oligosaccharides identified from sugar beet arabinan

Pools II_{30} and II_{100}	H-1	H-2	H-3	H-4	H-5R	H-5S	C-1	C-2	C-3	C-4	C-5
R α	5.265	4.04	4.04	4.24	3.769	3.87	104.01	84.18	78.71	84.23	69.69
R β	5.306	4.10	4.10	3.95	3.769	3.86	98.15	78.83	77.19	82.21	71.03
T	5.085	4.132	3.956	4.10	3.72	3.834	110.26	83.7 ^a	79.36	86.8 ^a	64.04
Pool III_{30}	H-1	H-2	H-3	H-4	H-5R	H-5S	C-1	C-2	C-3	C-4	C-5
R α	5.257	4.04	4.06	4.236	3.77	3.86	103.98	84.22	78.55	84.10	69.13
R β	5.312	4.10	4.10	3.95	3.78	3.85	98.18	78.90	77.16	82.21	70.69
A	5.116	4.293	4.04	4.197	3.768	3.877	110.26	82.03	84.94	86.0 ^a	63.9
T	5.17	4.144	3.948	4.04	3.717	3.842	109.89	84.05	79.38	86.73	63.99
Pool IV_{30}	H-1	H-2	H-3	H-4	H-5R	H-5S	C-1	C-2	C-3	C-4	C-5
R α	5.256	4.04	4.06	4.241	3.77	3.86	103.99	84.2	78.55	84.10	69.21
R β	5.308	4.10	4.10	3.95	3.78	3.85	98.19	78.88	77.15	82.16	70.73
A	5.122	4.294	4.10	4.319	3.856	3.95	110.29	81.92	85.2	84.52	69.29
T3	5.165	4.14	3.96	4.05	3.713	3.839	109.97	84.05	79.39	86.77	63.99
T5	5.097	4.14	3.96	4.115	3.734	3.839	110.18	83.78	79.39	86.83	63.99
Pool IV_{100}	H-1	H-2	H-3	H-4	H-5R	H-5S	C-1	C-2	C-3	C-4	C-5
R α	5.26	4.04	4.06	4.242	3.78	3.86	103.99	84.17	78.58	84.10	69.21
R β	5.307	4.10	4.10	3.95	3.78	3.85	98.19	78.86	77.22	82.18	70.73
A	5.253	4.31	4.19	4.19	3.77	3.89	109.14	88.0 ^a	82.9	85.4 ^a	63.54
T2	5.189	4.13	3.97	4.08	3.727	3.84	109.86	84.1	79.31	86.98	63.93
T3	5.165	4.15	3.96	4.05	3.718	3.84	109.7	84.02	79.37	86.83	63.97
Pool V_{30}	H-1	H-2	H-3	H-4	H-5R	H-5S	C-1	C-2	C-3	C-4	C-5
R α	5.26	4.04	4.05	4.24	3.77	3.86	103.99	84.21	78.56	84.10	69.22
R β	5.3	4.10	4.10	3.96	3.78	3.85	98.17	78.89	77.20	82.20	70.75
A	5.12 ^a	4.29 ^a	4.11	4.32	3.85	3.95	110.2	82.0 ^a	85.18	84.5 ^a	68.71
T3	5.16	4.14	3.96	4.05	3.725	3.84	110.04	84.07	79.40	86.77 ^a	63.97
B	5.125	4.3	4.04	4.221	3.77	3.88	110.2	82.04	84.95	86.08	63.89
T3	5.164	4.14	3.96	4.05	3.725	3.84	109.86	84.07	79.4	86.85 ^a	63.97
Pool V_{100}	H-1	H-2	H-3	H-4	H-5R	H-5S	C-1	C-2	C-3	C-4	C-5
R α	5.26	4.04	4.05	4.24	3.782	3.86	104.03	84.2	78.62	84.12	69.41
R β	5.30	4.10	4.10	3.96	3.782	3.85	98.2	78.9	77.20	82.14	70.96
A	5.260	4.315	4.256	4.32	3.860	3.95	109.2	87.8 ^a	83.12	84.0	68.88
T2	5.189	4.14	3.97	4.08	3.725	3.84	109.8	84.2	79.40	86.92	63.96
T3	5.165	4.15	3.96	4.05	3.725	3.84	109.8	84.0	79.40	86.9	63.96
T5	5.092	4.14	3.96	4.11	3.725	3.84	110.19	83.93	79.44	86.69	63.96
Pool VI_{30}	H-1	H-2	H-3	H-4	H-5R	H-5S	C-1	C-2	C-3	C-4	C-5
R α	5.26	4.04	4.06	4.24	3.77	3.85	103.98	84.21	78.56	84.1	69.22
R β	5.31	4.10	4.10	3.95	3.77	3.85	98.20	78.88	77.20	82.21	70.80
A	5.12 ^a	4.290	4.12	4.32	3.85	3.96	110.3 ^a	82.09	85.13	84.66	68.72
T3	5.162	4.15	3.96	4.05	3.72	3.84	109.94	84.09	79.40	86.74	63.95 ^b
B	5.133	4.303	4.10	4.346	3.77	3.85	110.21	81.9	85.21	84.66	69.27
T3	5.162	4.15	3.96	4.05	3.72	3.84	109.94	84.09	79.40	86.74	63.95 ^b
T5	5.098	4.14	3.96	4.12	3.73	3.84	110.23	83.8	79.44	86.83	64.00 ^b
Pool VII_{30}	H-1	H-2	H-3	H-4	H-5R	H-5S	C-1	C-2	C-3	C-4	C-5
R α	5.26	4.04	4.06	4.24	3.773	3.86	104	84.22	78.55	84.10	69.2
R β	5.31	4.1	4.1	3.96	3.773	3.86	98.2	78.87	77.20	82.10	70.69
A	5.12 ^a	4.3	4.1	4.32	3.85	3.96	110.3 ^a	81.94 ^a	85.17	84.51	69.27 ^a
T3	5.164	4.15	3.96	4.05	3.73	3.84	109.96	84.08	79.40	86.74 ^f	63.9 ^h
B	5.09	4.14	4.05	4.23	3.807	3.901	110.3 ^a	83.72 ^a	79.37	85.08	69.07
C	5.127	4.3	4.1	4.32	3.85	3.96	110.27 ^a	81.97 ^a	85.17	84.51	69.38 ^a
T3	5.164	4.15	3.96	4.05	3.73	3.84	109.96	84.08	79.40	86.77 ^f	63.96 ^h
T5	5.097	4.14	3.96	4.12	3.73	3.84	110.2	83.79 ^a	79.44	86.83	64.00 ^h
Pool $VIII_{100}$	H-1	H-2	H-3	H-4	H-5R	H-5S	C-1	C-2	C-3	C-4	C-5
R α	5.26	4.04	4.05	4.24	3.77	3.86	104	84.2	78.60	84.2	69.8
R β	5.31	4.09	4.1	3.96	3.77	3.86	98.2	78.9	77.20	82.1	71.2
A	5.10 ^a	4.14	4.04	4.22	3.9	3.807	110.34	84.08 ^f	79.40	85.0 ^a	69.21
B	5.13	4.29	4.12	4.32	3.86	3.96	110.24	82.05	85.12	84.44	68.86
T3	5.162	4.15	3.96	4.05	3.73	3.84	110.02	84.08 ^f	79.40	86.75	63.95
C	5.273	4.33	4.261	4.344	3.86	3.96	109.11	87.63	83.07	84.19	68.86
T2	5.191	4.14	3.97	4.08	3.73	3.85	109.68	84.21	79.40	86.92	63.95
T3	5.162	4.15	3.96	4.05	3.73	3.84	109.78	84.11 ^f	79.40	86.87	63.95
T5	5.092	4.14	3.96	4.12	3.73	3.84	110.26	83.96 ^f	79.47	86.68	63.95

* Signal broadening or splitting due to anomerization effect; superscript values may have to be interchanged.

Dimers

NMR analysis of the pools II_{30} and II_{100} resulted in identical NMR data (**Table 2**). The component present was identified as an α -(1,5)-arabinobiose, which confirms the HPAEC results (data not shown). The NMR data are in agreement with data for α -(1,5)-arabinobiose¹¹.

Trimers

HPAEC analysis of pools III_{30} and III_{100} reveals a major peak in the HPAEC chromatogram at 19.1 min for both samples, not co-eluting with any linear α -(1,5)-linked AOS standard (**Figures 2B** and **3B**). MALDI-TOF MS indicates the presence of an oligomer with a degree of polymerization (DP) of 3 for both pools. Apparently, both pools contain the same AOS (denoted 3.1) with a purity of > 90% determined by HPAEC. NMR analysis was carried out with pool III_{30} . The major component (3.1) could be assigned as a dimeric α -(1,5)-linked arabinan backbone with an α -(1,3)-linked arabinose residue at the non-reducing end (**Table 3**; structure 3.1) due to the following NMR characteristics: compared to the data for α -(1,5)-arabinobiose, the α -(1,3)-linkage of a third arabinose residue (**Table 3**, T-residue) is indicated by a cross-peak in the HMBC between H-1 of this T-residue and the C-3 of the A-residue (**Figure 4**, T1/A3). The downfield shift of 5.6 ppm for C-3 in the arabinose A-residue relative to the C-3 of the T-residue of an α -(1,5)-arabinobiose and the smaller upfield shifts for C-2 and C-4 of 1.4 ppm and 0.8 ppm, respectively, confirm the α -(1,3)-linkage of the arabinose T-residue (**Table 2**¹²⁻¹⁴). To enable the distinction between the linear α -(1,5)-linked arabinotriose (3.0) and the novel branched arabinotriose, the peak at 19.1 min was denoted 3.1.

Tetramers

Pools IV_{30} and IV_{100} contain oligomers of DP 4 as analyzed with MALDI-TOF MS (**Figures 2B** and **3B**, inset tables). HPAEC analysis of IV_{30} showed one major peak, which elutes at the retention time of the linear α -(1,5)-linked arabinotetraose (**Figure 2B**; 22.3 min). To investigate if a co-eluting branched AOS is present, pool IV_{30} has been analyzed by NMR. In the ¹³C-spectra of pool IV_{30} the downfield shift of 5.4 ppm for the C-5 of the A-residue (**Tables 2** and **3**; structure 4.2) compared to the A-residue of the component 3.1 in pool III_{30} indicates the presence of an additional α -(1,5)-linked residue. An upfield shift of 1.5 ppm for the C-4 of the A-residue (**Table 2**) and a HMBC cross-peak

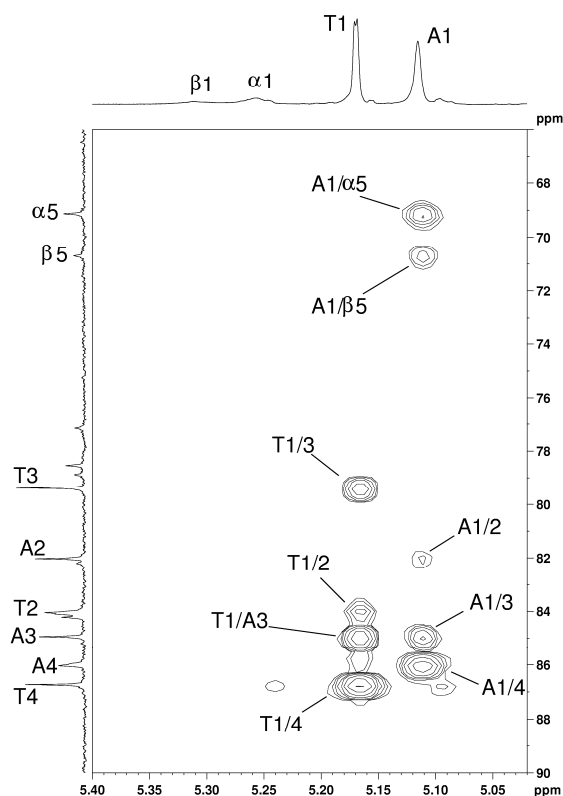


Figure 4 [^1H , ^{13}C]-HMBC spectrum of pool III_{30} (zoom at 5.40–5.00 ppm (^1H) and 66–90 ppm (^{13}C), respectively); T and A as indicated in **Tables 2** and **3**.

between H-1 of the T5-residue and C-5 of the A-residue confirms the presence of an α -(1,5)-linked T5-residue (**Table 2**). Following these NMR data, the component present in pool IV_{30} (denoted 4.2) could be assigned as a trimeric α -(1,5)-linked arabinan backbone with an α -(1,3)-linked arabinose residue attached at the middle arabinose unit (**Table 3**; structure 4.2). Thus, NMR data reveal that the main tetrameric component in the D-30 digest is a branched AOS (4.2) instead of the linear α -(1,5)-linked AOS (4.0). These two structures are apparently coeluting in HPAEC with the separation conditions used.

According to HPAEC analysis, the pool IV_{100} contains two major peaks (**Figure 3B**; 18.2 min (denoted 4.1) and 22.3 min (4.0 or 4.2)) next to a number of minor peaks. NMR analysis confirms the presence of two major components. The first component is identical to the one assigned in pool IV_{30} (4.2). The second component could be identified having an

H-1 signal shifted downfield to 5.253 ppm of the A-residue (**Tables 2 and 3**; structure 4.1). The HMBC shows a cross-peak with the C-2 of this residue (arabinose-A), and from this C-2 a cross-peak with another H-1 can be found in the HMBC, indicating an α -(1,2)-linkage. Signals for an α -(1,3)-linked T3-residue were also found. Compared to pool *III*₃₀ (3.1), the C-2 of the A-residue is shifted downfield with 6.0 ppm and the C-3 and C-1 are shifted upfield with 2.0 ppm and 1.1 ppm, respectively (**Table 2**), confirming the α -(1,2)-linkage of the T2-residue in pool *IV*₁₀₀ (4.1). Conclusively, the NMR data reveal the second component (denoted 4.1) as a dimeric α -(1,5)-linked arabinan backbone with an α -(1,2)-linked and an α -(1,3)-linked arabinose residue at the non-reducing end (**Table 2**; structure 4.1).

Pentamers

MALDI-TOF MS reveals that only oligomer(s) with DP 5 are present in both pools (*V*₃₀ and *V*₁₀₀, inset table in **Figures 2B and 3B**). According to HPAEC, pool *V*₃₀ consists of two major oligosaccharides present in about equal amounts (**Figure 2B**; denoted 5.1 and 5.2; 22.6 min and 26.5 min, respectively), whereas pool *V*₁₀₀ showed the presence of only one major peak at 22.6 min (denoted 5.1; **Figure 3B**).

The first component (5.1; 22.6 min) elutes close to the retention time of the linear α -(1,5)-linked arabinotetraose (**Figure 3B**; 4.0; 22.3 min). The second component, present in *V*₃₀, represents another DP 5-AOS (5.2; 26.5 min; **Figure 3B**) with substantially different retention behavior compared to AOS 5.1, but with a similar retention behavior compared to the linear α -(1,5)-linked arabinopentaose (5.0; 25.6 min). For further characterization of the AOS 5.1, the pool *V*₁₀₀ was analyzed by NMR as this pool contains the AOS in high purity. In pool *V*₁₀₀ all signals for the A-residue typical for (1,2), (1,3), and (1,5)-linkages as identified in *IV*₃₀ and *IV*₁₀₀ are present. Firstly, the H-1 at 5.26 ppm and the C-2 at 87.8 ppm indicate a (1,2)-linkage. Secondly, the chemical shift of C-3 at 83.12 ppm, which results from the combination of a downfield shift due to a (1,3)-linkage and a small upfield shift due to a (1,2)-linkage, indicates a (1,3)-linkage in combination with a (1,2)-linkage. Thirdly, the C-5 at 68.88 ppm indicates a (1,5)-linkage (**Table 2**). These data are in good agreement with Capek et al.¹¹. In the HMBC cross-peaks between all three terminal residues (T2, T3, and T5) and the A-residue could be assigned (**Figure 5**), resulting in a structure as shown in **Table 3** (structure 5.1). The cross-peaks denoted as X (most likely C-4) and Y are not belonging to the main component as is clear from the ¹³C-spectrum, in which the signals belonging to this cross-peak are too low. The signals are

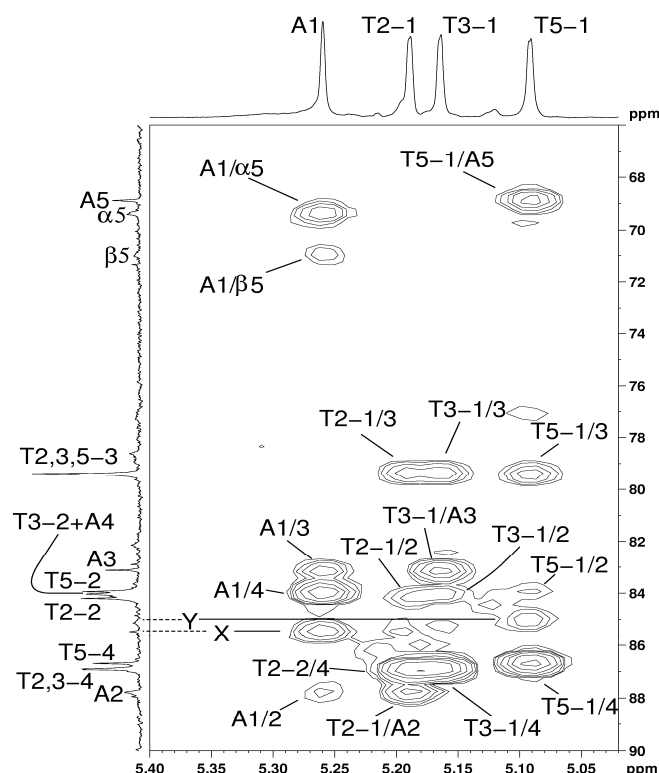


Figure 5 [^1H , ^{13}C]-HMBC spectrum of pool V_{100} (zoom at 5.40–5.00 (^1H) and 66–90 (^{13}C), respectively); T_n , A, B and C as indicated in **Tables 2** and **3**; X and Y are explained in the text.

visible in the HMBC due to the higher sensitivity of this proton detected 2D experiment and due to the high intensity of cross-peaks between H-1 and C-4 in arabinoses.

Although a mixture of two major compounds was present in pool V_{30} , with component 5.1 (pool V_{100}) as one of them, it was possible to determine the structure of the second compound, because of the presence of three characteristic signals: A signal at 86.08 ppm, assigned as C-4 of the B-residue with only an α -(1,3)-linked arabinose attached to it (compare with pool III_{30} (3.1)), and two signals at 85.18 ppm and 84.95 ppm for the A-residue and B-residue, respectively (**Tables 2** and **3**). This is typical for C-3 signals in arabinoses with only α -(1,3)-linked arabinose attached to it. Due to proximity of these two C-3 signals, the almost identical assignments for the two T3-residues and the lower resolution of the 2D HMBC experiment, only one combined cross-peak in the HMBC

confirms the two α -(1,3)-linkages. A cross-peak between H-1 of the B-residue and C-5 of the A-residue connects the two α -(1,3)-substituted arabinoses (data not shown). Cross-peaks between the A-residue and the reducing end arabinose complete the assignment of this structure, resulting in the structure as shown in **Table 3** for component 5.2.

HPAEC analysis of the pools VI_{30} and VI_{100} reveals the presence of each one major peak at 28.4 min and 25.5 min, respectively (**Figures 2B** and **3B**). As MALDI-TOF MS shows the presence of only oligomers of DP 6, these AOS are assigned as 6.2 and 6.1, respectively. NMR analysis shows that the pool VI_{30} is similar to pool V_{30} with respect to the presence of two (1,3)-linked residues as indicated by two signals for C-3 at 85.13 and 85.21 ppm (**Table 2**) together with a combined cross-peak with H-1 of the T3-residues, and a cross-peak between H-1 of the B-residue and C-5 of the A-residue (data not shown). In pool VI_{30} the C-4 signal of the B-residue indicates the presence of an additional (1,5)-linked T5-residue, confirmed by a cross-peak between H-1 of the T5-residue and C-5 of the B-residue in the HMBC (data not shown). Following the NMR data, compound 6.2 could be assigned as tetrameric α -(1,5)-linked arabinan backbone with α -(1,3)-substitution of single arabinose residues at the two middle arabinose units as depicted in **Table 3** (structure 6.2).

Hexamers

HPAEC analysis of the pools VI_{30} and VI_{100} reveals the presence of each one major peak at 28.4 min and 25.5 min, respectively (**Figures 2B** and **3B**). As MALDI-TOF MS shows the presence of only oligomers of DP 6, these AOS are assigned as 6.2 and 6.1, respectively. NMR analysis shows that the pool VI_{30} is similar to pool V_{30} with respect to the presence of two (1,3)-linked residues as indicated by two signals for C-3 at 85.13 and 85.21 ppm (**Table 2**) together with a combined cross-peak with H-1 of the T3-residues, and a cross-peak between H-1 of the B-residue and C-5 of the A-residue (data not shown). In pool VI_{30} the C-4 signal of the B-residue indicates the presence of an additional (1,5)-linked T5-residue, confirmed by a cross-peak between H-1 of the T5-residue and C-5 of the B-residue in the HMBC (data not shown). Following the NMR data compound 6.2 could be assigned as tetrameric α -(1,5)-linked arabinan backbone with α -(1,3)-substitution of single arabinose residues at the two middle arabinose units as depicted in **Table 3** (structure 6.2).

In pool VI_{100} signals similar to those in pool IV_{100} could be assigned (**Table 2**), indicating that the same structural element, an arabinose with (1,2)- and (1,3)-linked arabinose residues attached to it, must be present. The two residues between this element and the

reducing end, needed to complete the structure could not be assigned due to a large heterogeneity in the spectra. Thus, even though HPAEC showed only one major peak at 25.5 min, NMR analysis revealed that more than one component must be present, indicating insufficient separation of HPAEC for these compounds.

Heptamers

The pool *VII*₃₀ shows one major peak at 31.2 min during HPAEC analysis (**Figure 2B**; denoted 7.1), co-eluting with the linear α -(1,5)-linked AOS (7.0). MALDI-TOF MS analysis shows the presence of an oligomer of DP 7. NMR analysis shows that the pool *VII*₃₀ has all the features of pool *VI*₃₀: two (1,3)-linked arabinose residues (T3-residues) and one (1,5)-linked T5-residue (**Table 2**). An additional signal at 85.08 ppm, assigned as C-4, indicates the presence of an additional (1,5)-linked arabinose in the backbone. Two positions for this additional residue are possible: Between the two (1,3)-substituted arabinoses (T3) or between the first (1,3)-substituted arabinose (T3) and the reducing end (**Table 3**; structure 6.2). The first possibility with (1,3)-linked residues on the A-residue and the C-residue, respectively, represents the main component in this pool (7.1). HMBC cross-peaks between the H-1 of the C-residue and the C-5 of the B-residue confirm this assignment (data not shown), resulting in the structure as depicted in **Table 3** (structure 7.1). The latter possibility would result in slightly different signals for the C-5 of the reducing end and is found for the component in *VIII*₁₀₀ (see discussion there).

According to HPAEC and MALDI-TOF MS analysis the pool *VII*₁₀₀ contains a mixture of components with DP 6 and DP 7, thus, no further NMR analysis was done for pool *VII*₁₀₀.

Octamers

HPAEC analysis of pool *VIII*₁₀₀ reveals the presence of one major peak at 31.2 min, co-eluting with the linear α -(1,5)-linked arabinooheptaose (7.0) and component 7.1. MALDI-TOF MS results show the presence of mainly DP 8, thus, the unknown component represents an arabinooctaose (denoted 8.1) with a substantially different retention behavior compared to linear α -(1,5)-linked arabinooctaose (8.0; 33.4 min; **Figure 3B**). NMR analysis shows that in pool *VIII*₁₀₀ all signals of a triple substituted arabinose are present as were assigned for *V*₁₀₀ (compare pool *V*₁₀₀ with *VIII*₁₀₀ in **Table 2**). In the HMBC at the position of H-1 of the T3-residues two cross-peaks are found with two different C-3 signals: at 83.07 ppm (C-residue, **Tables 2 and 3**), characteristic for a (1,3)-linkage in

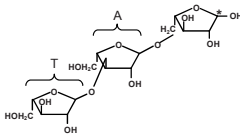
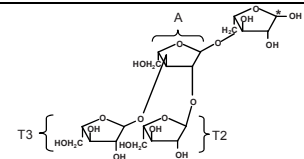
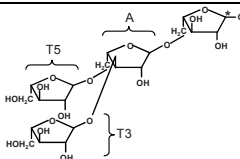
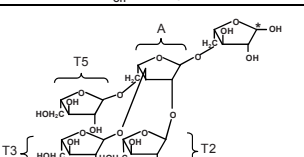
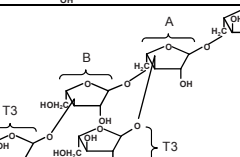
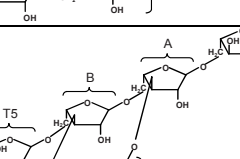
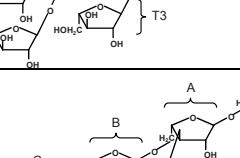

combination with a (1,2)-linkage as mentioned in pool V_{100} , and at 85.12 ppm (B-residue, **Tables 2** and **3**), indicating a (1,3)-linkage without (1,2)-substitution at the same residue (similar to IV_{30} (4.2), V_{30} (5.2), VI_{30} (6.2), and VII_{30} (7.1)). As in VII_{30} a C-4 signal at 85.0 ppm indicates the presence of an additional (1,5)-linked arabinose residue, which is located next to the reducing end due to a clear anomerization effect of this signal (A-residue, **Tables 2** and **3**). This is, furthermore, substantiated by cross-peaks in the HMBC between the H-1 of this A-residue and the C-5 signals of the reducing end (R α/β). The chemical shifts of these C-5 carbons are slightly different for those of all structures with a (1,3)-substituted A-residue, but resembles the chemical shifts found for α -(1,5)-arabinobiose, confirming the presence of an arabinose residue attached to the reducing end with no (1,3)-substitution (**Table 2**). Following all the NMR data, component 8.1, which is present in $VIII_{100}$, has a structure as depicted in **Table 3**.

Overview of AOS identified from sugar beet arabinan

In **Table 3** an overview of the structures of all identified branched AOS derived from sugar beet arabinan is given as based on extensive NMR analysis. All of them consist of an α -(1,5)-linked backbone of L-arabinosyl residues. Two main structural features could be identified among all identified AOS, varying in their type of linkages and the degree of substitution. AOS of the first series contain a structure with double substituted α -(1,2)- and α -(1,3)-linked L-arabinosyl residues (4.1, 5.1, 8.1; **Table 3**, series 1). An additional single substituted α -(1,3)-linked L-arabinosyl residue may be present within the same molecule as identified in component 8.1 (**Table 3**). AOS of the second series carry single substituted α -(1,3)-linked arabinose(s) (**Table 3**; series 2). Components with either one or two α -(1,3,5)-linkages were identified (3.1, 4.2 and 5.2, 6.2, 7.1, respectively).

None of the structures identified was substituted at the arabinose at the reducing end, which is in contrast with the synthesized methyl 2-O-, methyl 3-O- and methyl 5-O- α -L-arabinofuranosyl- α -L-arabinofuranosides as described by Kaneko et al¹⁵. The isolated component 3.1 is similar to an earlier described feruloylated arabinose-oligosaccharide with an α -L-arabinosyl residue linked at O-3 and a ferulic acid attached at O-2 of the non-reducing end of an α -(1,5)-linked dimeric backbone of L-arabinosyl residues, which has been isolated from spinach leaves¹⁶ and sugar beet pulp¹⁷.

Table 3 Structures of arabino-oligosaccharides identified from sugar beet arabinan (series 1 and 2) as obtained after degradation of sugar beet arabinan with the arabinohydrolases Abn1, Abn2, and Abn4 followed by Biogel P2 fractionation (D-30 and D-100, respectively)

	Structures of identified arabino-oligosaccharides from sugar beet arabinan	
	Series 1	Series 2
DP 3		
DP 4		
DP 5		
DP 6		
DP 7		
DP 8		

Almost all AOS of the second series (**Table 3**; 3.1, 4.2, 5.2, 6.2, and 7.1) were exclusively present in the D-30 digest, while the three isolated AOS belonging to the first series were mainly present in the D-100 digest. This indicates a different degradability of the structures by the arabinofuranosidase Abn4. Abn4 seems to be able to remove α -(1,3,5)-linked L-arabinosyl residues (present in the AOS of the second series; **Table 3**), whereas a α -(1,2,3,5)-linked double substituted structure as present in the AOS of the first series (**Table 3**) is not degradable by the arabinofuranosidase Abn4. Further investigation of the precise mode of action and specificity of the arabinohydrolases is currently ongoing.

Conclusions

Eight novel neutral branched AOS have been isolated from sugar beet arabinan after enzyme digestion with two different mixtures of the *C. lucknowense* arabinohydrolases Abn1, Abn2, and Abn4. NMR analysis revealed two series of branched AOS varying in the type of linkage. To the best of our knowledge, this is the first characterization of such branched AOS. These AOS may now be used for (further) characterization of arabinan-specific enzymes as well as for possible exploration of their prebiotic potential.

Acknowledgments

This study is partly carried out with financial support from the Commission of the European Communities (WallNet: 'Functional Genomics for Biogenesis of the Plant Cell Wall', Marie Curie Contract Number: MRTN-CT-2004-512265) and the Dutch Ministry of Economic Affairs via an EOS-LT grant (<http://www.senternovem.nl/eos/index.asp>).

References

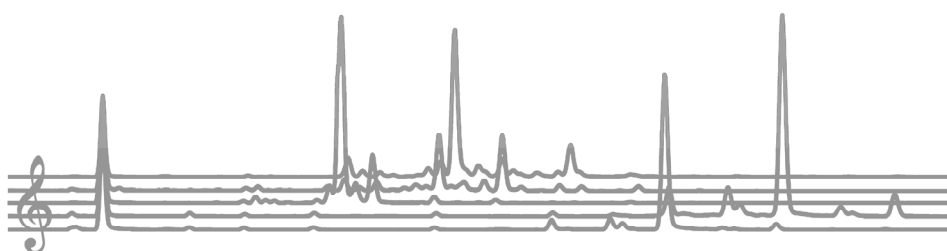
1. Albersheim, P.; Darvill, A.G.; O'Neill, M.A.; Schols, H.A.; Voragen, A.G.J., in: Visser, J., Voragen, A.G.J. (eds), Progress in Biotechnology 14: Pectins and pectinases, proceedings of an Int. Symp., Elsevier, Amsterdam, The Netherlands, **1996**, p. 47-55.
2. Ralet, M.C.; Thibault, J.F. *Biomacromolecules*, **2002**, *3*, 917-925.
3. Ridley, B.L.; O'Neill, M.A.; Mohnen, D.A. *Phytochemistry*, **2001**, *57*, 929-967.

4. Voragen, A.G.J.; Pilnik, W.; Thibault, J.F.; Axelos, M.A.V.; Renard, C.M.G.C. in: Stephen, A.M. (editor), *Food polysaccharides and their applications*, **1995**, Marcel Dekker Inc., New York, USA, p. 287-339.
5. Beldman, G.; Schols, H.A.; Pitson, S.M.; Searle-van Leeuwen, M.F.; Voragen, A.G.J., in Sturgeon, R.G. (Editor), *Advances in Macromolecular Carbohydrate Research*, Vol. 1, JAI Press Inc., Greenwich, United Kingdom, **1997**, p. 1-64.
6. Weinstein, L.; Albersheim, P. *Plant Physiology*, **1979**, *63*, 425-432.
7. Ishii, T. *Plant and Cell Physiology*, **1994**, *35*, 701-704.
8. Levigne, S.V.; Ralet, M.C.J.; Quemener, B.C.; Pollet, B.N.L.; Lapierre, C.; Thibault, J.F.J. *Plant Physiology*, **2004**, *134*, 1173-1180.
9. Kühnel, S.; Hinz, S.W.A.; Pouvreau, L.; Visser, J.; Schols, H.A.; Gruppen, H. *Bioresource Technol.*, *accepted for publication*, DOI 10.1016/j.biortech.2010.05.070.
10. Suzuki, Y.; Tanaka, K.; Nano, T.; Asakura, T.; Muramatsu, N. *Japan Soc. Horticultural Sci*, **2004**, *73* (6), 574-579.
11. Cros, S.; Imbert, A.; Bouchemal, N.; Dupenhoat, C.H.; Perez, S. *Biopolymers*, **1994**, *34*, 1433-1447.
12. Capek, P.; Toman, R.; Kardosova, A.; Rosik, J. *Carbohydr. Res.*, **1983**, *117*, 133-140.
13. Dourado, F.; Cardoso, S.M.; Silva, A.M.S.; Gama, F.M.; Coimbra, M.A. *Carbohydr. Polym.*, **2006**, *66*, 27-33.
14. Cardoso, S.M.; Silva, A.M.S.; Coimbra, M.A. *Carbohydr. Res.*, **2002**, *337*, 917-924.
15. Kaneko, S.; Kawabata, Y.; Ishii, T.; Gama, Y.; Kusakabe, I. *Carbohydr. Res.*, **1995**, *268*, 307-311.
16. Ishii, T.; Tobita, T. *Carbohydr. Res.*, **1993**, *248*, 179-190.
17. Colquhoun, I.J.; Ralet, M.C.; Thibault, J.F.; Faulds, C.B.; Williamson, G. *Carbohydr. Res.*, **1994**, *263*, 243-256.
18. McCleary, B.V.; Cooper, J.M.; Williams, E.L. *Pat. Application*, GB 88283809, **1989**.
19. Tollier, M.T.; Robin, J.P. *Ann. Technol. Agric.*, **1979**, *28*, 1-15.
20. Ahmed, E.R.A.; Labavitch, J.M. *J. Food Biochem.*, **1978**, *1*, 361-365.
21. Verhoef, R.; Beldman, G.; Schols, H.A.; Siika-Aho, M.; Ratto, M.; Buchert, J.; Voragen, A.G.J. *Carbohydr. Res.*, **2005**, *340*, 1780-1788.

Chapter 5

LC/CE-MS tools for the analysis of complex arabino-oligosaccharides

Westphal, Y., Kühnel, S., Schols, H.A., Voragen, A.G.J., Gruppen, H.,
Carbohydrate Research, *accepted for publication*.



Abstract

Recently, various branched arabino-oligosaccharides as present in a sugar beet arabinan digest were characterized using NMR. Although HPAEC often has been the method of choice to monitor the enzymatic degradation reactions of polysaccharides, it was shown that HPAEC was incapable to separate all known linear and branched arabino-oligosaccharides present. As this lack of resolution might result in an incorrect interpretation of the results, other separation techniques were explored for the separation of linear and branched arabino-oligosaccharides. The use of porous-graphitized carbon liquid chromatography with evaporative light scattering and mass detection as well as capillary electrophoresis with laser-induced fluorescence and mass detection demonstrated the superiority of both the techniques toward HPAEC by enabling the separation and unambiguous identification of almost all the linear and branched arabino-oligosaccharides available. The elution behavior of all arabino-oligosaccharides for the three tested separation techniques was correlated with their chemical structures and conclusions were drawn for the retention mechanisms of the arabino-oligosaccharides on the different chromatographic and electrophoretic systems. The combination of the elution/migration behavior on LC/CE and the MS fragmentation patterns of the arabino-oligosaccharides led to the prediction of structures for new DP 6 arabino-oligosaccharides in complex enzyme digests.

Introduction

Arabinans are branched polysaccharides with a linear backbone of α -(1,5)-linked arabinosyl residues, which can be single or double substituted at O-2 and/or O-3 with α -linked L-arabinosyl residues, which again may be further branched^{1,2}. In addition, the arabinan of sugar beet cell walls can be feruloylated at the O-2 and/or O-5 position of one of the arabinose moieties^{3,4}.

Recently, the degradation of sugar beet arabinan by using pure and well-defined arabinohydrolases from *Chrysosporium lucknowense*⁵ was described. Two distinct series of branched arabino-oligosaccharides (AOS) were isolated and identified using NMR analysis⁶. The first series consists of oligomers having a backbone of α -(1,5)-linked L-arabinosyl residues, of which some are double substituted with α -(1,2)- and α -(1,3)-linked L-arabinosyl residues. An additional single substitution of α -(1,3)-linked L-arabinose may be present⁶. The second series contains oligomers having a backbone of α -(1,5)-linked L-arabinosyl residues being substituted on one or two places with a single α -L-(1,3)-linked arabinose unit.

For the elucidation of the fine structure of arabinans derived from various sources and for the identification and characterization of novel arabinan degrading enzymes, the separation and detection of as many as possible linear and branched AOS within a complex arabinan enzyme digest are desirable. Chromatographic separation of the linear α -(1,5)-linked AOS, similar to many other oligosaccharides, is generally performed by high-performance anion-exchange chromatography (HPAEC) in combination with a pulsed amperometric detector (PAD)⁵⁻⁸. However, recently it was shown that HPAEC-PAD has insufficient resolution to separate all linear and branched AOS⁶. Various AOS were co-eluting, which can result in an incorrect interpretation of AOS present in a complex mixture. Therefore, other separation techniques are required.

Capillary electrophoresis with laser-induced fluorescence detection (CE-LIF) has been reported to be a suitable tool to analyze complex oligosaccharides derived from cell wall polysaccharides in a short time (20 min⁹⁻¹²). Furthermore, CE-MSⁿ analysis allows the identification of (unknown) cell wall-derived oligosaccharides in complex mixtures^{9,10}. Porous-graphitized carbon liquid chromatography with evaporative light scattering and mass detection (PGC-HPLC-ELSD/MS) was recently introduced to a broad range of oligosaccharides derived from cell wall polysaccharides including linear α -(1,5)-linked

AOS¹³. Good separation of many neutral oligosaccharides was demonstrated following a distinct mechanism based on planarity of the oligosaccharides.

In this study, both CE-LIF(-MS) and PGC-HPLC-ELSD/MS were explored on their capability to be used for the simultaneous separation and detection of the linear and branched AOS in complex mixtures. The combination of elution/migration behavior on LC and CE, and the MS fragmentation patterns will be discussed with respect to their potential as prediction tools for unknown arabino-oligosaccharide structures within complex mixtures whenever NMR analysis is not possible due to the heterogeneity of the sample.

Materials and Methods

Materials

Linear α -(1,5)-linked AOS (DP 2-8) were purchased from Megazyme International Ltd (Bray, Ireland), and were denoted 2.0, 3.0, 4.0, 5.0, 6.0, 7.0, and 8.0, respectively. Branched AOS were isolated from sugar beet arabinan by enzyme digestions with pure arabinohydrolases (Abn1, Abn2, and Abn4, *Chrysosporium lucknowense*) followed by purification of the branched oligosaccharides⁶. These fractions containing purified AOS were used for the identification of peaks in the different separation techniques. An overview of all the linear and branched AOS is given in **Table 1**. To produce a suitable sample, two arabinan digests (D-30 and D-100)⁶ were mixed 1:1 to ensure a complex arabinan enzyme digest for comparative analysis. This mixture will be referred to as D-30/100.

High performance anion-exchange chromatography with pulsed amperometric detection

An HPAEC system (ICS-3000, Dionex Corporation, Sunnyvale, CA, USA) was equipped with a CarboPac PA-1 column and a CarboPac PA-1 guard column (2 mm ID x 250 mm and 2 mm ID x 25 mm; Dionex Corporation). A flow of 0.3 mL/min was used and the temperature was kept at 20 °C. AOS (injection volume 10 μ L; 10 to 100 μ g/mL) were separated using a gradient with 0.1 M NaOH (A) and 1 M NaOAc in 0.1 M NaOH (B): 0-36 min from 0% B to 42% B, 36-42 min at 100% B and 42-57 min at 0% B⁶.

Table 1 Overview of the chemical structures and simplified representations of linear and branched arabino-oligosaccharides (AOS) derived from sugar beet arabinan (DP 3-8) – part I.

Structures of AOS (DP 3-8)		
Component	Chemical structure	Simplified structure
Series 0 (linear α-(1,5)-linked AOS)		
3.0-8.0		
Series 1 (branched AOS with α-(1,2)- and α-(1,3)-substitution)		
4.1		
5.1		
8.1		

Table 1 Overview of the chemical structures and simplified representations of linear and branched arabinooligosaccharides (AOS) derived from sugar beet arabinan (DP 3-8), part II.

Structures of AOS (DP 3-8)		
Component	Chemical structure	Simplified structure
Series 2 (branched AOS with single α -(1,3)-substitution)		
3.1		
4.2		
5.2		
6.2		
7.1		

Porous-graphitized-carbon liquid chromatography with evaporative light scattering and mass detection

PGC-HPLC-ELSD/MS was performed on a Thermo Accela UHPLC system (Waltham, MA, USA) equipped with a Hypercarb column (PGC, 100 x 2.1 mm, 3 μ m) in combination with a Hypercarb guard column (10 x 2.1 mm, 3 μ m Thermo Electron Corporation). Elution was performed with a flow rate of 0.4 mL/min and a column oven temperature of 70 °C. The injection volume was set to 10 μ L (0.1-0.4 mg/mL for purified AOS and 5 mg/mL for sugar beet arabinan digest D30/100). The following eluents were used: Millipore water (A), acetonitrile (B) and 0.2% (w/v) trifluoroacetic acid (TFA) in water (C). To all the eluents 25 μ M lithium acetate was added to ensure lithium adduct formation of all components during the MS analysis. The following elution profile was used: 0-1 min, isocratic 100% A, 1-15 min, linear gradient from 0-27.5% (v/v) B, 15-28 min linear gradient from 27.5-60% B and concomitant linear gradient from 0-10% (v/v) C, 28-31 min linear gradient from 60-80% B and from 10-20% C, 31-35 min isocratic 80% B and 20% C, 35-36 min from 80% B and 20% C to 100% A, 36-41 min equilibration with 100% A. The PGC-column was coupled to a 1:1-splitter (Accurate, Dionex Corporation) directing the eluent both to an ELSD 85 evaporative light scattering detector (Sedere, Alfortville, France) and to an ESI-MSⁿ-detector (LTQ XL MS, ion trap, Thermo Electron Corporation, Sunnyvale, CA, USA). The drift tube temperature of the ELSD was set to 50 °C and the gain to 12. MS-detection was performed in positive mode using a spray voltage of 4.6 kV and a capillary temperature of 260 °C and auto-tuned on arabinotetraose (m/z 553). The ion trap was closed either after 10 ms or when an intensity of 3×10^5 was reached to enable the detection of minor components and to avoid the overload of the MS by abundant components. The MSⁿ-experiments were performed using wide band activation and based on dependent scan-settings (Xcalibur software, Thermo Electron Corporation).

For modeling of the 3D-structure of the linear and branched AOS the software ChemBio Office 2010 (CambridgeSoft Corporation, Cambridge, MA, USA) was used.

Capillary electrophoresis with laser-induced fluorescence and MS detection

Labeling of samples and standards

CE-LIF analysis

To about 0.1 mg of sample D-30/100 and 20 nmol of each purified AOS, 5 nmol maltose was added as internal standard and mobility marker. These mixtures were dried using the

SpeedVac Concentrator Savant ISS110 (Thermo Electron Corporation) and subsequently labeled with the fluorescent 9-aminopyrene-1,4,6-trisulfonate (APTS) for 90 min at 60 °C using the ProteomeLab Carbohydrate Labeling and Analysis Kit (Beckman Coulter, Fullerton, CA, USA). The derivatized samples (4 µL) were diluted 500 times prior to CE-LIF analysis.

CE-MS analysis

Arabinose and arabinobiose present in sample D-30/100 were removed prior to CE-MS analysis by solid phase extraction (SPE) on non-porous graphitized carbon cartridges (150 mg; Alltech, Deerfield, IL, USA) as described previously¹¹. Two percent acetonitrile in water (v/v) was used to elute the arabinose and arabinobiose, the oligomers of DP ≥ 3 were eluted with 25% acetonitrile in water (v/v). After air-drying of the 25% acetonitrile (v/v) fraction, the material was re-dissolved in Millipore water.

Purified AOS (~ 50 nmol) and the SPE-treated sample D-30/100 (0.1 mg carbohydrate) were labeled as described above. Ten nmol maltose was added as internal standard and mobility marker. The derivatized samples (4 µL) were diluted 37.5 and 125 times for the SPE-treated sample D-30/100 and the purified AOS standards, respectively, prior to CE-LIF-MS analysis.

Capillary electrophoresis with laser-induced fluorescence detection

CE-LIF was performed on a ProteomeLab PA 800 characterization system (Beckman Coulter, Fullerton, CA, USA), equipped with an internal laser-induced fluorescence detector (LIF; excitation: 488 nm, emission 520 nm; Beckman Coulter) and a polyvinyl alcohol (N-CHO)-coated capillary (50 µm ID x 50.2 cm (Beckman Coulter), detector after 40 cm), kept at 25 °C. Samples were loaded hydrodynamically (7 s at 0.5 psi) on the capillary. Separation was performed in the reversed polarity mode (30 kV, 20 min) in 25 mM acetate buffer (pH 4.75) containing 0.4% polyethylene oxide as provided in the ProteomeLab Carbohydrate Labeling and Analysis Kit (Beckman Coulter). Peaks were integrated manually using Chromeleon software 6.8 (Dionex Corporation).

Capillary electrophoresis with mass detection

CE-MS was performed on a P/ACE™ System MDQ (Beckman Coulter). Opposite to CE-LIF, for CE-MS analysis a fused silica capillary (50 µm ID x 85 cm (Beckman Coulter)) and MS compatible buffers were used. This CE-MS set-up results in a 5-6 times

increase of the migration time (~ 50-60 min) and a significant loss of resolution compared to CE-LIF analysis. A capillary window after 60 cm was fitted with an ellipsoid for LIF detection to enable the monitoring of the elution profile prior to MS analysis. An external LIF detector was used (excitation: 488 nm, emission: 520 nm; Picometrics ZetaLIF discovery system; Picometrics, Toulouse, France). LIF signals were sent to Beckman 32Karat software via an Agilent SSXL4002 converter (Agilent Technologies, Santa Clara, CA, USA). Separation was performed in the reversed polarity mode (20 kV, 60 min) in 0.3% (v/v) formic acid at a capillary temperature of 15 °C. Samples were injected for 2 s at 10 psi¹⁰.

The ESI-MS (LTQ, ion trap, Thermo Electron Corporation) was operated in negative mode using a spray voltage of 2.0 kV and an MS-capillary temperature of 190 °C. The end of the CE capillary was installed in front of the ESI source by leading it through a T-part designed in our laboratory¹⁹ and provided the coaxial addition of a sheath liquid (50/50 isopropanol/water) at 2.5 µL/min via a 5 mL syringe (Hamilton, Reno, NV, USA) coupled to an automated syringe pump (Pump 11 Pico Plus, Harvard apparatus, Holliston, MA, USA). Mass spectra were acquired from m/z 300 to 1500. MSⁿ was performed in the data-dependent mode using a window of m/z 1 and collision energy of 38%. MSⁿ data were interpreted using Xcalibur software 2.0.7 (Thermo Electron Corporation). Base peak chromatograms are shown in their smoothed forms.

Results and discussion

Separation of AOS with HPAEC-PAD, PGC-HPLC-ELSD/MS and CE-LIF(-MS)

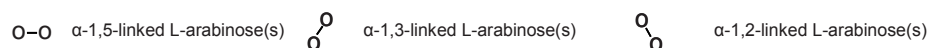
Recently, a range of branched AOS derived from sugar beet arabinan was purified and characterized⁶. Two arabinan digests were produced enzymatically (D-30 and D-100) containing several branched AOS⁶. In this study, these two enzyme digests were mixed in a ratio of 1:1 resulting in a complex mixture of branched AOS. This sample, referred to as D-30/100, as well as linear and branched AOS standards (**Table 1**), were analyzed with three different separation tools (HPAEC-PAD, PGC-HPLC-ELSD/MS, and CE-LIF-MS) to explore the capability of these separation techniques for the characterization of AOS. An overview of the retention times and the relative migration times of all AOS under investigation is given in **Table 2**.

Table 2 Overview of the retention times of various linear and branched AOS on HPAEC-PAD and PGC-HPLC-ELSD/MS, and the relative migration times of these AOS on CE-LIF.

Component	Schematic structure	Retention time [min]		Relative migration time ^a
		HPAEC	PGC-HPLC ^b	CE-LIF ^c
1.0		3.9	< 1.2	0.864
2.0		14.2	3.5	0.972
3.0		19.1	7.4	1.078
4.0		22.3 ^j	9.8	1.188
5.0		25.7 ^f	11.3 ^l	1.293 ^m
6.0		28.6 ^e	12.7	1.398
7.0		31.1 ⁱ	13.8 ^k	1.500
8.0		33.4	14.9	1.605
3.1		19.1	7.1	1.056
4.2		22.3 ^j	9.3	1.146
5.2		26.5	10.7	1.230
6.2		28.5 ^e	12.1	1.313
7.1		31.2 ⁱ	13.4	1.413
4.1		18.2	8.5	1.139
5.1		22.6	10.3	1.211
8.1		31.2 ⁱ	13.9 ^k	1.470
6.1a ^d	not known	25.5 ^f	11.4 ^l	1.297 ^m
6.1b ^d	not known	25.5 ^f	11.7	1.354

^a Migration time in relation toward maltose.^b Retention time based on MS detection.^c CE-LIF measurements.^d 6.1a and 6.1b may be interchanged for CE and PGC-HPLC measurements; in HPAEC denoted as 6.1^{e,f,g,h,i,j,k,l,m} Components carrying the same superscript letter co-elute.

* reducing end



HPAEC-PAD

In **Figure 1** the HPAEC-PAD elution pattern of sample D-30/100 is given. The identification of the AOS is based on the analysis of purified linear and branched AOS (**Table 1**). The retention times are listed in **Table 2** indicating co-elution with letters in superscript. Only about half of the AOS present in the D-30/100 sample were separated when using HPAEC and the gradient used (**Figure 1** and **Table 2**), while 56% of the AOS co-elute with at least one other AOS as already discovered earlier⁶. Online- or offline-coupled MS analysis will not support the identification of co-eluting AOS having the same degree of polymerization (DP) (e.g., 4.0 and 4.2, 6.0 and 6.2, 7.0 and 7.1), even though it might support the identification of co-eluting components differing in their DP (e.g., 5.0 and 6.1, 7.0/7.1 and 8.0). As the additional benefit of MS analysis for the characterization of complex arabinan digests is rather low due to insufficient separation and resolution, no further experiments were performed with offline- and online-MS coupling.

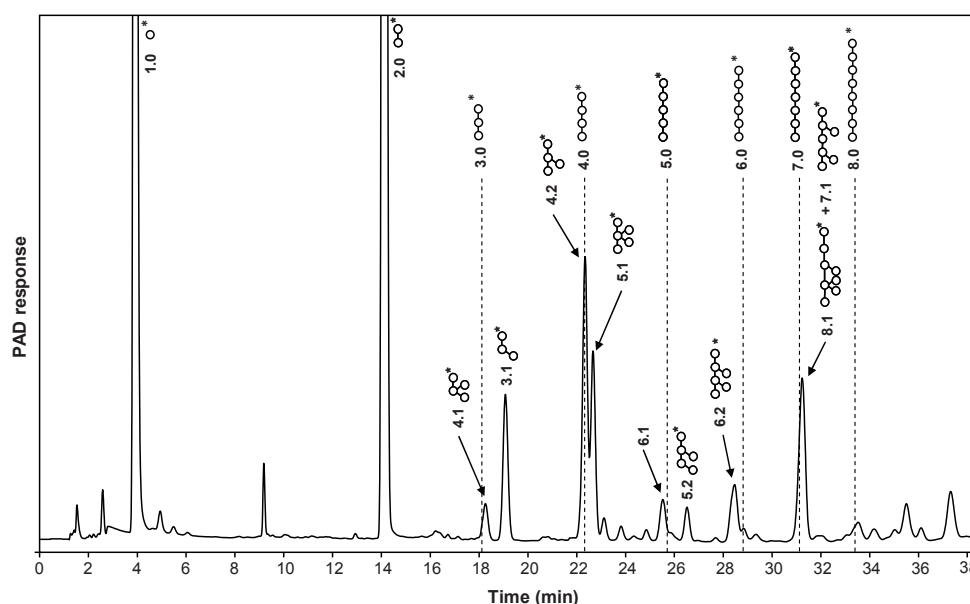


Figure 1 HPAEC-PAD elution pattern of the AOS sample D-30/100 including numerical and graphical annotation according to **Table 1**, indication of linear α -(1,5)-linked AOS with dashed lines (DP 1-8; denoted as 1.0-8.0).

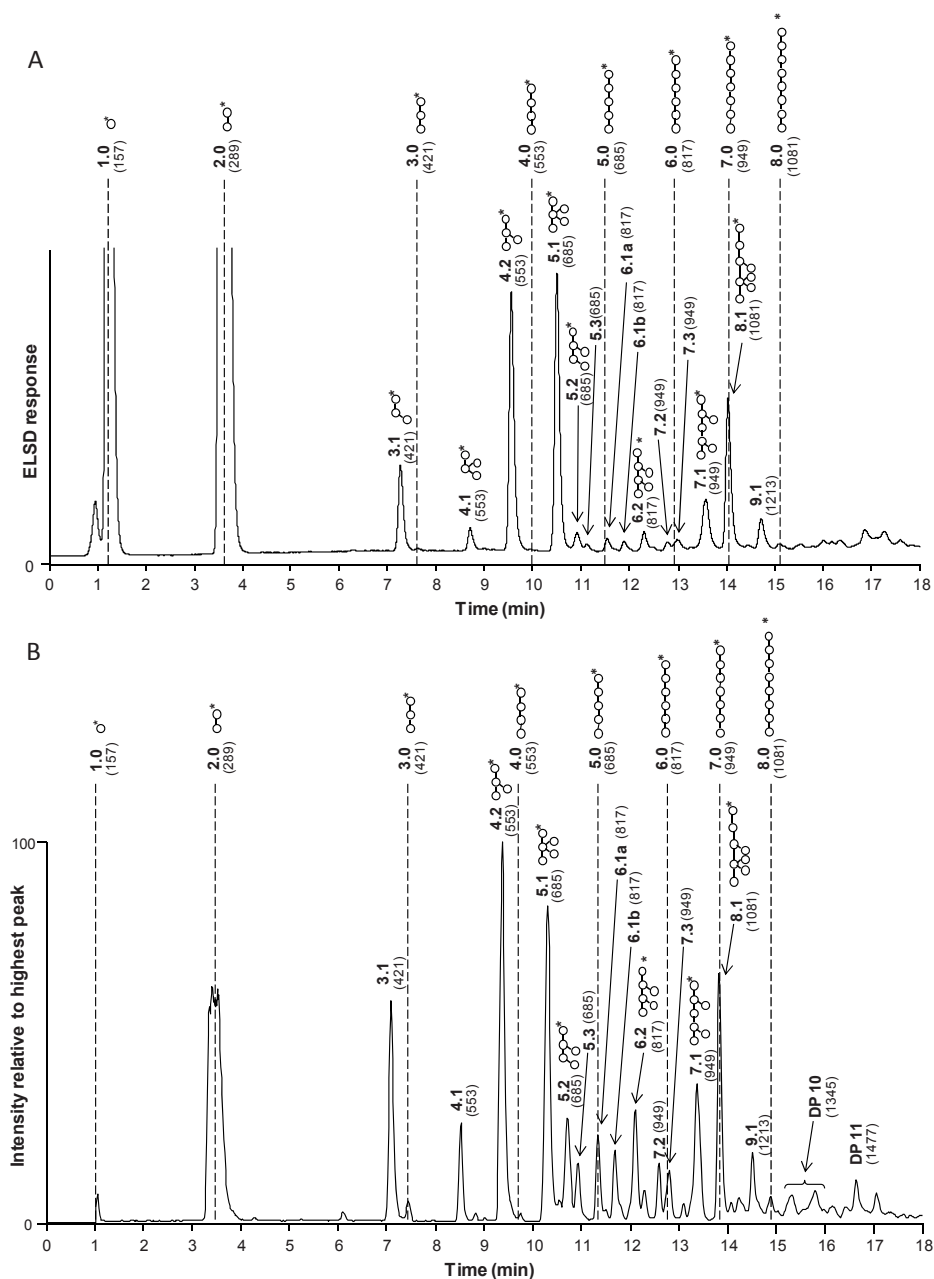


Figure 2 PGC-HPLC elution pattern of the AOS sample D-30/100 including numerical and graphical annotation according to **Table 1**: ELS-pattern (**A**) and MS base peak chromatogram (**B**); indication of linear α -(1,5)-linked AOS with dashed lines (DP 1-8; denoted as 1.0-8.0).

PGC-HPLC-ELSD/MS

In **Figure 2** the PGC-HPLC elution patterns with ELS- (**Figure 2A**) and MS- (**Figure 2B**) detection of the sample D-30/100 are presented. Numerical and graphical presentations of the identified AOS are added based on retention times and online-recorded MS spectra of the purified linear and branched AOS. The differences in the response between ELS- and MS-detection can be explained by two factors: 1) the logarithmical detection of the ELSD, and 2) the flexible closing of the ion trap during MS detection. Using a flexible ion trap time allows the mass spectrometric analysis of compounds present in very low amounts, although minor compounds will be overestimated during MS analysis this way. The online-MS-coupling of PGC-HPLC ensures MSⁿ data for all the peaks present in the ELSD chromatogram without any loss of resolution (**Figure 2A** and **2B**). About 80% of all AOS present in D-30/100 were separated using PGC-HPLC-ELSD/MS (**Figure 2** and **Table 2**). Opposite to HPAEC, PGC-HPLC-ELSD/MS enabled for example the separation of the arabinotetraoses 4.0 and 4.2 as well as the arabinohexaoses 6.0 and 6.2. Furthermore, the analysis of the purified fraction (pool VI₁₀₀⁶) containing AOS 6.1 revealed the presence of two main components instead of one component as was suggested by HPAEC analysis. Online-MS data for both the peaks revealed the presence of only DP 6-AOS (*m/z* 817), and thus these AOS were denoted as 6.1a and 6.1b in **Figure 2** and **Table 2**.

Only four of the eighteen AOS under investigation co-elute on PGC-HPLC-ELSD/MS (**Figure 2** and **Table 2**): 1) AOS 5.0 and 6.1a (11.3-11.4 min), and 2) AOS 7.0 and 8.1 (13.8-13.9 min). Due to the performed online-coupled MS analysis the identification of these co-eluting AOS is possible as the corresponding *m/z*-values differ due to different degrees of polymerization. Furthermore, with PGC-HPLC-ELSD/MS analysis, some unknown AOS became visible (e.g., denoted as 5.3, 7.2, 7.3, and 9.1 in **Figure 2**), which represent unidentified branched AOS.

CE-LIF(-MS)

To explore the capability of both CE-LIF and CE-MS to separate all AOS under investigation, various purified linear and branched AOS (**Table 1**) and the sample D-30/100 were derivatized and the labeled AOS were subjected to CE-LIF and CE-MS analysis, respectively.

In **Figure 3** the CE-LIF electropherogram of sample D-30/100 is presented, including graphical and numerical annotations of the AOS (**Table 1**). About 90% of the AOS under investigation were separated by CE-LIF: only AOS 5.0 and 6.1a co-migrated (6.4 min;

Figure 3). In **Table 2** an overview of the relative migration times of all AOS is given. As migration times may vary slightly in between CE-LIF runs, it was chosen to list the migration times normalized on the internal standard and mobility marker maltose resulting

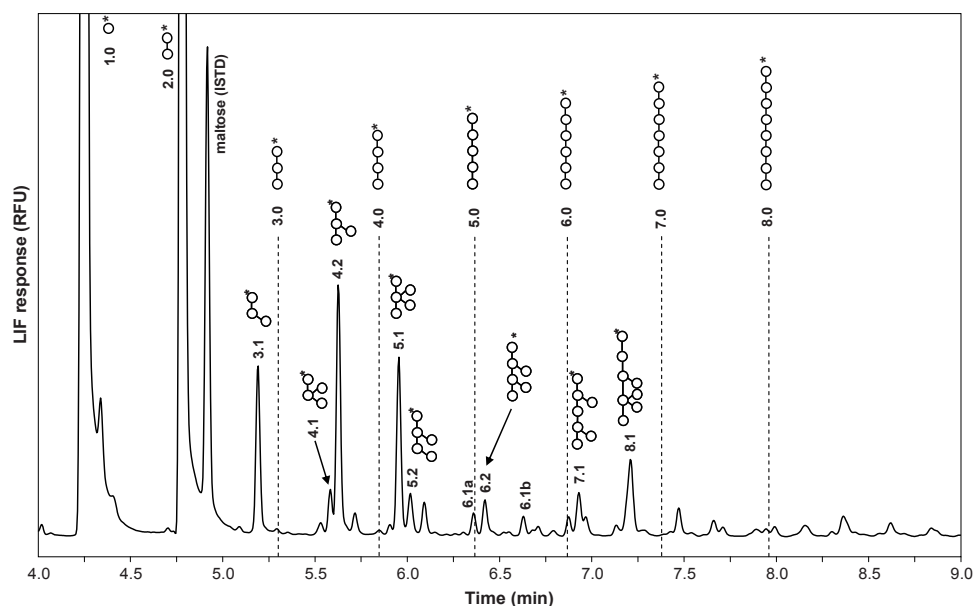


Figure 3 CE-LIF migration pattern of the AOS sample D-30/100 including numerical and graphical annotation of the AOS according to **Table 1**; indication of linear α -(1,5)-linked AOS with dashed lines (DP 1-8; denoted as 1.0-8.0).

in relative migration times (**Table 2**). Co-elution of AOS 4.1 and 4.2 as well as AOS 5.1 and 5.2 in CE-MS analysis due to the significant lower resolution compared to CE-LIF analysis prevents the identification of these components based on CE-MSⁿ experiments. In agreement with PGC-HPLC-MS/ELSD, CE-LIF analysis of the purified fraction containing the DP 6-AOS 6.1a and 6.1b (pool VI_{100}^6) confirmed the presence of two components (**Figure 3**). The annotation of both components as hexamers was confirmed by CE-MS analysis (m/z 624.6, representing a DP 6-AOS with APTS ($z = -2$) label attached).

Even though MSⁿ data is limited for a few AOS, CE-MS analysis can support the identification of (unknown) peaks in the CE-LIF electropherogram.

Correlation of elution/migration times and the degree of polymerization for AOS

To explore the elution behavior of the linear and branched AOS using all three separation tools in more detail and to evaluate the potential of these separation techniques to be used as a tool to predict the structure of (unknown) AOS, the retention times or the relative migration times were evaluated in more detail.

HPAEC-PAD

In **Figure 4A** the retention times using HPAEC-PAD are plotted against the DP for all the linear and branched AOS of DP 2 to 8 (**Table 1**). In general, the retention times of the AOS increase with increasing DP (**Figure 4A**). Having the same DP, AOS carrying single α -(1,3)-linked L-arabinosyl residues (series 2, **Table 1**) have a very similar retention behavior compared to the linear α -(1,5)-linked AOS. For DP 4, DP 6, and DP 7, the corresponding AOS even co-elute (4.0 and 4.2, 6.0 and 6.2, 7.0 and 7.1). For DP 3 and DP 5, the corresponding AOS (3.0 and 3.1, and 5.0 and 5.2) are separated. The substitution of an α -(1,3)-linked L-arabinosyl residue(s) at the middle arabinose(s) within the α -(1,5)-linked backbone, as is the case for AOS 4.2, 6.2 and 7.1 (**Table 1**), does not affect the retention times significantly compared to the linear α -(1,5)-linked AOS resulting in co-elution. In contrast, the presence of an α -(1,3)-linked L-arabinosyl residue attached at the non-reducing end prolongs the retention time in that range that it results in good separation of those AOS (3.1 and 5.2) from the corresponding linear α -(1,5)-linked AOS (3.0 and 5.0, respectively; **Figure 4A**). AOS carrying a double substituted α -(1,2,3,5)-linked structure within the molecule (AOS 4.1, 5.1 and 8.1, **Table 1**) elute significantly earlier compared to the corresponding linear α -(1,5)-linked AOS (4.0, 5.0 and 8.0, **Table 1**) and branched AOS carrying single α -(1,3)-linked L-arabinosyl residues (AOS 4.2, 5.2, **Table 1**). This tremendous decrease of retention in HPAEC due to a double substituted α -(1,2,3,5)-linked structure might be due to a conformational change resulting in a lower interaction of the oxyanions, which are formed at pH 12, with the functional groups of the stationary phase in HPAEC^{14,15}.

PGC-HPLC-ELSD/MS

In **Figure 4B** the retention times on PGC-HPLC-ELSD/MS are plotted against the DP for the linear and branched AOS. The retention times of the AOS generally increase with increasing DP. Within one DP, the AOS elute strictly following the retention mechanism on

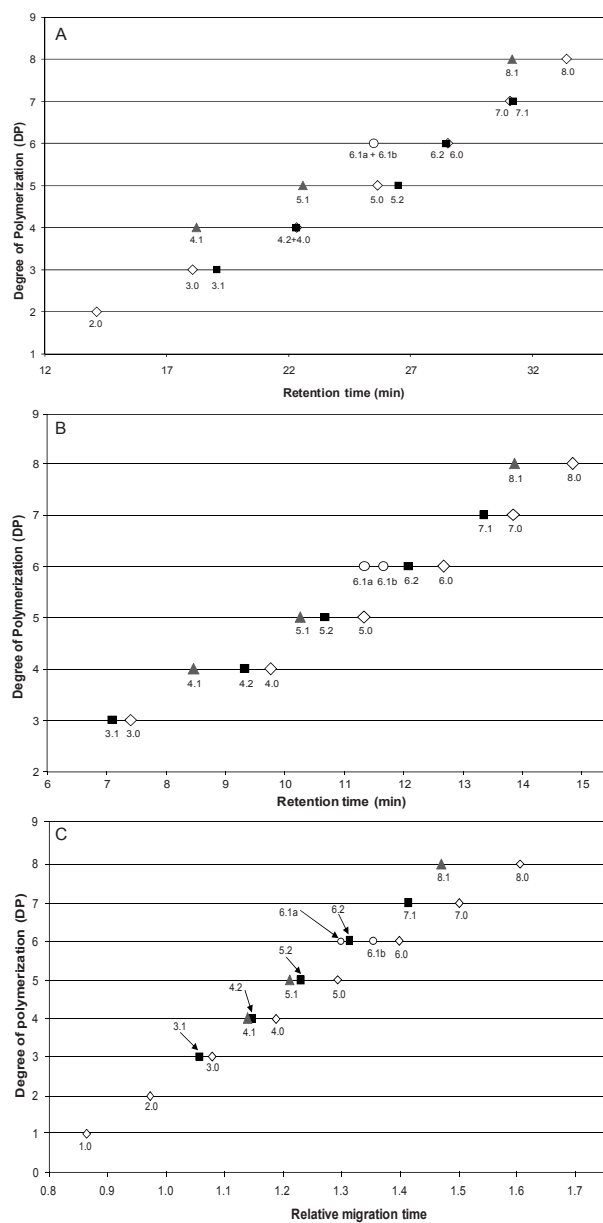


Figure 4 Retention times or relative migration times of various linear and branched AOS plotted against the degree of polymerization: HPAEC-PAD (A), PGC-HPLC-ELSD/MS (B) and CE-LIF (C) and; numerical annotation of the AOS according to **Table 1**. White diamonds: series 0-AOS; grey triangles: series 1-AOS; black squares: series 2-AOS; white circles: unknown DP6 AOS.

PGC based on conformation as was previously described for other carbohydrates^{13,16}. The more planar the molecule, the later the elution on PGC material. The linear α -(1,5)-linked AOS always elute the latest (**Figure 4B**), concluding that the linear α -(1,5)-linked AOS are the most planar. The presence of linkage types other than α -(1,5) results in earlier elution, and thus in a less planar conformation (e.g., AOS 3.0 and 3.1, 7.4 min and 7.1 min, respectively). While single substitution with α -(1,3)-linked L-arabinosyl residues as present in AOS 3.1, 4.2, 5.2, 6.2 and 7.1 results in a slight decrease of the retention time (~ 0.3 -0.5 min, **Figure 4B**), double substitution with α -linked L-arabinosyl residues at O-2 and O-3 results in a tremendous decrease of the retention time (~ 1 min, **Figure 4B**). This retention behavior is in agreement with the conformations of a single or double substituted structure within the AOS as predicted when using 3D-model software (ChemBio Office 2010). Single substitution with α -(1,3)-linked L-arabinosyl residue(s) leads to a branched AOS, which is still able to form a rather planar structure, even though interaction with the column material is slightly reduced resulting in a slight decrease in retention time. Double substitution with L-arabinosyl residues at O-2 and O-3 results in a more 'bulky' rather than planar conformation as one of the two substituted L-arabinosyl residues is forced to stick out of the planar dimension of the molecule (as modeled using ChemBio Office 2010 software).

The described retention behavior allows predictions concerning structural features within (un)known AOS (DP 3-8) based on the retention time. Whenever the retention time is lower than the retention time of a linear α -(1,5)-linked AOS (white diamonds in **Figure 4B**), other linkage types than α -(1,5) are present in the molecule resulting in a branched AOS. A retention time, which is clearly decreased (> 0.8 min) compared to the retention time of the linear AOS of the same DP, signalizes the presence of a double substitution with α -linked L-arabinosyl residues at O-2 and O-3 within the molecule. Whenever the retention time of an (un)known component shows only a slight decrease (~ 0.3 -0.5 min) of the retention time compared to the linear AOS, it is most likely that an AOS carrying single α -(1,3)-linked L-arabinosyl residue(s) is present.

In general, the retention times of linear and branched AOS (DP 3-8) on PGC-HPLC-ELSD/MS can be summarized as follows: $n.1 \ll n.2 < n.0$ with $n = \text{DP}$ for each AOS and the numbers indicating the AOS series (**Table 1**), even though some overlap of DP-clusters occurs (**Figure 4B**).

CE-LIF

In **Figure 4C** the relative migration time is plotted against the DP for linear and branched AOS. The migration order of the various AOS on CE-LIF (**Figure 4C**) reveals a linear correlation of the DP and the electrophoretic mobility for each of the AOS series (series 0, 1 and 2, respectively), which allows prediction of at least the structural elements of AOS based on the migration time. Generally, within one DP, linear α -(1,5)-linked AOS migrate clearly later than the branched AOS. AOS with an α -(1,2,3,5)-linked arabinose unit within the molecule (series 1, **Table 1**) migrate earlier than the α -(1,3)-linked AOS (series 2, **Table 1**). This migration behavior is similar to the PGC-HPLC-ELSD/MS elution behavior, even though the difference is rather small in CE-LIF compared to PGC-HPLC-ELSD/MS (e.g., 4.1 and 4.2, 5.1 and 5.2; **Figure 4B-C**). The only slight differences in electrophoretic mobility between AOS of series 1 and series 2, and the significantly decreased electrophoretic mobility of the linear AOS of the same DP, indicate that the migration mechanism for AOS is based on the hydrodynamic volume.

In general, the migration times of linear and branched AOS (DP 3-8) on CE-LIF can be summarized as follows: $n.1 < n.2 \lll n.0$ with $n = \text{DP}$ for each AOS and the numbers indicating the AOS series (**Table 1**), even though some overlap of DP-clusters occurs (**Figure 4C**).

MS² fragmentation as identification tool

In complex mixtures, whenever NMR is not suitable for analysis, predictive information of MS² fragmentation patterns derived from unknown AOS might be of great interest. The predictive potential of MS² fragmentation patterns of oligosaccharides was already described earlier for feruloylated mono- and disaccharides and α -(1,4)-linked oligosaccharides of, for example, glucose and galacturonic acid¹⁷.

During both, PGC-HPLC-MS and CE-MS analysis, online-MS² spectra of linear and branched AOS were recorded. We could observe good reproducibility for MS² fragmentation patterns in both LC and CE for the same component present in a purified fraction as well as in the mixture D-30/100 and for different runs. Consequently, the use of these MS² fragmentation patterns as a predictive tool to support identification of unknown AOS will be discussed in the following paragraphs.

PGC-HPLC-MS²

In **Figure 5** an overview of the obtained PGC-HPLC-MS² fragmentation patterns of AOS with DP 4 is given (m/z 553; 4.0, 4.1 and 4.2) to exemplify the potential of PGC-HPLC-MS² fragmentation patterns to be used as predictive tool within AOS analysis. Best MS² fragmentation patterns were obtained in positive mode with lithium adducts and the use of wide band activation. Both resulted in a three times increase of the smaller MS² fragments compared to the cross-ring cleavages of the arabinose at the reducing end. From electrospray-ion trap-MSⁿ studies of ¹⁸O-labeled DP 4-AOS (data not shown), we could conclude that the main cross-ring cleavages (m/z 463 and m/z 493 for DP 4 AOS, **Figure 5**) mainly occur at the reducing end, which is in agreement with research performed with feruloylated mono- and disaccharides¹⁷.

In the MS² fragmentation pattern of the linear α -(1,5)-linked arabinotetraose 4.0 (**Figure 5A**) fragments corresponding to cross-ring cleavages of the arabinose at the reducing end are abundant (e.g., m/z 463 (^{0,2}A₄) and m/z 493 (^{0,3}A₄)¹⁸), whereas the fragments corresponding to inter-carbohydrate cleavages are rather small, which is in good agreement with Quemener et al.¹⁷. The MS² fragmentation mechanisms are rather similar for all linear α -(1,5)-linked AOS. The MS² fragmentation patterns of the branched AOS as exemplified with 4.1 and 4.2 (**Figures 5B** and **5C**) show a decreased intensity of the fragment ions originated from cross-ring cleavages of the arabinose at the reducing end (m/z 463 (^{0,3}A₃) and m/z 493 (^{0,2}A₃)¹⁸) compared to fragment ions derived from inter-carbohydrate cleavages (e.g., m/z 421). This described decrease is even more severe for AOS 4.1 carrying a double substitution of α -L-arabinosyl residues at O-2 and O-3 within the molecule (4.1; **Figure 5B**). Even though the cross-ring cleavages occur mainly at the reducing-end arabinose, the branching points present in the molecule seem to influence the stability of the reducing end arabinose resulting in different relative abundances of these fragments. The ratios between the different inter-carbohydrate cleavages (DP 4: m/z 421, m/z 289 and m/z 157, **Figure 5**) also differ for differently linked AOS. The ratio m/z 289 to m/z 421 is significantly decreased in the branched AOS 4.1 and 4.2 (0.24 and 0.26, respectively; inset table in **Figure 5B** and **5C**) compared to the ratio for linear AOS (0.53; inset table in **Figure 5A**). However, a difference between the two branched DP 4-AOS 4.1 and 4.2 based on the differences in the ratios of the inter-carbohydrate cleavages, is not visible (**Figure 5B-C**). Thus, the presence of an α -(1,2)-linked L-arabinosyl residue instead of an α -(1,5)-linked L-arabinosyl residue at the non-reducing end does not influence the inter-carbohydrate cleavages significantly.

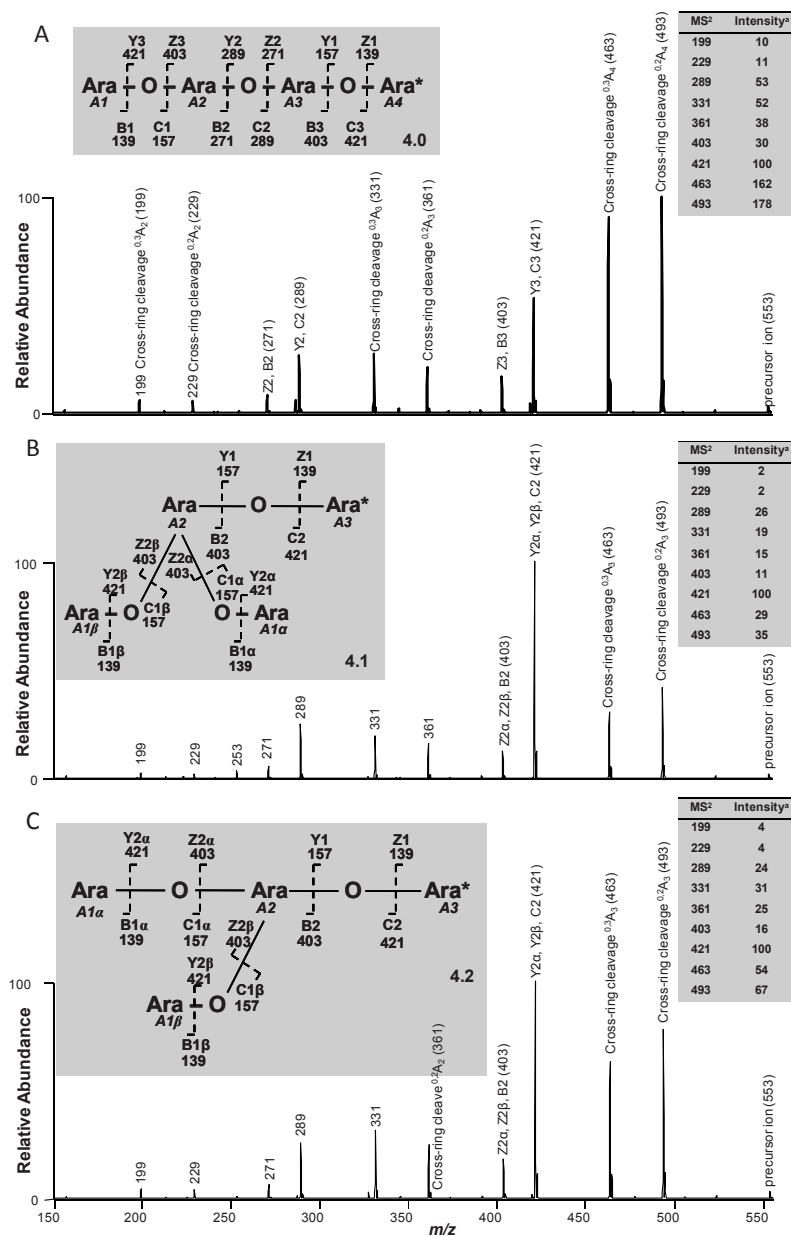


Figure 5 Online-recorded PGC-HPLC-MS² spectra of the AOS with DP = 4 (m/z 553): 4.0 (A), 4.1 (B) and 4.2 (C), including the simplified structures and indication of the inter-carbohydrate cleavages and the corresponding m/z – values for each AOS¹⁸; MS² fragments of online-recorded MS² spectra listed in inset table; ^a intensity is normalized toward fragment m/z 421 (set to 100).

Opposite to the general opinion that in MS^n analysis fragments corresponding to double cleavages do not or hardly occur, for branched AOS (DP 4-8) fragments derived from double cleavages occur on regular basis and to relative high amount as is exemplified for the AOS 4.1 and 4.2 in **Figures 5B** and **5C** (m/z 289).

The same trends as described for DP 4 were seen for all other AOS (DP 3-8). Thus, the ratios of inter-carbohydrate cleavages and especially the cross-ring cleavages at the reducing end depend on the linkages present within the oligomer.

CE- MS^2

CE-MS analysis is performed in negative mode to enable the detection of the negatively charged APTS-labeled AOS. Opposite to PGC-HPLC- MS^2 analysis, the main fragments in CE- MS^2 analysis are inter-carbohydrate-cleavages, whereas cross-ring cleavages do not occur as was already described earlier for other sugars in CE-MS analysis^{9,19}. APTS-labeled AOS occur in two different charge levels ($z = -2$ and -3), of which the charge $z = -2$

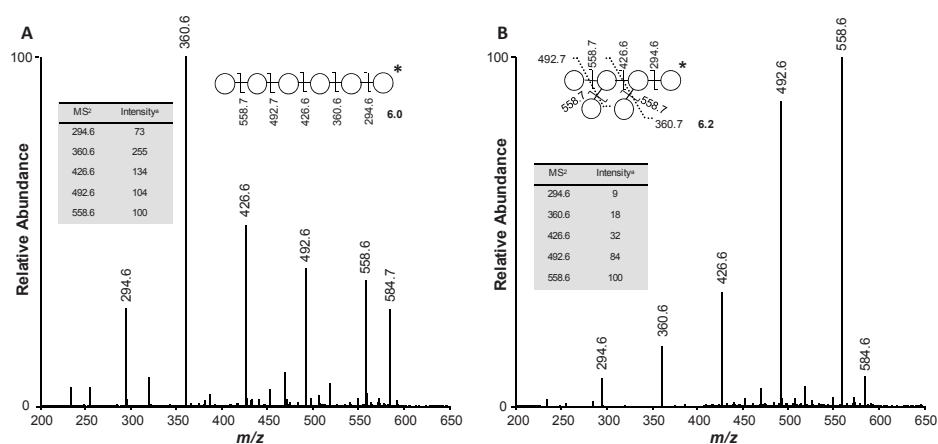


Figure 6 Online-recorded CE- MS^2 spectra of the AOS 6.0 (**A**) and 6.2 (**B**) (m/z 624.6), including the simplified structures and indication of the inter-carbohydrate cleavages; ^a intensity is normalized toward fragment m/z 558.6 (set to 100).

is abundant for most of the AOS. Good MS^2 spectra of almost all AOS were obtained. CE- MS^2 fragmentation of the linear AOS as is exemplified for the linear DP 6-AOS 6.0 in **Figure 6A** is rather straightforward. The MS fragmentation of the precursor ion of the doubly charged APTS-labeled AOS 6.0 (m/z 624.6) results in five main inter-carbohydrate

cleavages (**Figure 6A**). The main fragment is the labeled dimer with an m/z -value of 360.6. This fragment is the preferred fragment for all the linear AOS under investigation (DP 3-8). Branched AOS (series 1 and 2, **Table 1**) show a significantly different MS² fragmentation pattern compared to the linear α -(1,5)-linked AOS as is exemplified for AOS 6.2 (**Figure 6B**). The abundant fragment in the MS² fragmentation pattern of AOS 6.0 (m/z 360.6) represents only a minor fragment in the MS² fragmentation pattern of AOS 6.2 (**Figure 6B**). The abundant fragment for AOS 6.2 is m/z 558.6 (**Figure 6B**). Similar to PGC-HPLC-MS², double and even triple cleavages occur to a high extent in CE-MS². For example, fragment m/z 492.6 for AOS 6.2 can only be present in the MS² fragmentation pattern when a double cleavage has occurred (**Figure 6B**).

The ratio of fragment m/z 360.6 to fragment m/z 426.6 seems to be indicative for the presence of an α -(1,3)-linked arabinose attached to the second arabinose (counted from the reducing end). A ratio of 1.8 is characteristic for all linear AOS (DP 3-8), whereas a ratio of 0.5-1.0 seems to be characteristic for an α -(1,3)-linked arabinose attached to the second arabinose. The MS² fragmentation pattern of AOS 5.1 carrying a double substitution at the second arabinose, revealed a ratio of 0.2 (data not shown). Similar to PGC-HPLC-MS² fragmentation patterns, the ratios of the fragments in CE-MS² spectra allow the prediction of present structures within the molecule, even though a complete identification solely based on PGC-HPLC-MS² or CE-MS² data is hardly possible due the occurrence of multiple cleavages in branched AOS.

Prediction of the structures of the two unknown DP 6-AOS 6.1a and 6.1b

To demonstrate the strength of PGC-HPLC-ELSD/MS and CE-LIF-MS in AOS analysis to predict the structures of unknown AOS in complex mixtures, the structures of the DP 6-AOS 6.1a and 6.1b are predicted using retention and migration times as well as MS² fragmentation patterns in addition to given information based on enzymatic degradation.

Opposite to HPAEC, PGC-HPLC-ELSD/MS and CE-LIF-MS revealed that the DP 6-AOS denoted as 6.1 in **Figure 1**, consists of two unknown DP 6-AOS denoted as 6.1a and 6.1b (**Figures 2 and 3**). Theoretically, about 50 different structures are possible for a DP 6-AOS structure. However, since the enzyme cocktail used for preparation of the AOS⁶ was demonstrated to not release any AOS carrying a single α -(1,2)-linked L-arabinosyl residue, being branched at the reducing end arabinose or carrying two or more unbranched

α -(1,5)-linked arabinoses at the non-reducing end^{5,6}, these structures were excluded from the list of possible structures. A further limitation of the list of possible structures is based on the elution behavior of AOS 6.1a and 6.1b on PGC-HPLC-ELSD/MS (**Figure 4B**). Both components show a significant decrease of the retention time compared to the linear AOS (-1.3 min and -1.0 min for 6.1a and 6.1b, respectively), giving strong evidence that a double substitution is present in both structures. After all these limitations, an overview of the four remaining possibilities for the AOS 6.1a and 6.1b is given in **Figure 7**.

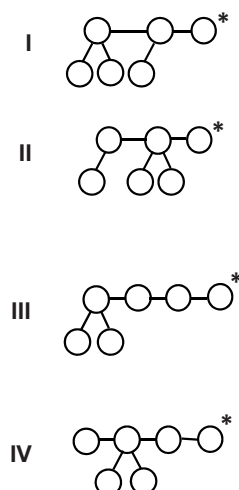


Figure 7 A list of possible structures (I-IV) for the AOS 6.1a and 6.1b.

PGC-HPLC-MS² and CE-MS² spectra of AOS 6.1a (**Figures 8C and 9A**) revealed that the AOS 6.1a has a similar fragmentation pattern as AOS 6.2 (**Figures 8B and 6B**). In the CE-MS² spectra, the ratio of fragment m/z 360.6 to m/z 426.6 of 0.3 for AOS 6.1a indicates a single α -(1,3)-linked L-arabinosyl residue at the second arabinose (counted from the reducing end) as present in AOS 6.2. This conclusion leads to structure I in **Figure 7**. Even though complete annotation of all fragment ions is not possible, the prediction of structure I is in good agreement with 1) the high electrophoretic mobility in CE-LIF and 2) the low retention time in PGC-HPLC-ELSD/MS.

The PGC-HPLC-MS² fragmentation pattern of AOS 6.1b (**Figure 8D**) equals more the fragmentation pattern of the linear AOS 6.0 (**Figure 8A**) than AOS 6.1a (**Figure 8C**) based

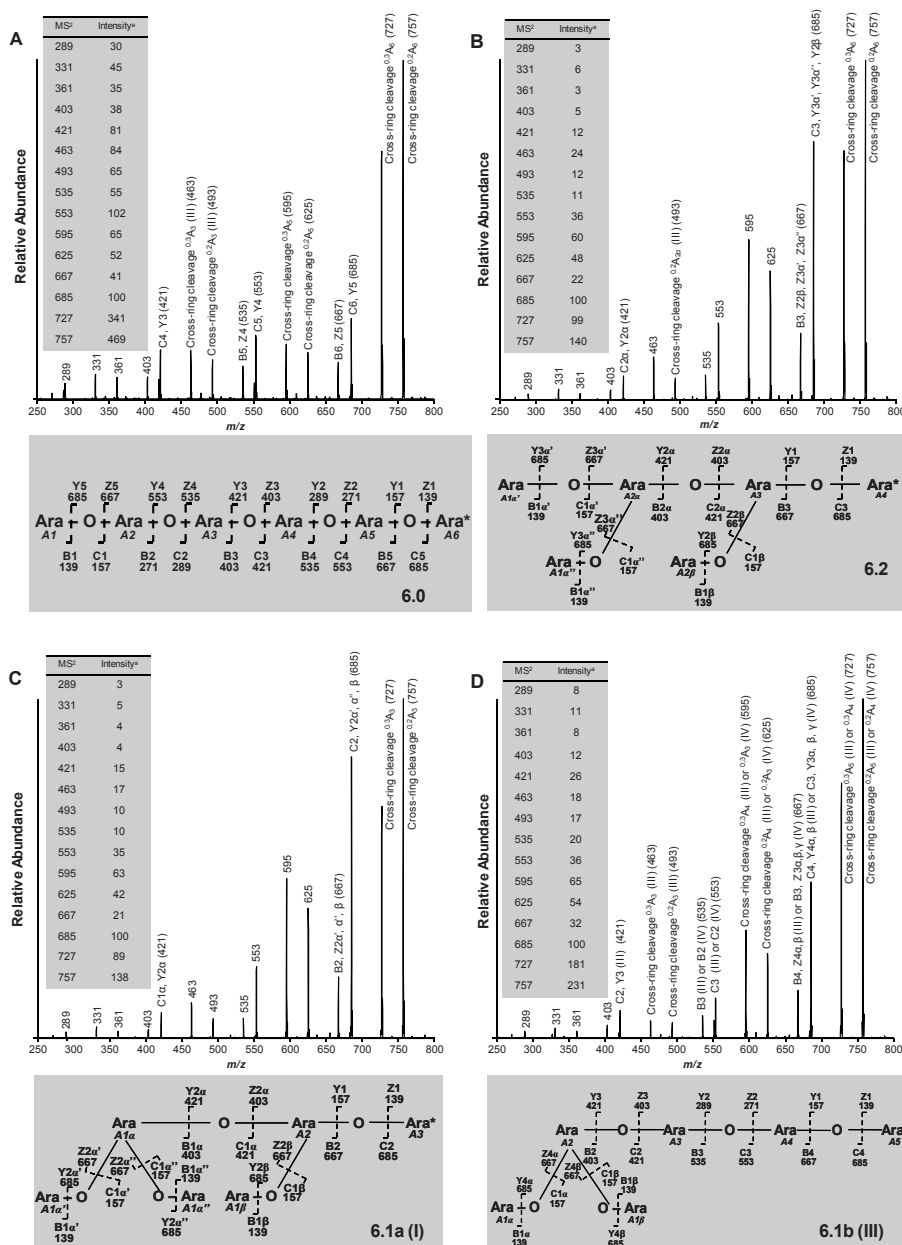


Figure 8 Online-recorded PGC-HPLC-MS² spectra of the AOS with DP 6 (m/z 817): 6.0 (A), 6.2 (B), 6.1a (C) and 6.1b (D), including the simplified structures and indication of the inter-carbohydrate and the corresponding m/z – values for each AOS; ^a intensity is normalized toward fragment m/z 685 (set to 100). Roman numbers (I,III, IV) are given according to structures in **Figure 7**.

on the abundant cross-ring cleavages (m/z 757 and m/z 727), indicating that the part at the reducing end consists of unbranched α -(1,5)-linked arabinoses. The CE-MS² fragmentation pattern of AOS 6.1b shows two abundant fragments: m/z 360.6 and m/z 558.6, while the fragments m/z 426.6 and m/z 492.6 are present in minor relative abundances (**Figure 9B**). The ratio of fragment m/z 360.6 to m/z 426.6 for AOS 6.1b is with 3.5 even higher than for linear AOS as discussed earlier (**Figure 6A**). This indicates an unbranched arabinobiose at the reducing end. Furthermore, it can be hypothesized that a double substituted structure is present at the non-reducing end hindering the production of fragment m/z 426.6. From the presented data we can suggest AOS 6.1b to be structure III (**Figure 7**) as also suggested from its CE migration behavior. Furthermore, an enzymatic treatment of AOS 6.1b with an overdose of Abn1⁵ resulted in the AOS 4.1 (**Table 1**) and arabinobiose as end products.

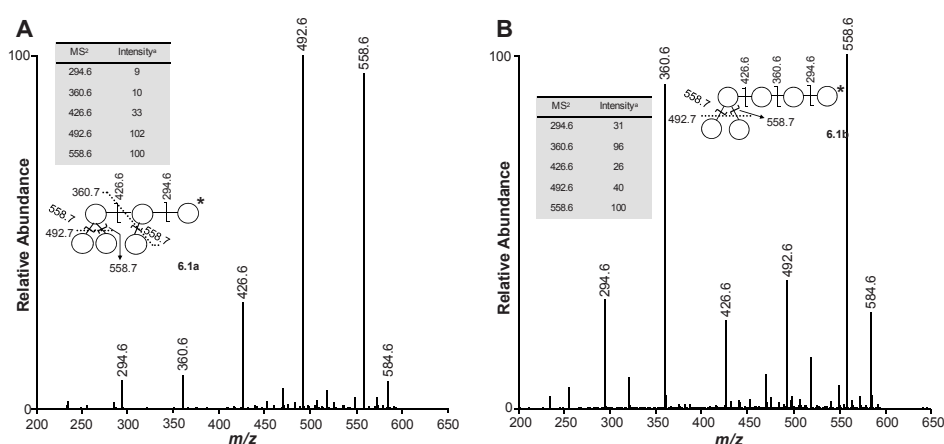


Figure 9 Online-recorded CE-MS² spectra of the AOS 6.1a (**A**) and 6.1b (**B**) (m/z 624.6), including the simplified structures and indication of the inter-carbohydrate cleavages¹⁸, ^a intensity is normalized toward fragment m/z 558.6 (set to 100).

Although we did not succeed in the complete annotation of AOS 6.1a and 6.1b by NMR⁶, some characteristic signals in NMR analysis confirm the presence of a double substituted structure at the non-reducing end (comparable to structure 4.1, **Table 1**) and the presence of an α -(1,3)-linked L-arabinosyl residue (similar to structure 4.2, **Table 1**). Thus, the available NMR data of this heterogeneous mixture are in agreement with the proposed structures for 6.1a (I) and 6.1b (III) (**Figure 7**).

Conclusions

This study demonstrated that both PGC-HPLC-ELSD/MS and CE-LIF enabled better separation of the linear and branched AOS under investigation compared to HPAEC-PAD, demonstrating the superiority of both methods for the characterization of AOS. For PGC-HPLC-ELSD/MS online-MS-coupling is rather straightforward and supplies direct MSⁿ information without loss of resolution. Furthermore, the elution order, as well as the online-recorded MS² spectra, supports the identification or at least prediction of unknown AOS significantly. CE-LIF represents as well a promising separation tool for the characterization of AOS in complex mixtures due to the good resolution of almost all AOS, the short analysis time (15 min) and, even more important, mole-based detection as was demonstrated for various galactose-oligosaccharides previously¹².

Acknowledgements

This study is partly carried out with financial support from the Commission of the European Communities (WallNet: “Functional Genomics for Biogenesis of the Plant Cell Wall”, Marie Curie contract number: MRTN-CT-2004-512265) and the Dutch Ministry of Economic Affairs via an EOS-LT grant (<http://www.senternovem.nl/eos/index.asp>).

The authors would like to thank Edwin Bakx and René Kuijpers for the fruitful discussions concerning the (CE-) MS analysis.

References

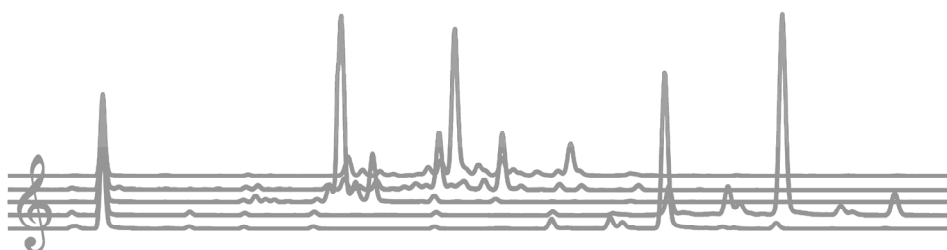
1. Beldman, G.; Schols, H.A.; Pitson, S.M.; Searle-van Leeuwen, M.F.; Voragen, A.G.J., in Sturgeon, R.G. (Editor), *Advances in Macromolecular Carbohydrate Research*, Vol. 1, JAI Press Inc., Greenwich, United Kingdom, **1997**, p. 1-64.
2. Weinstein, L.; Albersheim, P. *Plant Physiology*, **1979**, *63*, 425-432.
3. Ishii, T. *Plant and Cell Physiology*, **1994**, *35*, 701-704.
4. Levigne, S.V.; Ralet, M.C.J.; Quemener, B.C.; Pollet, B.N.L.; Lapierre, C.; Thibault, J.F.J. *Plant Physiology*, **2004**, *134*, 1173-1180.
5. Kühnel, S.; Hinz, S.W.A.; Pouvreau, L.; Visser, J.; Schols, H.A.; Gruppen, H. *Bioresource Technol.*, **2010**, *accepted for publication*, DOI 10.1016/j.biortech.2010.05.070.
6. Westphal, Y.; Kühnel, S.; de Waard, P.; S.W.A., H.; Schols, H.A.; Voragen, A.G.J.; Gruppen, H. *Carbohydr. Res.*, **2010**, *345*, 1180-1189. *This thesis, Chapter 4*

7. Lee, Y.C. *J. Chromatogr. A*, **1996**, 720, 137-149.
8. Schols, H.A.; Mutter, M.; Voragen, A.G.J.; Niessen, W.M.A.; Vanderhoeven, R.A.M.; Vandergreef, J.; Bruggink, C. *Carbohydr. Res.*, **1994**, 261, 335-342.
9. Kabel, M.A.; Heijnis, W.H.; Bakx, E.J.; Kuijpers, R.; Voragen, A.G.J.; Schols, H.A. *J. Chromatogr. A*, **2006**, 1137, 119-126.
10. Albrecht, S.; Schols, H.A.; van den Heuvel, E.; Voragen, A.G.J.; Gruppen, H. *Electrophoresis*, **2010**, 31, 1264-1273.
11. Albrecht, S.; van Muiswinkel, G.C.J.; Schols, H.A.; Voragen, A.G.J.; Gruppen, H. *J. Agric. Food. Chem.*, **2009**, 57, 3867-3876.
12. Albrecht, S.; Schols, H.A.; Klarenbeek, B.; Voragen, A.G.J.; Gruppen, H. *J. Agric. Food. Chem.*, **2010**, 58, 2787-2794.
13. Westphal, Y.; Schols, H.A.; Voragen, A.G.J.; Gruppen, H. *J. Chromatogr. A*, **2010**, 1217, 689-695. *Chapter 3*
14. Johnson, D.C.; Dobberpuhl, D.; Roberts, R.; Vandeberg, P. *J. Chromatogr.*, **1993**, 640, 79-96.
15. Pastell, H., *PhD thesis, Preparation, structural analysis and prebiotic potential of arabinoxylo-oligosaccharides*, University of Helsinki, Helsinki, Finland, **2010**.
16. Pereira, L. *J. Liq. Chromatogr. Related Technol.*, **2008**, 31, 1687-1731.
17. Quemener, B.; Ralet, M.C. *J. Mass Spectrom.*, **2004**, 39, 1153-1160.
18. Domon, B.; Costello, C.E. *Glycoconjugate J.*, **1988**, 5, 397-409.
19. Hilz, H.; de Jong, L.E.; Kabel, M.A.; Schols, H.A.; Voragen, A.G.J. *J. Chromatogr. A*, **2006**, 1133, 275-286.

Chapter 6

Mode of action of *Chrysosporium lucknowense* C1 arabinohydrolases

Kühnel, S., Westphal, Y., Hinz, S.W.A., Schols, H.A., Gruppen. H.,
submitted for publication.



Abstract

In the present work, the mode of action of four *Chrysosporium lucknowense* C1 arabinohydrolases was determined to ensure the controlled and effective degradation of arabinan. The active site of endo-arabinanase Abn1 has at least six subsites, of which the subsites -1 to +2 have to be occupied for hydrolysis. Abn1 was able to hydrolyze a branched arabinohexaose with a double substituted arabinose at subsite -2 and is, therefore, side chain tolerant. The exo acting enzymes Abn2, Abn4 and Abf3 release arabinobiose (Abn2) and arabinose (Abn4 and Abf3) from the non-reducing end of reduced arabinose oligomers. Abn2 binds the two arabinose units only at the subsites -1 and -2. Abf3 prefers small oligomers over large oligomers. It is able to hydrolyze all linkages present in beet arabinan, including the linkages of double substituted residues. Abn4 is more active toward polymeric substrate and only removes the linkages of single substituted arabinosyl residues.

Introduction

Sugar beet pulp consists to 75% (w/w) of carbohydrates on dry matter basis¹. Up to one third of the carbohydrate material is polymeric arabinan, a heavily branched, complex neutral sugar side chain of pectic rhamnogalacturonan-I². Sugar beet arabinan has a backbone of linear α -(1,5)-linked arabinofuranose units. Monomeric or oligomeric arabinofuranose branches are linked to the backbone via α -(1,2)-linkages and α -(1,3)-linkages. The oligomer side chains may even be further branched. A number of researchers report that up to 1% of the arabinose is present as terminal arabinopyranose (summarized in Beldman et al.³). The degradation of such a heavily branched carbohydrate requires the concerted action of a number of powerful arabinohydrolases. Arabinohydrolases are a group of enzymes that belong to the glycoside hydrolase families GH 3, 27, 43, 51 54, 62 and 93 (<http://www.cazy.org>).

Endo-arabinanases belong to GH family 43. They hydrolyze the α -(1,5)-linkages in the unsubstituted regions of the arabinan backbone with an inverting mode of action⁴. Endo-arabinanases prefer polymers over oligomers. Their activity decreases with decreasing degrees of polymerization⁵. Arabinotriose is the smallest substrate for the enzyme and it is hydrolyzed to arabinose and arabinobiose as the main products upon end point hydrolysis². Structural studies of a GH family 43 endo-arabinanase from *Geobacillus stearothermophilus* revealed that the substrate binding site is a binding cleft that can harbor at least 5 arabinose units in which arabinotriose occupies the subsites -1 to +2⁴.

Exo-arabinanases belong to GH families 43 and 93 and release arabinose, arabinobiose or arabinotriose from the non-reducing end of the α -(1,5)-linked arabinan backbone⁶⁻⁸. All of these enzymes specifically release only one product and preferably act on linear arabinan. The conformation of the substrate binding site greatly determines the enzymes mode of action. Proctor and co-workers⁹ could change the mode of action of GH family 43 exo-arabinanase 43A from *Cellvibrio japonicus* into an endo-mode of action by redesigning its binding site.

Arabinofuranosidases active toward arabinan belong to the GH families 43, 51, 54 (<http://www.cazy.org>) and are able to release arabinose monomers from the non-reducing ends of arabinan. Besides their structural classification, they are classified according to their substrate specificity into arabinofuranosidases A+B and arabinofuranohydrolases specific toward arabinoxylans³. Arabinofuranosidase A (AbfA) and arabinofuranosidase B (AbfB) are both active toward arabinose oligomers and *p*-nitrophenyl arabinofuranoside

(pNP-Ara). Their activities differ toward polymeric substrates as AbfA is inactive toward linear arabinan and much less active than AbfB toward branched arabinan².

The genome of the ascomycete *Chrysosporium lucknowense* (C1) encodes 14 enzymes that putatively release arabinose or arabinose oligomers from arabinan¹⁰. Kühnel and co-workers¹¹ purified and characterized four enzymes that act in synergy on the degradation of sugar beet arabinan. C1 arabinohydrolase digests of branched arabinan contain a mixture of linear and branched arabinose oligomers¹². No detailed information is available about the mechanism how the C1 arabinohydrolases act in synergy. This information is necessary to ensure a controlled and efficient degradation of the substrate.

In this research branched arabinose oligomers and reduced linear arabinose oligomers are used to determine the substrate specificity and mode of action of the C1 endo-arabinanase Abn1, exo-arabinanase Abn2 and the two arabinofuranosidoases Abn4 and Abf3.

Materials and Methods

Enzyme subsites were named following the nomenclature for sugar-binding subsites in glycosyl hydrolases¹³. Centrifugation was always performed at room temperature at $15\,000 \times g$ for 10 min.

Materials

The C1 enzymes Abn1, Abn2, Abn4 and Abf3 were purified previously by Kühnel and co-workers¹¹. Their activities are given in **Table 1**. Linear arabinose oligomers in the range from DP 2-7 used for incubations and for the production of reduced arabinose oligomers

Table 1 Activities of C1 arabinohydrolases. Linear and branched arabinan from sugar beet. 1 U = 1 μ mol (product)/ min * mg (enzyme)

	Activity (U/mg)	Substrate
Abn1	26.0	linear arabinan
Abn2	7.1	linear arabinan
Abn4	9.5	branched arabinan
Abf3	21.4	pNP-Ara

were purchased from Megazyme (Bray, Ireland). Linear and branched sugar beet arabinan were from British Sugar (Peterborough, United Kingdom). Branched arabinose oligomers were produced, purified and characterized by Westphal and co-workers¹². Other chemicals were from Merck or Sigma-Aldrich.

Activity of C1 arabinohydrolases toward reduced arabinose oligomers

Production of reduced arabinose oligomers

Arabinose and arabinose oligomers in the range from DP 2-7 (5 mg each) were reduced with 7.5 mg sodium borohydride in 0.2 mL ammonium hydroxide (1.5 M) for 1 h at ambient temperature. The reaction was stopped by the addition of glacial acetic acid until gas formation ceased (pH < 5). Methanol (1 mL) was added to remove the sodium borohydride as volatile trimethylborate and the samples were dried under a stream of air. The methanol washing was repeated two times. Samples were dissolved in water and the reduction was verified by HPAEC.

Activity of C1 arabinohydrolases toward reduced arabinose oligomers

Pure, reduced arabinose oligomers in the range from DP 2-7 (25 µL; 2 mg/mL) were mixed with 25 µL enzyme solution in 100 mM sodium acetate buffer (Abn1 and Abn2: 0.35 mU, Abn4: 0.3 mU and Abf3: 0.4 mU). The samples were incubated for 1 h, 15 h and 20 h with an additional dose of fresh enzyme (4 mU in 10 µL) added after 15 h. After incubation, the samples were diluted 20 times, boiled (t = 5 min) and centrifuged. The supernatant was analyzed by HPAEC.

C1 arabinohydrolase activities toward branched arabinose oligomers

Branched arabinose oligomers (0.1 mg) were incubated for 2 h at 30 °C with Abn1 (30 mU), Abn4 (20 mU) or Abf3 (20 mU) in a total volume of 100 µL. After incubation, the samples were diluted with 400 µL water and boiled for 5 min. After centrifugation, the supernatant was analyzed by PGC-HPLC-MS.

Product inhibition of C1 arabinohydrolases

Abn1 and Abn2

Product inhibition of Abn1 and Abn2 was studied toward linear arabinan in the presence of arabinobiose as the end product for both enzymes. Abn1 and Abn2 (6 mU) were incubated for 1 h at 30 °C with 0.5 mg linear arabinan and arabinobiose (0, 0.1, 0.5, 1, 2, 3, 4 and 5 mg) in 100 µL total volume. The samples were subsequently boiled ($t = 5$ min) and centrifuged. The supernatant was transferred into a HPLC vial and subjected to HPSEC analysis.

Abn4 and Abf3

The product inhibition of Abn4 and Abf3 was studied toward pNP-Ara in the presence of arabinose. Abn4 (0.5 mU) and Abf3 (1 mU) were incubated for 30 min at 30 °C in a microtiter plate in 200 µL total volume, including 10 mM sodium acetate buffer (pH 5.0), 0.5 mM pNP-Ara and arabinose monomer concentrations from 0-500 mM. The pH was adjusted to pH 10 with 50 µL sodium carbonate (0.5 M) and the amount of free *p*-nitrophenol was determined photospectrometrically at 405 nm. A *p*-nitrophenol standard curve (10-500 µM) was used for quantification. Abf3 inhibition kinetics were studied with a slightly modified protocol: $t = 15$ min, $V = 200$ µL, 100 µL pNP-Ara (0.25-2.5 mM), 50 µL arabinose (0-2 M), 40 µL sodium acetate buffer (50 mM, pH 5.0) and 10 µL Abf3 (1 mU).

Chromatography

High performance size exclusion chromatography (HPSEC) was performed on a Dionex Ultimate 3000 system (Dionex, Sunnyvale, CA, USA) equipped with a set of four TSK-Gel superAW columns (Tosoh Bioscience, Tokyo, Japan) in series: guard column (6 mm ID × 40 mm) and separation columns 4000, 3000 and 2500 (6 mm ID × 150 mm). The samples (10 µL; 5 mg/mL) were eluted with filtered aqueous 0.2 M sodium nitrate at 40 °C at a flow rate of 0.6 mL/min. Elution was followed by refractive index detection (Shodex RI 101; Showa Denko K.K., Kawasaki, Japan).

The monomer and oligomer carbohydrate levels of the digests were analyzed by high performance anion exchange chromatography (HPAEC) according to Albrecht and co-workers¹⁴. Arabinose and arabinose oligomers (10 µL; 50-100 µg/mL) were eluted in 0.1 M sodium hydroxide with an adapted sodium acetate (NaOAc) elution profile: A

gradient of 0-350 mM NaOAc over 30 min, 1 M NaOAc for 10 min and 0 M NaOAc for 15 min (equilibration).

Branched oligomers were separated and identified by HPLC-MS with a porous graphitized carbon (PGC) column according to Westphal and co-workers¹⁵.

Results and discussion

Mode of action of C1 arabinohydrolases toward reduced arabinose oligomers

Abn1

The action of Abn1 toward reduced arabinose oligomers is shown in **Figure 1**. Abn1 can degrade reduced arabinose oligomers with $DP \geq 3$ and shows higher activities with increasing degree of polymerization (**Figure 1A**). Reduced arabinobiose is the smallest labeled compound identified in all digests and it is the first product formed in DP 3-5 oligomer digests (no further data shown). This indicates that the +1 subsite of Abn1 cannot be occupied by a reduced arabinose moiety. The preferred hydrolyzed linkage shifts one arabinose unit toward the non-reducing end for DP 6 and DP 7 oligomers, which results in arabinotriose and reduced arabinotriose or reduced arabinotetraose as the main primary products from DP 6 or DP 7, respectively (**Figure 1B**). All produced oligomers with $DP \geq 3$ are subject to further hydrolysis that yields arabinose, arabinobiose and reduced arabinobiose as final products. The reduction of the free aldehyde groups causes structural and conformational changes within the molecule. Nevertheless, Abn1 could degrade reduced arabinotriose and arabinoheptaose with the same activity and specificity as non-reduced arabinotriose and arabinoheptaose (no further data shown). Therefore, it can be concluded that the action of Abn1 is not influenced by the modification of the reducing end group. The data presented in **Figure 1** suggests that the substrate binding site of Abn1 recognizes at least six arabinose units, when the reduced arabinose is not considered to be specifically recognized. The degradation of reduced arabinotriose shows that two α -(1,5)-linked arabinose units that cover the subsites -1 and +1 are a prerequisite for hydrolysis. The additional arabinose at position -2 in reduced arabinotetraose does not greatly alter the activity of Abn1. In contrast, an additional arabinose unit at position -3 in reduced arabinopentaose increases the activity by more than 50% (**Figure 1A,C**). A similar

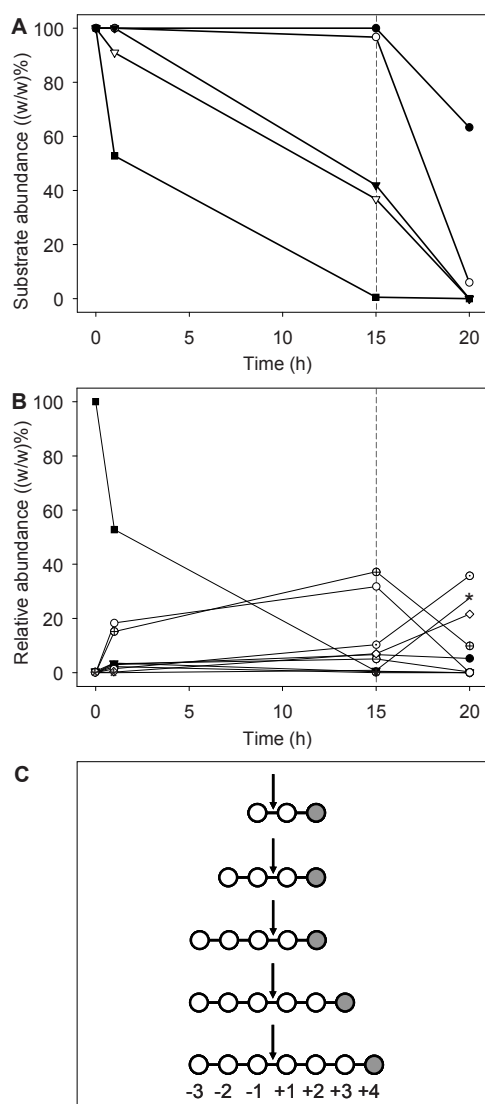


Figure 1 Abn1 activity toward reduced arabinose oligomers. (A) Time dependent consumption of pure reduced arabinose oligomers in the range from DP 3-7. (B) Product formation from reduced arabinose oligomers: ● reduced arabinotriose, ○ reduced arabinotetraose, ▼ reduced arabinopentaose, ▽ reduced arabinohexaose, ■ reduced arabinoseptaose, * arabinose, ⊙ arabinobiose, ⊕ arabinotriose, ⊖ arabinotetraose, ⊗ arabinopentaose, grey dashed line: fresh ten fold enzyme dose added after 15 h incubation. (C) Schematic mode of action of Abn1 toward reduced arabinose oligomers and main products formed after first hydrolysis step. White circles: arabinose units, grey circles: reduced arabinose, arrows: primarily hydrolyzed linkage by Abn1, numbers from -3 to +4: predicted binding subsites of Abn1.

behavior can be noticed between DP 5 and 6, where an additional arabinose unit at position +2 from the active site does not change the activity of Abn1, whereas the activity still increases from DP 6 to DP 7. The activity increase from DP 4 to DP 5 and DP 6 to DP 7 is connected to the presence of an additional arabinose at subsites -3 and +3, respectively. This suggests that these subsites have a higher binding affinity than the subsites -2 and +2. The lower binding affinity of the subsites -2 and +2 also explains the unaltered Abn1 activity toward DP 3 and 4 and DP 5 and 6, respectively.

Abn2

When reduced arabinose oligomers from DP 3-7 are digested with Abn2, arabinobiose is released together with arabitol or reduced arabinobiose from oligomers with uneven or even DP, respectively (**Figure 2A**). The data obtained confirms that Abn2 hydrolyzes its substrate from the non-reducing end. It recognizes two arabinose units next to the non-reducing end. The +1 position from the active site (in case of reduced arabinotriose the arabitol) does not prevent the binding and hydrolysis of the substrate. This suggests a rather unspecific +1 subsite since arabitol can be considered as structurally different from an arabinofuranose of the arabinan backbone. However, the enzyme activity is decreasing with decreasing DP which suggests that Abn2 recognizes parts of the substrate on the plus side of the active site as well. Carapito and co-workers determined the crystal structure of a GH family 93 arabinobiohydrolase from *Fusarium graminearum*¹⁶. They describe the substrate binding site as a cleft with a very defined -1 subsite and a more open -2 subsite. Toward the reducing end, only the +1 subsite could be identified from where the cleft opens and does not allow any further prediction of additional subsites¹⁶. Abn2 also belongs to GH family 93 and has the same mode of action as the *F. graminearum* arabinobiohydrolase. Therefore, it could also have a similar conformation of the substrate binding site.

Abn4

Abn4 is a GH family 43 arabinofuranosidase that is mainly active toward the side chains of branched arabinan and shows some activity toward linear arabinose oligomers with $DP \geq 4$ ¹¹. In this case, the activities toward reduced linear arabinose oligomers are much lower than the activities toward non-reduced linear arabinose oligomers. Abn4 is not active toward reduced arabinotetraose and reduced arabinopentaose. Reduced arabinohexaose and reduced arabinohexaose are degraded to yield reduced arabinopentaose (10%) and reduced

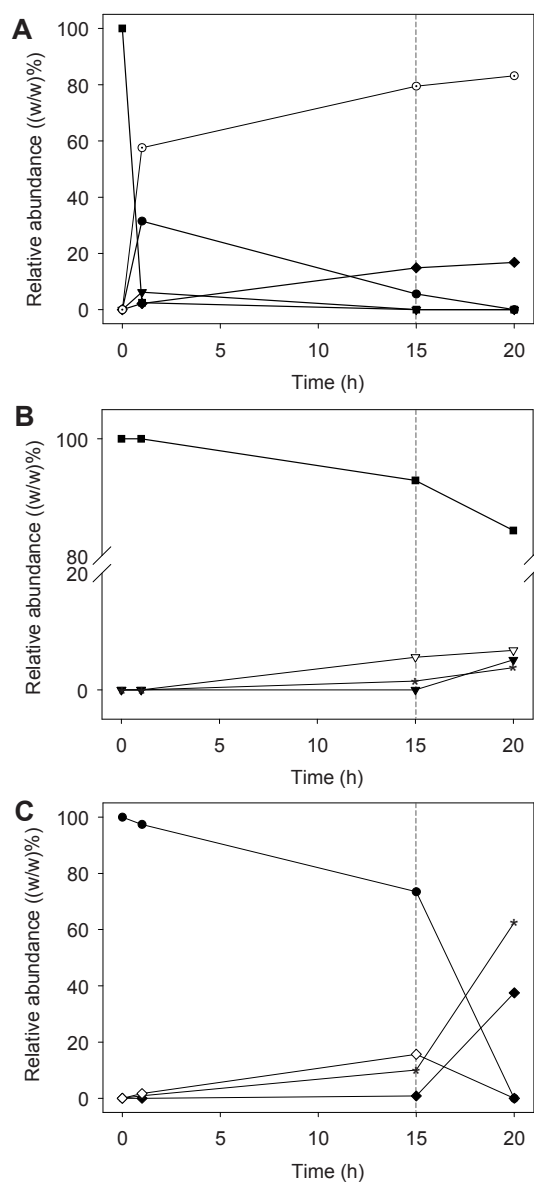


Figure 2 Time curves of C1 arabinohydrolases Abn2, Abn4 and Abf3 toward pure, reduced arabinose oligomers. (A) Abn2 toward reduced arabinoheptaose, (B) Abn4 toward reduced arabinoheptaose, (C) Abf3 toward reduced arabinotriose. ◆ arabinitol, ◇ reduced arabinobiose, ● reduced arabinotriose, ▼ reduced arabinopentaoise, ▽ reduced arabinohexaoise, ■ reduced arabinoheptaose, * arabinose, ○ arabinobiose, grey line: fresh ten fold enzyme dose added after 15 h incubation.

arabinohexaose (15%), respectively (**Figure 2B**). These values show that Abn4 removes a terminal arabinose unit from the non-reducing end of the molecule. It is likely that the alditol decreases the substrate binding to Abn4 and, by this, reduces enzyme activity. Since Abn4 belongs to GH family 43 it is structurally more similar to endoarabinanases or GH family 43 exoarabinanases than to GH family 51 or 54 arabinofuranosidases. Abn4 could have a rather large substrate binding site that recognizes a large part of the substrate. GH family 43 exo-arabinanase 43A from *Pseudomonas cellulosa* / *Cellvibrio japonicus* could be converted from an exo-mode of action to an endo-mode of action by changing two amino acid residues that stucked out into the binding cleft of the enzyme^{9,17}. The main difference between Abn4 and exo-arabinanase 43A is the linkage specificity and released product. Unlike exo-arabinanase 43A, Abn4 removes single arabinose side chains from polymeric arabinan. The low activity toward arabinose oligomers suggests that the substrate binding site of Abn4 recognizes a larger part of the arabinan backbone. The binding of the substrate occurs with an endo-mode of action, whereas the product release follows an exo-mode of action.

According to this data Abn4 is not part of the arabinofuranosidase family A or B or arabinoxylan arabinofuranohydrolase as described by Beldman and co-workers³. It is suggested to preliminary designate Abn4 as exo-arabinanase. Structural characterization of the enzyme (e.g. by crystallography) could give more insight into the structure-function relationship of Abn4.

Abf3

Abf3 is a GH family 51 arabinofuranosidase that releases arabinose from arabinoxylan and from linear and branched arabinose oligomers^{10,11}. It can be seen from **Figure 2C** that Abf3 removes single arabinose units from the non-reducing end of reduced arabinotriose. Abf3 activity toward reduced arabinose oligomers was five to ten times lower than Abf3 activity toward pNP-Ara. It is most active toward reduced arabinobiose. The clear preference for smaller oligomers and the lack of activity toward polymeric substrate indicates that Abf3 acts toward arabinose oligomers like expected for an arabinofuranosidase A^{3,11}.

Product inhibition

Arabinobiose was added to Abn1 and Abn2 digests of linear arabinan since it is the main product that accumulates upon end point conversion. The reaction was followed by HPSEC (**Figure 3A,B**). The linear arabinan polymer elutes at 9.8 min and is rapidly degraded to intermediate and small molecular mass materials that elutes from 11.5-15.0 min. The main peak at 14.75 min shows the increasing arabinobiose levels in the samples. The insert represents a zoom into the high molecular mass region in the range from 8.5-14.0 min.

Abn1

Abn1 is not inhibited in the degradation of linear arabinan even when 50 mg/mL arabinobiose were added to the mixture (**Figure 3A**). Some variation in the release of small molecular mass material can be observed. Digests with 25 and 50 mg/mL arabinobiose show the release of slightly more oligomers that elute at 13.2 min, 13.5 min and 13.9 min than digests with less arabinobiose. From HPSEC it is not possible to confirm if this increase is correlated with a decrease in arabinose and arabinobiose release. Such a decrease could indicate product inhibition when small molecular mass compounds serve as substrates. From the data presented in **Figure 3A** it can be concluded that Abn1 has a very high binding affinity toward linear arabinan. The data is also in line with the data presented in **Figure 1A**, where a very low activity toward reduced arabinotriose was observed.

Abn2

Unlike Abn1, Abn2 is very sensitive to product inhibition (**Figure 3B**). The addition of 1 mg/mL arabinobiose reduces Abn2 activity with about 25% and it further declines by 80% and 95% at concentrations of 5 and 10 mg/mL arabinobiose, respectively, as estimated from the surface area decrease in the range of 8.5-14.0 min. These data suggest a similar binding affinity of Abn2 toward linear arabinan and its product arabinobiose. This assumption is supported by the results from an earlier section, where it is shown that Abn2 does not recognize more than two arabinose units at the -2 and -1 subsite. Both enzymes were also incubated with linear arabinan in the presence of 150 mg/mL arabinose. None of the enzymes showed any product inhibition. Therefore, a specific binding of arabinose by Abn1 and Abn2 can be excluded (no further data shown).

Abn4 and Abf3

The exo-arabinanase Abn4 does not show any product inhibition when incubated with arabinose (**Figure 3C**). On the contrary, 50 mM arabinose seems to stabilize the enzyme and leads to a 30% increase in enzyme activity. This increase in activity is also seen when glucose was added to the mixture. However, 50 mM sodium acetate buffer, xylose or inositol do not have any effect on the enzyme activity (no further data shown). It can be concluded that Abn4 is positively affected by the presence of certain sugars. The Abf3 activity is reduced by 20% in the presence of 500 mM arabinose (**Figure 3C**). A linear

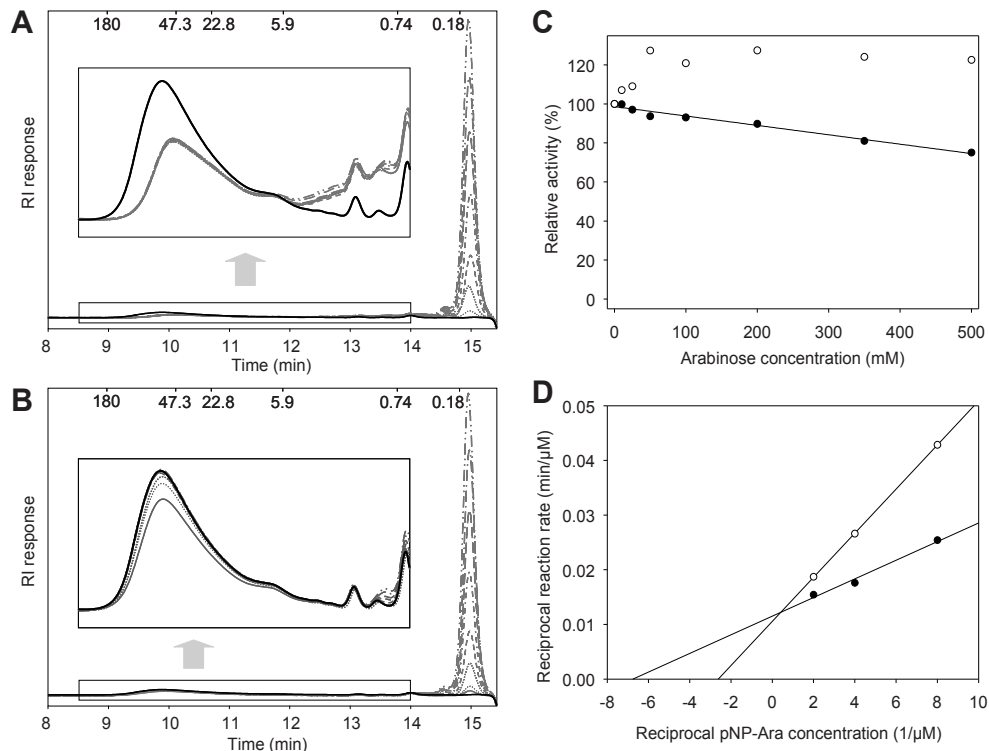


Figure 3 Product inhibition of C1 arabinohydrolases. Linear arabinan degradation by Abn1 (A) and Abn2 (B) in the presence of 0-50 mg/mL arabinobiose ($t = 14.75$ min), upper X-Axis: Molecular masses of pullulan standards (in kDa), black line: blank, grey line: 0 mg/mL arabinobiose, grey dashed/dotted lines: 1, 5, 10, 20, 30, 40, 50 mg/mL arabinobiose with increasing peak area at 14.75 min. (C) Abn4 and Abf3 activity toward pNP-Ara (0.5 mM) in the presence of 0-500 mM arabinose. (D) Lineweaver-Burke-Plot of Abf3 toward pNP-Ara (from 0.125-0.5 mM) with 0 mM arabinose (●) and 500 mM arabinose (○).

correlation between product concentration and Abf3 activity was observed. Abf3 digests with different initial substrate concentrations were analyzed to determine the inhibition mechanism. From the Lineweaver-Burke-Plot shown in **Figure 3D** it can be seen that Abf3 product inhibition follows a competitive mechanism. The product can bind to the active site with a much lower affinity than the substrate. Abf3 activity is fully recovered when the substrate concentration is increased to 5 mM pNP-Ara.


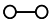
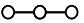
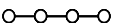
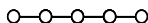
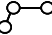
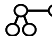
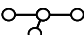
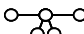
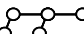
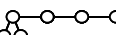
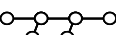
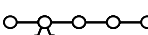
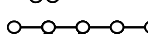
Activity of C1 arabinohydrolases toward branched arabinose oligomers

Activity toward branched arabinopentaose isoforms

The activities of Abn4 and Abf3 were tested toward branched arabinose oligomers to determine the linkage specificity of the enzymes. The branched pentamers used consist of three α -(1,5)-linked arabinose units that carry two arabinose side groups. The middle arabinose of the 5.1 isoform is double substituted with one α -(1,2)-linked and one α -(1,3)-linked arabinose whereas the middle arabinose and the terminal non-reducing arabinose of the 5.2 isomer are single substituted with two α -(1,3)-linked arabinose units (**Table 2**). From **Figure 4A** it can be seen that the branched arabinose pentaose mix mainly contains two structures that are differently degraded by Abn4 and Abf3 (lines II-IV). The evaporative light scattering (ELS) signal allows the quantification of the compounds present and the formation of arabinose monomers. **Figure 4B** shows the MS signal of the same samples, in which minor compounds are more pronounced (e.g., the 4.2 and 6.2 oligomers, **Figure 4B**, line I).

Abn4 can only degrade the 5.2 isomer (**Figure 4**, line II). It releases the α -(1,3)-linked side groups from the pentamer 5.2, which leads to the release of arabinose and arabinotriose as the end products of the reaction. The oligomer 4.2 (**Table 2**) is formed as an intermediate product. This could suggest that the terminal α -(1,3)-linked arabinose at the end of the molecule is preferred over the α -(1,3)-linked arabinose attached to the second arabinose. Abn4 also releases linear arabinotetraose which is derived from the branched hexamer 6.2 (**Figure 4**, line II). The pentamer 5.1 cannot be degraded by Abn4. It can, therefore, be concluded that Abn4 cannot hydrolyze the linkages of double substituted arabinose from arabinose oligomers.

Table 2 Branched arabinose oligomer structures according to Westphal and co-workers^{12,15}. Horizontal white dots: α -(1,5)-linked arabinofuranose units, branches attached on the lower left side: α -(1,3)-linked arabinofuranose side chain, branches attached on the lower right side: α -(1,2)-linked arabinofuranose side chain

Component	Schematic structure	PGC-HPLC-MS Retention time (min)
1.0		< 1.0
2.0		3.5
3.0		7.5
4.0		9.7
5.0		11.4
3.1		7.2
4.1		8.5
4.2		9.4
5.1		10.4
5.2		10.8
6.1b*		11.8
6.2		12.2
7.2**		13.2
8.1		13.9

* predicted structure confirmed by the degradation of 8.1 by Abf3 and Abn1

** proposed structure based on the degradation of 8.1 by Abn4

In contrast to Abn4, Abf3 can degrade both branched arabinopentaose isomers over time (**Figure 4**, line III). The amount of enzyme required for the degradation is similar to the amount needed for the degradation of the linear pentamer. The double substituted isomer 5.1 is converted into 4.1 ($t = 8.5$ min) by the removal of the terminal α -(1,5)-linked arabinose residue from the non-reducing end of the molecule. The 4.1 peak accumulates over time and is further degraded to monomer when a 10-fold overdose Abf3 is added to the mixture (**Figure 4**, line IV). The isomer 5.2 is degraded to the structure 4.2 by the hydrolysis of the terminal α -(1,3)-linkage at the non-reducing end (**Figure 4B**, line III, $t = 9.4$ min). Subsequently, the molecule is further degraded to two trimers 3.0 and 3.1 that

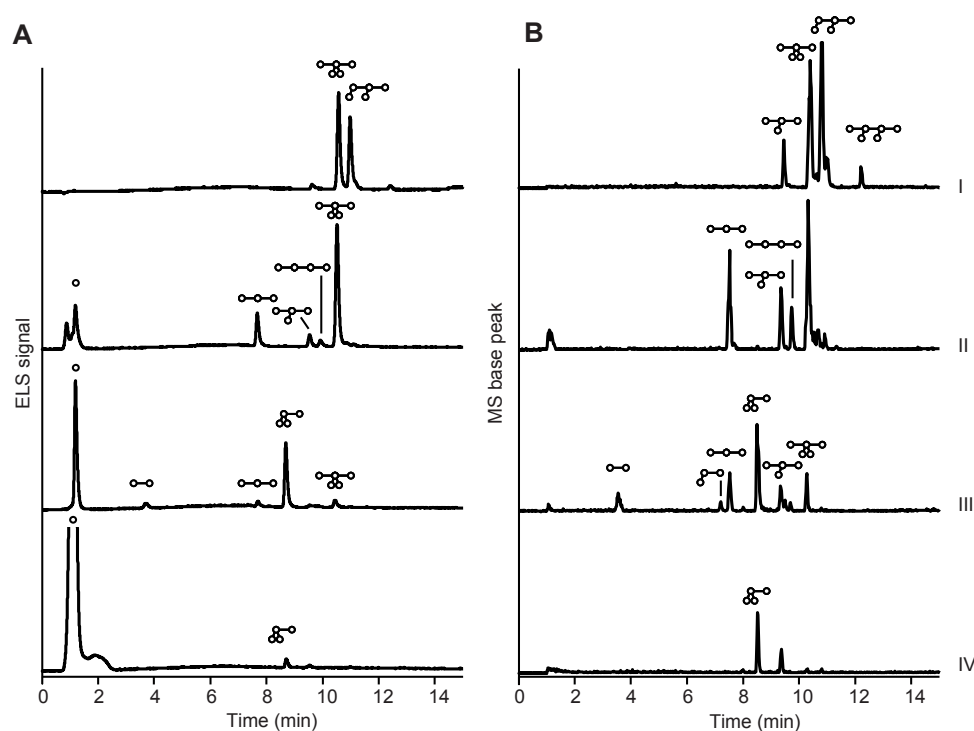


Figure 4 Time dependent degradation of the arabinopentaose isomers by Abf3 and Abn4. (A) PGC-HLPC-ELSD retention time profiles of the branched arabinopentaose mix (BAP), (B) PGC-HPLC-MS retention time profiles of BAP. (I) BAP (blank), (II) BAP digested with Abn4, (III) BAP digested with Abf3, (IV) BAP digested with ten fold concentration Abf3 ($t = 3\text{h}$).

elute at 7.5 min and 7.2 min, respectively. Both trimers are then converted to arabinobiose and subsequently to arabinose as end product (**Figure 4**, line IV). With respect to Abf3 it can be concluded that it can degrade all linkages present in 5.1 with a clear preference for single substituted sugars in proximity of the non-reducing end. The double substituted arabinose side chains are also degraded. However, the activity is 10-fold lower compared to the hydrolysis of a single α -(1,3)-linkage or α -(1,5)-linkage. The absence of any intermediate degradation products smaller than the 4.1 oligomer is in support of this behavior (**Figure 4A**).

Activity toward branched arabinooctaose

The C1 arabinohydrolases Abn1, Abn4 and Abf3 were sequentially tested toward the branched arabinooctaose isomer 8.1 to get more insight in structural limitations of enzymatic degradation. From **Figure 5A** it can be seen that Abn1 is not active toward 8.1 (line II). Abn4 has a low activity toward 8.1. It either can remove the terminal α -(1,5)-linked at the non-reducing end of the backbone or the α -(1,3)-linked arabinose side group and releases an arabinoheptaose isomer that elutes at 13.4 min (line III). This isomer can be degraded by Abn1 to the known arabinopentaose isomer 5.1 and arabinobiose (line IV). Therefore, the structure of the arabinoheptaose released by Abn4 is concluded to be as shown in structure 7.2 (**Table 2**). The data shows that Abn4 cannot remove the terminal non-reducing α -(1,5)-linked arabinose from 8.1. It releases the single substituted α -(1,3)-linked arabinose. This release is much slower than the removal of the α -(1,3)-linked arabinose units from 5.2. It is likely that the neighboring double substituted arabinose residue decreases the binding affinity of Abn4 toward its substrate. The highest activity of Abn4 is predicted toward α -(1,2)-linked arabinose since no oligomers with a single substituted α -(1,2)-linked arabinose could be isolated by Westphal and co-workers¹².

Regarding Abn1, these data show that it is side chain tolerant. Abn1 can hydrolyze the α -(1,5)-linkage of the backbone in the presence of a double substituted arabinose residue at -2. From the data shown in **Figure 1A** it was concluded that the binding affinity of the -2 and +2 subsites of Abn1 are much lower than the binding affinities of the neighboring subsites. The lower binding affinity of the -2 subsite is accompanied by a decreased substrate specificity that allows Abn1 to hydrolyze the 7.2 isomer.

Abf3 degrades 8.1 to the arabinohexaose isomer 6.1b (**Figure 5**, line V) that can be further degraded by Abn1 to give arabinobiose and 4.1 (no further data shown). It confirms that Abf3 can hydrolyze both, α -(1,3)-linked and α -(1,5)-linked arabinose. The appearance of the 7.2 isomer suggests a slight preference of the α -(1,3)-linked arabinose over the α -(1,5)-linked arabinose (line V) since this peak was the only arabinoheptaose structure that was released by Abf3.

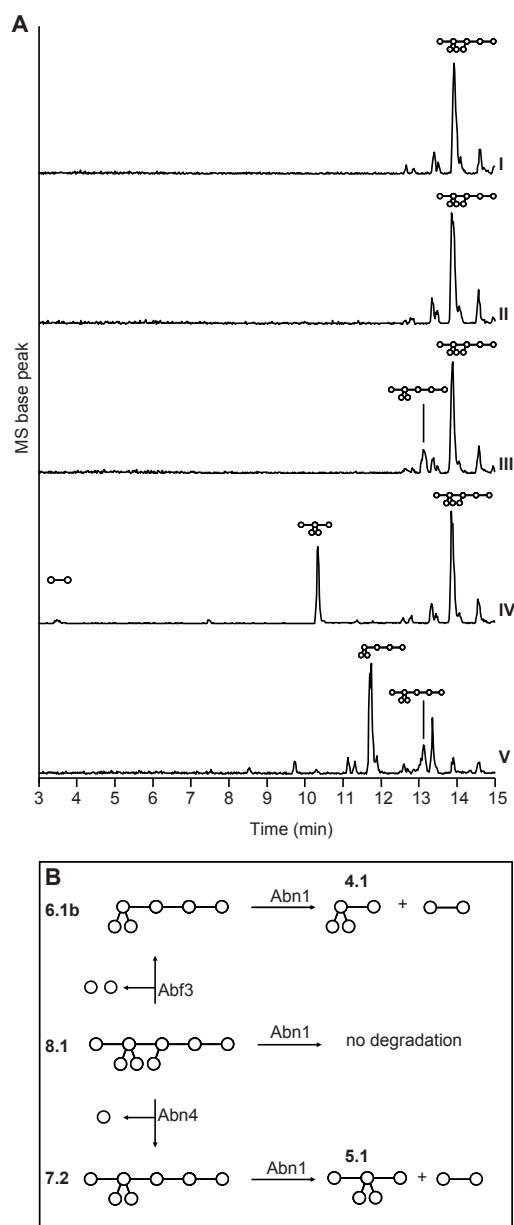


Figure 5 Degradation of branched arabinooctaose 8.1 by C1 arabinohydrolases. (A) HPLC-PGC-MS elution profile of 8.1 (I), 8.1 treated with Abn1 (II), 8.1 treated with Abn4 (III), sample III treated with Abn1 (IV) and 8.1 treated with Abf3 (V). (B) Schematic representation of branched arabinooctaose degradation by Abf3, Abn4 and Abn1.

Conclusions

The C1 arabinohydrolases have different modes of action and substrate specificities. The exo-arabinanase Abn2 releases arabinobiose from the non-reducing end of the α -(1,5)-linked arabinan backbone and prefers, like Abn1, polymers over oligomers. Endo-arabinanase Abn1 can hydrolyze substrates that carry a double substitution at the subsite -2 and is therefore considered as side chain tolerant. The arabinohydrolases Abn4 and Abf3 release arabinose monomers from the non-reducing end of the molecule with different linkage specificities (summarized in **Table 3**). The enzymes characterized allow the controlled and efficient degradation of arabinan to either monomers, or, by partial degradation, to branched arabinose oligomers.

Table 3 Linkage specificity of Abn4 and Abf3. Activities given for the preferred substrate: Abn4: branched arabinan, Abf3: linear and branched arabinose oligomers, * not determined

Linkage	α -(1,2)	α -(1,3)	α -(1,5)	α -(1,2) and α -(1,3)
Abn4	++	+	\pm	-
Abf3	n.d.*	++	++	+

Acknowledgements

The work has been financed in part by the Dutch Ministry of Economic Affairs via an EOS-LT grant (<http://www.senternovem.nl/eos/index.asp>).

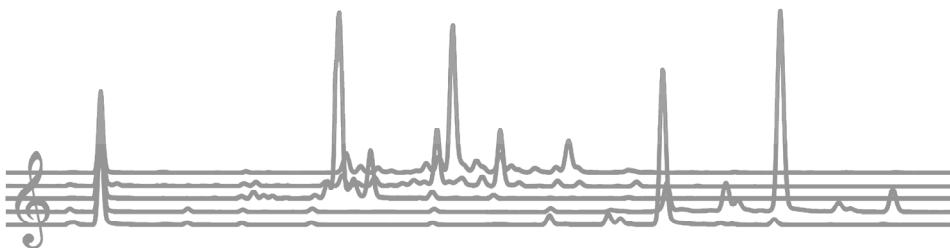
References

1. McCready, R.M. *J. Am. Soc. Sugar Beet*, **1966**, *14*, 260.
2. Rombouts, F.M.; Voragen, A.G.J.; Searle-van Leeuwen, M.F.; Geraeds, C.C.J.M.; Schols, H.A.; Pilnik, W. *Carbohydr. Polym.*, **1988**, *9*, 25-47.
3. Beldman, G.; Schols, H.A.; Pitson, S.M.; Searle-van Leeuwen, M.F.; Voragen, A.G.J., in Sturgeon, R.G. (Editor), *Advances in Macromolecular Carbohydrate Research*, Vol. 1, JAI Press Inc., **1997**, Greenwich, United Kingdom, p. 1-64.

4. Alhassid, A.; Ben-David, A.; Tabachnikov, O.; Libster, D.; Naveh, E.; Zolotnitsky, G.; Shoham, Y.; Shoham, G. *Biochem. J.*, **2009**, *422*, 73-82.
5. Dunkel, M.P.H.; Amado, R. *Carbohydr. Res.*, **1995**, *268*, 151-158.
6. Ichinose, H.; Yoshida, M.; Fujimoto, Z.; Kaneko, S. *Appl. Microbiol. Biot.*, **2008**, *80*, 399-408.
7. Sakamoto, T.; Thibault, J.F. *Appl. Environ. Microbiol.*, **2001**, *67*, 3319-3321.
8. Kaji, A.S., K. *Agr. Biol. Chem. Tokyo*, **1984**, *48*, 67-72.
9. Proctor, M.R.; Taylor, E.J.; Nurizzo, D.; Turkenburg, J.P.; Lloyd, R.M.; Vardakou, M.; Davies, G.J.; Gilbert, H.J. *P. Natl. Acad. Sci.*, **2005**, *102*, 2697-2702.
10. Hinz, S.W.A.; Pouvreau, L.; Joosten, R.; Bartels, J.; Jonathan, M.C.; Wery, J.; Schols, H.A. *J. Cereal Sci.*, **2009**, *50*, 318-323.
11. Kühnel, S.; Hinz, S.W.A.; Pouvreau, L.; Visser, J.; Schols, H.A.; Gruppen, H. *Bioresource Technol.*, **2010**, *accepted for publication*, DOI 10.1016/j.biortech.2010.05.070.
12. Westphal, Y.; Kühnel, S.; de Waard, P.; S.W.A., H.; Schols, H.A.; Voragen, A.G.J.; Gruppen, H. *Carbohydr. Res.*, **2010**, *345*, 1180-1189. *This thesis, Chapter 4*
13. Davies, G.J.; Wilson, K.S.; Henrissat, B. *Biochem. J.*, **1997**, *321*, 557-559.
14. Albrecht, S.; van Muiswinkel, G.C.J.; Schols, H.A.; Voragen, A.G.J.; Gruppen, H. *J. Agric. Food. Chem.*, **2009**, *57*, 3867-3876.
15. Westphal, Y.; Kühnel, S.; Schols, H.A.; Voragen, A.G.J.; Gruppen, H. *Carbohydr. Res.*, **2010**, *submitted for publication*. *This thesis, Chapter 5*
16. Carapito, R.; Imberty, A.; Jeltsch, J.M.; Byrns, S.C.; Tam, P.H.; Lowary, T.L.; Varrot, A.; Phalip, V. *J. Biol. Chem.*, **2009**, *284*, 12285-12296.
17. Nurizzo, D.; Turkenburg, J.P.; Charnock, S.J.; Roberts, S.M.; Dodson, E.J.; McKie, V.A.; Taylor, E.J.; Gilbert, H.J.; Davies, G.J. *Nat. Struct. Biol.*, **2002**, *9*, 665-668.

Chapter 7

Concluding remarks



Research motives

The plant cell wall represents a crucial and very complex structure surrounding the plant cells. It is responsible for various functions of the plant cell including stability and rigidity, flexibility and protection. Especially during plant growth, the plant cell wall needs to adapt continuously to fulfill all these functions^{1,2}. The main components are the cell wall polysaccharides cellulose, hemicelluloses and pectin, which are known to be very complex macromolecules. Furthermore, the occurrence and chemical fine structure of these cell wall polysaccharides differ depending on the plant origin and developmental stage.

Detailed and efficient characterization of the complex cell wall polysaccharides, and products thereof, are important in food and non-food applications and processing, including bio-active compounds and bio ethanol production. To enable a good characterization of all these complex cell wall polysaccharides, suitable (and fast) analytical tools are required. Since polysaccharides are usually too complex to be characterized as such, the aim of the present PhD thesis was to extend the current analytical tool box to enable the separation of complex mixtures containing neutral and acidic cell wall derived oligosaccharides. Therefore, various LC and CE-MS approaches were explored for a broad range of neutral and acidic cell wall derived oligosaccharides to be used as screening, fingerprinting and/or prediction tool within cell wall analysis.

Screening for *Arabidopsis* plants varying in cell wall polysaccharide structure

A multi-enzyme assisted method for the screening of *Arabidopsis* mutants is described in chapter 2. This method is a further development of the OLIMP (oligosaccharide mass profiling) method³, in which a MALDI-TOF MS based screening method was set-up for xyloglucan (XG) derived oligosaccharides after enzymatic degradation of the xyloglucan by xyloglucan-endo-glucanase (XEG)⁴. In contrast, in our research a mixture of ten pure and well-defined enzymes was added to the alcohol insoluble solids (AIS) of the samples in order to degrade cellulose, hemicelluloses and pectin: Endo-glucanase I, cellobiohydrolase (CBH), XEG, β -(1,4)-xylanase, endo-polygalacturonanase (endo-PG), pectin methyl esterase (PME), rhamnogalacturonan hydrolase (RGH), xylogalacturonan hydrolase (XGH), α -(1,5)-arabinanase and β -(1,4)-galactanase. In contrast to present literature, demonstrating a MALDI-TOF MS screening method after enzymatic degradation of one

single polysaccharide as described for XG and homogalacturonan^{3,5,6}, our approach provides a fingerprint of all enzyme-accessible *Arabidopsis* cell wall polysaccharides in a single MALDI-TOF mass spectrum. This multi-enzyme assisted screening method was validated with leaf material derived from known *Arabidopsis* cell wall mutants (*qual*, *mur3* and *xgd1*). Differences in the relative abundance of the oligosaccharides released can mostly be linked to a distinct polysaccharide and its variability. For example, the cell wall mutant *qual* being deficient in homogalacturonan (HG)^{7,8} showed a clear decrease in HG oligosaccharides released within the MALDI-TOF mass spectrum after digestion with the enzyme cocktail (chapter 2).

Furthermore, the use of CE-LIF for the detection of the oligosaccharides released after degradation with the enzyme cocktail was demonstrated to have potential in the screening for *Arabidopsis* analysis. The CE-LIF electropherograms obtained from leaf material of the known *Arabidopsis* mutants *qual* and *mur3* after enzymatic degradation showed clear differences compared to the corresponding wild-type plants (chapter 2). Since most mutants having extremely different cell wall compositions might have been recognized already, we anticipate that future *Arabidopsis* mutants will mainly differ in the quantity and relative abundances of the polysaccharides present. Therefore, the demand of screening methods enabling quantifications of the oligosaccharides released will increase significantly in future. CE-LIF enables a mol-based-detection^{9,10} and is suitable for the analysis of very small amounts of sample. Even though not performed in this research, CE-LIF enables the quantification of the oligosaccharides released, when a suitable internal standard is used during analysis.

As the focus in *Arabidopsis* research is directed to the analysis of hypocotyls, both MALDI-TOF MS and CE-LIF approaches were downscaled to hypocotyl level. Even though some limitations were required with respect to the analysis of *Arabidopsis* hypocotyls, we could successfully distinguish mutant *Arabidopsis* hypocotyls from the corresponding wild type hypocotyls addressing *gaut13* as an interesting candidate for further analysis (chapter 2).

The enzyme cocktail as flexible analytical tool

The enzymes added to the enzyme cocktail were chosen based on cell wall composition in order to degrade all enzyme-accessible plant cell wall polysaccharides. A second prerequisite of enzymes selected was their ability to release structural information containing oligosaccharides. An exception was the addition of pectin methyl esterase

(PME), which removes methyl esters in the samples in order to enhance the HG degradation by endo-PG (as also done before⁶). Although some structural information will be lost, significant amounts of characteristic methyl-esterified oligosaccharides remain in the digest (chapter 2) as PME is not able to remove all methyl esters present¹¹.

Use of additional enzymes

The availability of more and more genomes being completely sequenced, and the therefore target-oriented search for novel enzymes has already and will in future support the identification and characterization of many enzymes, which might be used to further enhance the degradation of polysaccharides within this multi-enzyme assisted screening method.

To comprise differences in methyl ester distribution patterns between mutant and wild type plants the addition of pectin lyase to the enzyme cocktail might be a good alternative. Pectin lyase is known to cleave the linkage between two methyl esterified α -(1,4)-linked galacturonic acid units (chapter 1,¹²). Since pectin lyase would not work on low methyl esterified pectin, a mixture of endo-PG and pectin lyase within the enzyme cocktail could be tested as well.

The use of more enzymes being more tolerant against acetyl or feruloylated groups or methyl esters than the ones tested would increase the amount and number of liberated oligosaccharides without losing diagnostic information. Thus, a valuable supplement of the enzyme cocktail would be, for example, the recently described rhamnogalacturonan hydrolase being tolerant toward acetyl groups¹³.

Xylogalacturonan, as present in alcohol insoluble solids, was hardly digested by xylogalacturonan hydrolase. This is most likely due the presence of methyl esterification. To confirm this assumption and to enable the release of characteristic xylogalacturonan derived oligosaccharides, it would be of great interest to find and use a xylogalacturonan hydrolase, which is tolerant toward variations at the xylogalacturonan backbone as was previously described for rhamnogalacturonan hydrolase¹³.

Arabino-, galacto- and arabinogalacto-oligosaccharides released are only present in minor amounts in both MALDI-TOF mass spectra and CE-LIF electropherograms of *Arabidopsis* leaf and hypocotyl tissues. Thus, it can be hypothesized that the addition of α -(1,5)-arabinanase and β -(1,4)-galactanase was not sufficient to degrade the complex side chains of RG-I. The additional use of arabinofuranosidases, exo-arabinanases or

β -galactosidases could support the degradation of these RG-I side chains, even though complete degradation toward monomers has to be avoided¹⁴⁻¹⁷.

Furthermore, pectin acetyl esterase, rhamnogalacturonan acetyl esterase and ferulic acid esterase could be added in the enzyme cocktail in order to liberate more material as these accessory enzymes remove acetyl or feruloylated groups, respectively. These groups hinder the glycohydrolases to work resulting in too large oligosaccharides to be included in our analysis. The accessory enzymes would liberate more material, although the obtained MALDI-TOF MS fingerprint may be less diagnostic as differences in the characteristic distribution patterns would be reduced.

The cell wall polysaccharide rhamnogalacturonan (RG-II), which is reported to be important for plant growth^{18,19}, is not covered in the multi-enzyme assisted screening method (chapter 2) as enzymes required for the degradation of RG-II have not yet identified²⁰. The addition of glycohydrolases releasing diagnostic oligosaccharides from RG-II enabling MALDI-TOF MS or CE-LIF detection would increase the value of this multi-enzyme assisted screening method significantly. A MALDI-TOF MS fingerprinting method for RG-II using mild acid for hydrolysis as has recently been presented²⁰ represents a good supplementation to our approach as well, allowing the detection of *Arabidopsis* mutants deviating in the RG-II structure.

Implications for other fields of research

As described above the multi-enzyme assisted screening method (chapter 2) can easily be extended by other (novel) enzymes depending on the research question. For example, the method might be used for the screening of cell wall polysaccharide mutants from *Brachypodium distachyon*, the upcoming model plant for temperate grasses²¹. Another application field might be the determination of the degree of ripeness for fruits and vegetables (e.g. tomatoes, mango's). The structure of the cell wall polysaccharides of fruits and vegetables changes during ripening. Therefore, enzymatic or even chemical degradation prior to MALDI-TOF MS and CE-LIF detection of the diagnostic oligosaccharides will then provide information of the maturation state of the fruits and vegetables. The screening of by-products from food production for further valorization, and the screening of food processing steps and biochemical processes are two other possible application fields for a MALDI-TOF MS and CE-LIF screening method of diagnostic oligosaccharides.

Enzyme-assisted screening methods are very powerful techniques to provide a fast overview of the enzyme-accessible cell wall polysaccharides in a sample. However, some peaks cannot be annotated unambiguously due to the same m/z value for two or more components within a complex oligosaccharide mixture (chapter 2). Therefore, the use of MALDI-TOF-TOF-MS enabling easy MS² measurements might overcome this drawback.

Another great improvement would be the application of these enzyme-assisted screening methods directly on the material without any purification step needed before. Recently, Obel and co-workers introduced the ‘in-situ’-analysis of xyloglucan (XG) oligosaccharides for *Arabidopsis* roots and stems by MALDI-TOF MS, which even allowed the analysis of XG oligosaccharides at different localizations within one *Arabidopsis* organ⁶. This approach should definitely be extended to all enzyme-accessible cell wall polysaccharides. This will provide a fingerprint of the entire enzyme-accessible cell wall at distinct localizations within one *Arabidopsis* plant or parts of fruits, vegetables or cereals (even after processing to foods). A continuation would be the localization of certain polysaccharide features such as RG-I and HG or the distribution of acetylated or methyl esterified oligosaccharides using imaging software. One drawback of these MALDI-TOF MS based screening methods is the lacking quantification of the oligosaccharides released. Furthermore, the production of too many monomers could hinder the detection of MALDI-TOF MS.

Another option to enable the screening of enzyme-accessible cell wall polysaccharides would be the use of an ESI-ion mobility-MS after direct injection of the multi-enzyme digest. No crystallization on the MALDI plate is necessary, and thus the variations due to the crystallization would be omitted. Furthermore, as separation is not only based on size but as well on conformational differences, even oligosaccharide isomers with the same m/z -values, which cannot be distinguished by MALDI-TOF MS, can be separated with ion mobility. This will result in a mapping of all oligosaccharides released enabling as well the distinction of isomeric oligosaccharides, as e.g. released by xylans and arabinans.

PGC-HPLC in cell wall analysis

PGC-HPLC-ELSD/MS is already known for some time and has frequently been used in the analysis of human milk oligosaccharides, glycoproteins, cyclodextrins, aromatic and polar compounds for some time²²⁻²⁷. Only few examples for the use of PGC-HPLC-ELSD/MS for cell wall derived oligosaccharides have been described,

including maltodextrins and galactans^{28,29}. In our research we could demonstrate that PGC-HPLC-ELSD/MS is suitable for the analysis of a broad range of cell wall derived oligosaccharides including α -(1,5)-arabino-, β -(1,4)-xylo-, β -(1,4)-galacto-, α -(1,4)-gluco-, β -(1,4)-gluco-, β -(1,4)-manno- and α -(1,4)-galacturono-oligosaccharides (chapter 3). Within homologous series of neutral oligosaccharides, the retention time is based on size. In between homologous series of neutral oligosaccharides, a clear correlation between planarity of the molecule and retention time on PGC-material could be found for all tested cell wall oligosaccharides. This is in good agreement with the known mechanism on PGC material²²: The more planar the molecule, the later the elution. Thus, β -(1,4)-xylo- and β -(1,4)-gluco-oligosaccharides elute significantly later than the rest of the oligosaccharides investigated. This retention behavior is quite predictive and can be used for the prediction of unknown oligosaccharide structures as exemplified by arabino-oligosaccharides in chapter 5 and has already been demonstrated for a selection of human milk oligosaccharides earlier³⁰. The software program ChemBio Office 2010 (Cambridge Soft Corporation, Cambridge, MA, USA) allowed the simplified modeling of the 3D-structures of carbohydrates, which facilitates the identification of unknown peaks within the chromatograms based on their 3D-conformation (chapter 5).

The retention time of charged oligosaccharides is based on their charge, even though neutral side chains having strong influence on the conformation of the molecules may lead to a separation of oligosaccharides carrying the same charge (chapter 3).

The identification of oligosaccharides by PGC-HPLC-ELSD/MS is expected to be a 'second-step' technique. Thus, the user should have already some basic knowledge of the sample (e.g. sugar composition) before using this advanced HPLC-MS technique. Main application fields within cell wall analysis will, most likely, be the analysis of enzyme resistant cereal, fruit and vegetable structures within food and non-food processes as well as the monitoring of enzymatic degradations as demonstrated in chapter 6. For the analysis of small amounts of sample, e.g. in *Arabidopsis* hypocotyl analysis, the use of PGC-capillaries or even the use of nano-LC ('microfluidic glycochips') systems as described for human milk oligosaccharides³¹ might be a good possibility.

PGC-HPLC, similar to other liquid chromatography methods, is a rather versatile method. A broad range of cell wall derived oligosaccharides was already included in our research (chapter 3), although quite some oligosaccharides released from the cell wall were not included: e.g., feruloylated arabino-glucurono-xylo-oligosaccharides or arabino-

oligosaccharides, acetylated HG or RG-I oligosaccharides, (galacto-gluco)-manno-oligosaccharides, and branched arabinogalacto-oligosaccharides. Preliminary results (not shown) indicated that the gradient may be adapted depending on the interaction of the oligomers with the PGC material, while also other organic and acidic modifiers may be needed.

Similar to RP-HPLC, PGC-HPLC separates both α - and β - forms of the oligomer to a certain extent, which is not desired. It leads to a broad peak or even a double peak for every component in the chromatogram complicating the chromatogram significantly. In addition to the use of higher temperature as used in our research to avoid α - and β -separation (chapter 3), another option might be the reduction of the oligosaccharides prior to analysis^{30,32} in order to have better peak shapes and a better resolution. Furthermore, the sugar would be labeled at the reducing end, which would support the MSⁿ analysis.

CE-LIF-MS in cell wall analysis

Although other analytical tools are available to analyze complex mixtures (chapter 1), we focused on the comparison of PGC-HPLC with CE-LIF-MS. The latter had been described to be a very promising method due to the very good resolution of many neutral and acidic cell wall derived oligosaccharides in short time⁹. Furthermore, CE-LIF is suitable for small sample amounts, as was demonstrated with the analysis of *Arabidopsis* hypocotyls in chapter 2, and allows mole-based detection. However, even though CE-LIF enables the separation of many oligosaccharides and CE-MS-coupling allows powerful MS fragmentations of labeled oligosaccharides, the resolution in CE-MS is much lower compared to CE-LIF analysis as already observed by others and is also addressed for arabino-oligosaccharides in chapter 5. CE-MS² fragmentation patterns were shown to be very informative. However, due to co-elution, MS² spectra could not be obtained for all arabino-oligosaccharides present in a complex mixture (chapter 5). The loss of resolution is mainly due to the use of another capillary and MS-compatible buffer when compared to CE-LIF. To improve the separation during CE-MS analysis another capillary should be used, preferably the same as used for CE-LIF. However, we did not succeed in establishing a stable ion spray and ion current when using the “CE-LIF”-capillary during CE-MS analysis. New CE-MS interfaces under development may take us a step forward. Another possibility would be the coupling of a mass spectrometer equipped with an ion mobility

device. Even though co-elution of the oligosaccharides occurs, the labeled oligosaccharides might then be separated due to different conformations of the molecule.

We think that PGC-HPLC-ELSD/MS and CE-LIF-MS are compulsory techniques in oligosaccharide research. In combination, these techniques are very powerful tools to enable the characterization of complex cell wall derived oligosaccharide mixtures as was already shown for arabino-oligosaccharides in chapter 5.

Branched arabino-oligosaccharides

Two unique series of branched arabino-oligosaccharides were isolated from sugar beet arabinan. Both series consist of a backbone of α -(1,5)-linked L-arabinosyl residues. In one series the α -(1,5)-linked arabinan backbone was only substituted with single α -(1,3)-linked L-arabinosyl residue(s), while the backbone of the other series carried a double substitution of α -(1,2) and α -(1,3) L-arabinosyl residues and might carry an additional single α -(1,3)-linked L-arabinosyl residue (chapter 4). These arabino-oligosaccharides could also be identified in *Arabidopsis* stems derived from *arad1* and *Col0* plants after digestion with a mixture of arabinohydrolases of *Chrysosporium lucknowense* as used in chapter 4 for sugar beet arabinan (data not shown). During our analysis we could not isolate any arabino-oligosaccharides carrying a single α -(1,2)-linked L-arabinosyl residue (chapters 4 and 5). Thus, it is hypothesized that the exo-arabinanase Abn4 used for the preparation of the arabino-oligosaccharides has the highest activity toward a single α -(1,2)-linked arabinose (chapter 6). The attachment of ferulic acid to the arabino-oligosaccharides is a common feature in sugar beet arabinan³³⁻³⁵. Due to a strong alkali-treatment during extraction of sugar beet arabinan (British Sugars, Peterborough, United Kingdom), these feruloylated groups were removed. For further research, it would be very interesting to study the action of the arabino-hydrolases Abn1, Abn2, Abn4 and Abf3 derived from *C. lucknowense*¹⁵ (chapters 4 and 6) on feruloylated arabinan.

Furthermore, it might be of great interest to test the isolated branched arabino-oligosaccharides upon their prebiotic effects. Linear arabino-oligosaccharides were demonstrated to have prebiotic effects^{36,37}, thus the branched structures are hypothesized to be even less degraded in the proximal part of the colon and might reach the distal part of

the gastrointestinal tract, in which many colonic diseases, such as ulcerative colitis and tumors, occur^{38,39}.

Another possible use for the arabino-oligosaccharides isolated, is the use for competitive inhibition assays of monoclonal antibodies raised against e.g. arabinan, arabinogalactan or even arabinoxylan⁴⁰. And even more interesting would be the isolation of highly defined monoclonal antibodies being directed to e.g. double substituted L-arabinosyl residues within branched arabinan by immunizing with the arabino-oligosaccharides isolated (chapter 4). The resulting monoclonal antibodies might be used to study the distribution of branched arabinan within the cell wall of various plants and developmental stages of a plant.

LC/CE-MS analysis of arabino-oligosaccharides

The separation of linear and branched arabino-oligosaccharides was not possible with commonly used HPAEC-PAD as about half of the components co-eluted with at least one other arabino-oligosaccharide (chapter 5). In contrast, PGC-HPLC-ELSD/MS and CE-LIF enabled the separation of 70-85% of all arabino-oligosaccharides. An example of HPAEC failing to give sufficient information on the purity of reference oligosaccharides is our discovery that some batches of commercially available 'pure' arabinotetraose still contain 1-15% of a branched arabinotetramer (4.2, chapter 5) as recognized by PGC-HPLC and CE-LIF. Thus, PGC-HPLC-ELSD/MS and CE-LIF were in favor for further in-depth-characterization of arabinan-degrading enzymes (chapter 6). Due to the good separation on PGC-HPLC-ELSD/MS of the branched arabino-oligosaccharides and the online-MS detection, easy annotation of almost all peaks could be achieved and the mode of action of the enzymes studied could be described (chapter 6). Furthermore, the predictive retention behavior of PGC-material together with the controlled enzyme treatment and LC- and CE-MS fragmentation patterns allowed the prediction of the structure of two arabino-oligosaccharides of DP 6 (chapter 5). This combined approach certainly can be applied to any other cell wall derived oligosaccharide, such as oligosaccharides derived from arabinoxylan, arabinogalactan type I and II, galacto-gluco-mannan and acidic oligosaccharides derived from homogalacturonan-, rhamnogalacturonan I and xylogalacturonan. It should be noted that some optimization of the LC-gradient may be needed for the acidic oligosaccharides prior to possible prediction of their structures upon their retention times on PGC material. Thus, this technique enables the characterization of

various (novel) enzymes as well as the characterization of unknown oligosaccharides by combining the use of purified and well-defined enzymes and LC-MSⁿ information.

Due to the development of powerful MS and ELS detectors as well as columns with a higher separation efficiency allowing the detection and identification of many carbohydrates, we experience a revival of HPLC materials such as reversed phase, porous graphitized carbon and hydrophilic interaction chromatography (HILIC)⁴¹. Although not tested in this PhD thesis, it could be worthwhile to explore especially HILIC for a broad range of cell wall derived oligosaccharides as is done in our research for PGC (chapter 3). HILIC describes a mode of chromatography, in which a polar stationary phase (such as aminopropyl silica or amide-80⁴²) is used in combination with a less polar mobile phase. It has been described to be suitable to retain both neutral and acidic carbohydrates and thus could be a good alternative for the analysis of many cell wall oligosaccharides. However, the use of high concentration of organic modifiers might cause solubility problems of some higher oligomeric sugars.

LC-MS² fragmentation of unknown oligosaccharides

No unambiguous identification of the structures of the arabino-oligosaccharides was possible by LC-MS² fragmentation due to the fragmentation behavior of the branched arabino-oligosaccharides and the absence of a label at the reducing end (chapter 5). For other oligosaccharides such as oligosaccharides derived from homogalacturonan, RG-I, xylogalacturonan, arabinoxylan and xyloglucan as well as feruloylated arabino-oligosaccharides, it was shown that MS² fragmentation is a good possibility to identify the structures unambiguously⁴². To improve the LC-MS² fragmentation patterns of arabino-oligosaccharides in specific and all other oligosaccharides in more general during PGC-HPLC analysis, labeling of the oligosaccharides at the reducing end will help significantly. As water represents a great part of the eluents, ¹⁸O-labeling will most likely not be stable during a 45 min run at 70 °C. Another option could be the reduction of the oligosaccharides as already discussed earlier in this chapter. The use of charged labels is not preferred as elution will be significantly delayed and separation based on planarity within the neutral oligosaccharides will be reduced. The use of fluorescent labels such as 2-aminobenzoic acid (2-AA)⁴² could be a possible alternative.

For both, reduction and labeling, the production of double peaks due to anomerization would be eliminated as the reducing end is blocked. Furthermore, the label would simplify interpretation of MSⁿ data derived from the oligosaccharide of interest. However, the influence of the planar aromatic structure of the fluorescent label 2-AA on the retention time on PGC-material as well as the labeling/reduction efficiency has to be evaluated.

Final remarks

MS analysis is getting more and more important in cell wall analysis. MS analysis provides very characteristic data and allows identification of unknown structures in complex matrixes⁴², when NMR is only suitable after extensive and laborious purification efforts due to the heterogeneity of the sample. The bottleneck of MS analysis nowadays is the analysis of oligosaccharides having the same *m/z* values. To overcome this drawback, high resolution LC and CE techniques combined with mass spectrometers are required. Thereby, the revival of long-time-known LC-methods (RP, NP, HILIC, and PGC) as well as the development of novel techniques such as ESI-ion mobility-MS will boost the cell wall analysis in the near future.

References

1. Caffall, K.H.; Mohnen, D. *Carbohydr. Res.*, **2009**, *344*, 1879-1900.
2. Ridley, B.L.; O'Neill, M.A.; Mohnen, D.A. *Phytochemistry*, **2001**, *57*, 929-967.
3. Lerouxel, O.; Choo, T.S.; Seveno, M.; Usadel, B.; Faye, L.; Lerouge, P.; Pauly, M. *Plant Physiology*, **2002**, *130*, 1754-1763.
4. Pauly, M.; Andersen, L.N.; Kauppinen, S.; Kofod, L.V.; York, W.S.; Albersheim, P.; Darvill, A. *Glycobiology*, **1999**, *9*, 93-100.
5. Lionetti, V.; Raiola, A.; Camardella, L.; Giovane, A.; Obel, N.; Pauly, M.; Favaron, F.; Cervone, F.; Bellincampi, D. *Plant Physiology*, **2007**, *143*, 1871-1880.
6. Obel, N.; Erben, V.; Schwarz, T.; Kuhnelt, S.; Fodor, A.; Pauly, M. *Mol. Plant.*, **2009**, *2*, 922-932.
7. Bouton, S.; Leboeuf, E.; Mouille, G.; Leydecker, M.T.; Talbotec, J.; Granier, F.; Lahaye, M.; Hofte, H.; Truong, H.N. *Plant Cell*, **2002**, *14*, 2577-2590.
8. Orfila, C.; Sorensen, S.O.; Harholt, J.; Geshi, N.; Crombie, H.; Truong, H.N.; Reid, J.S.G.; Knox, J.P.; Scheller, H.V. *Planta*, **2005**, *222*, 613-622.
9. Kabel, M.A.; Heijnis, W.H.; Bakx, E.J.; Kuijpers, R.; Voragen, A.G.J.; Schols, H.A. *J. Chromatogr. A*, **2006**, *1137*, 119-126.

10. Albrecht, S.; Schols, H.A.; Klarenbeek, B.; Voragen, A.G.J.; Gruppen, H. *J. Agric. Food. Chem.*, **2010**, *58*, 2787-2794.
11. Versteeg, C.; Rombouts, F.M.; Pilnik, W. *Lebensmittel-Wissenschaft & Technologie*, **1978**, *11*, 267-274.
12. Benen, J.A.E.; Vincken, J.-P.; Alebeek, G.-J.W.M.v. in: Seymour, G.B., Knox, J.P. (eds.) *Pectins and their Manipulation*, Oxford, United Kingdom, **2002**, p. 174-221.
13. Normand, J.; Ralet, M.C.; Thibault, J.F.; Rogniaux, H.; Delavault, P.; Bonnin, E. *Appl. Microbiol. Biotechnol.*, **2010**, *86*, 577-588.
14. Beldman, G.; Schols, H.A.; Pitson, S.M.; Searle-van Leeuwen, M.F.; Voragen, A.G.J., in Sturgeon, R.G. (Editor), *Advances in Macromolecular Carbohydrate Research*, Vol. 1, JAI Press Inc., Greenwich, United Kingdom, **1997**, p. 1-64.
15. Kühnel, S.; Hinz, S.W.A.; Pouvreau, L.; Visser, J.; Schols, H.A.; Gruppen, H. *Bioresource Technol.*, **2010**, *accepted for publication*, DOI 10.1016/j.biortech.2010.05.070.
16. van de Vis, J.W.; Searle-van Leeuwen, M.J.F.; Siliha, H.A.; Kormelink, F.J.M.; Voragen, A.G.J. *Carbohydr. Polym.*, **1991**, *16*, 167-187.
17. Hinz, S.W.A.; Broek, L.A.M.; Beldman, G.; Vincken, J.-P. *Appl Microbiol Biotechnol.*, **2004**, *66*, 276-284.
18. O'Neill, M.A.; Eberhard, S.; Albersheim, P.; Darvill, A.G. *Science*, **2001**, *294*, 846-849.
19. O'Neill, M.A.; Ishii, T.; Albersheim, P.; Darvill, A.G. *Annual Review Of Plant Biology*, **2004**, *55*, 109-139.
20. Séveno, M.; Voxeur, A.; Rihouey, C.; Wu, A.M.; Ishii, T.; Chevalier, C.; Ralet, M.C.; Driouich, A.; Marchant, A.; Lerouge, P. *Planta*, **2009**, *230*, 947-957.
21. Christensen, U.; Alonso-Simon, A.; Scheller, H.V.; Willats, W.G.T.; Harholt, J. *Phytochemistry*, *71*, 62-69.
22. Pereira, L. *J. Liq. Chromatogr. Related Technol.*, **2008**, *31*, 1687-1731.
23. Gnoth, M.J.; Rudloff, S.; Kunz, C.; Kinne, R.K.H. *J. Biol. Chem.*, **2001**, *276*, 34363-34370.
24. Polyakova, Y.L.; Row, K.H. *Chromatographia*, **2007**, *65*, 59-63.
25. Polyakova, Y.; Row, K.H. *J. Liq. Chromatogr. Related Technol.*, **2005**, *282*, 3157-3168.
26. Barroso, B.; Dijkstra, R.; Geerts, M.; Lagerwerf, F.; van Veelen, P.; de Ru, A. *Rapid Commun. Mass Spectrom.*, **2002**, *16*, 1320-1329.
27. Antonio, C.; Larson, T.; Gilday, A.; Graham, I.; Bergström, E.; Thomas-Oates, J. *J. Chromatogr. A*, **2007**, *1172*, 170-178.
28. Ishimaru, M.; Smith, D.L.; Mort, A.J.; Gross, K.C. *Planta*, **2009**, *229*, 447-456.
29. Koizumi, K.; Okada, Y.; Fukuda, M. *Carbohydr. Res.*, **1991**, *215*, 67-80.
30. Pabst, M.; Bondili, J.S.; Stadlmann, J.; Mach, L.; Altmann, F. *Anal. Chem.*, **2007**, *79*, 5051-5057.
31. Ninonuevo, M.R.; Perkins, P.D.; Francis, J.; Lamotte, L.M.; LoCascio, R.G.; Freeman, S.L.; Mills, D.A.; German, J.B.; Grimm, R.; Lebrilla, C.B. *J. Agric. Food. Chem.*, **2008**, *56*, 4854-4854.

- 32. Stadlmann, J.; Pabst, M.; Kolarich, D.; Kunert, R.; Altmann, F. *Proteomics*, **2008**, *8*, 2858-2871.
- 33. Ralet, M.C.; Andre-Leroux, G.; Quemener, B.; Thibault, J.F. *Phytochemistry*, **2005**, *66*, 2800-2814.
- 34. Quemener, B.; Ralet, M.C. *J. Mass Spectrom.*, **2004**, *39*, 1153-1160.
- 35. Ishii, T. *Plant and Cell Physiology*, **1994**, *35*, 701-704.
- 36. Suzuki, Y.; Tanaka, K.; Nano, T.; Asakura, T.; Muramatsu, N. *Japan Soc. Horticultural Sci.*, **2004**, *73* (6), 574-579.
- 37. Van Laere, K.M.J.; Hartemink, R.; Bosveld, M.; Schols, H.A.; Voragen, A.G.J. *J. Agric. Food Chem.*, **2000**, *48*, 1644-1652.
- 38. Voragen, A.G.J. *Trends Food Sci. Tech.*, **1998**, *9*, 328-335.
- 39. Albrecht, S.; van Muiswinkel, G.C.J.; Schols, H.A.; Voragen, A.G.J.; Gruppen, H. *J. Agric. Food. Chem.*, **2009**, *57*, 3867-3876.
- 40. Verhertbruggen, Y.; Marcus, S.E.; Haeger, A.; Verhoef, R.; Schols, H.A.; McCleary, B.V.; McKee, L.; Gilbert, H.J.; Knox, J.P. *Plant Journal*, **2009**, *59*, 413-425.
- 41. Hemstrom, P.; Irgum, K. *J. Sep. Sci.*, **2006**, *29*, 1784-1821.
- 42. Maslen, S.L.; Goubet, F.; Adam, A.; Dupree, P.; Stephens, E. *Carbohydr. Res.*, **2007**, *342*, 724-735.

Summary

Plant cell walls surround and protect each cell present in plant tissues and are responsible for the stability and rigidity as well as the flexibility of the plant tissue. Especially during plant growth, the plant cell wall needs to adapt continuously to fulfill all these functions. The main components of the cell wall are the polysaccharides cellulose, hemicellulose and pectins. Chapter 1 gives a general introduction on the occurrence, chemical fine structures and biological variations of these plant cell wall polysaccharides. Furthermore, the main models concerning the architecture of the cell wall polysaccharides are addressed. Additionally, an overview of cell wall degrading enzymes including cellulases, hemicellulases and pectinases is presented. The separation and detection techniques commonly used for the analysis of cell wall derived mono-, oligo- and polysaccharides are briefly reviewed as well. The analysis of polysaccharides is mainly performed using time-consuming fractionation and purification steps followed by e.g. sugar (linkage) analysis and NMR. However, as analysis of the intact polysaccharides only provides limited information of its chemical fine structure, the main analytical tools revealing the chemical fine structure of the cell wall polysaccharides focus on the separation and detection of diagnostic oligosaccharides after controlled enzymatic or chemical degradation of the polysaccharides.

This PhD study focuses on 1) the development of high-throughput screening methods of both neutral and acidic cell wall derived oligosaccharides and 2) the development of analytical tools, which separate both neutral and acidic oligosaccharides and even enable a prediction on structural features within the molecule of interest based on retention time and online-recorded MSⁿ data.

Chapter 2 describes a multi-enzyme assisted screening method for mutant *Arabidopsis* plants deviating in the cell wall polysaccharide structures. By applying pure and well-defined cellulases, hemicellulases and pectinases to isolated *Arabidopsis* plant materials we aimed at the degradation of all enzyme-accessible plant cell wall polysaccharides. Matrix-Assisted Desorption/Ionization Time-of-Flight Mass Spectrometry (MALDI-TOF MS) detection provided a fast overview of the neutral and acidic oligosaccharides released (m/z 500-2000, about DP 3-12) resulting in a characteristic fingerprint in a single MALDI-TOF mass spectrum. Capillary Electrophoresis-Laser Induced Fluorescence (CE-LIF) detection was demonstrated to provide complementary information including the quantification of the oligosaccharides released on a mole-based detection principle. The methods were validated

with leaf tissues of known *Arabidopsis* mutants. Furthermore, downscaling of the method toward hypocotyl level was performed, even though this complicated the analysis significantly.

In Chapter 3 Porous-Graphitized-Carbon (PGC)-HPLC analysis with Evaporative Light Scattering (ELS) and MSⁿ detection was explored for a broad range of cell wall derived oligosaccharides. A water-acetonitrile-gradient for the first 15 minutes ensured good separation of almost all neutral oligosaccharides under investigation, including α -(1,5)-L-arabino-, β -(1,4)-D-xylo-, α -(1,4)-D-gluco-, β -(1,4)-D-gluco-, β -(1,4)-D-galacto- and β -(1,4)-D-manno-oligosaccharides. Within homologous series, the separation is based on size. In between the different homologous series, the separation is based on the conformation of the oligosaccharides: The more planar the molecule, the later the elution. Thus, β -(1,4)-D-xylo- and β -(1,4)-D-gluco-oligosaccharides elute significantly later than the rest of the neutral oligosaccharides. Using neutral acetylated β -(1,4)-D-xylo-oligosaccharides it could be demonstrated that acetylation results in significant increase of the retention time. The acidic α -(1,4)-D-linked galacturonic acid oligomers (DP 2-9) elute after the addition of the acidic modifier TFA. The separation of these charged oligomers is mainly based on charge as could be as well seen for other charged pectic oligomers (xylogalacturonan and rhamnogalacturonan-I oligosaccharides). Neutral side chains seem to influence only the retention behavior if they have a large conformational impact. Online-MS coupling facilitates the identification of the peaks present in the chromatograms significantly.

Chapter 4 describes the isolation and characterization of novel branched arabino-oligosaccharides from sugar beet arabinan. After enzymatic degradation with pure arabino-hydrolases from *Chrysosporium lucknowense* the arabino-oligosaccharides released were fractionated based on size and characterized by HPAEC-PAD and MALDI-TOF MS. NMR analysis of the purified fractions revealed the presence of two series of branched arabino-oligosaccharides. Both series consist of a backbone of α -(1,5)-linked L-arabinosyl residues being substituted with single L-arabinosyl residues. One series is only substituted with single α -(1,3)-linked L-arabinosyl residue(s), while the other series carries a double substitution of α -(1,2) and α -(1,3) L-arabinosyl residues and might carry an additional single α -(1,3)-linked L-arabinosyl residue.

HPAEC-PAD was shown to be incapable to separate many of the linear and branched arabino-oligosaccharides. Co-elution may lead to incorrect annotation of the arabino-oligosaccharides present in complex mixtures. Therefore, PGC-HPLC-ELSD/MS and

CE-LIF-MS were explored to enable the separation and characterization of all linear and branched arabino-oligosaccharides (Chapter 5). Correlations between the retention or migration behavior and the degree of polymerization were evaluated. Especially the retention behavior on PGC-material showed predictive potential depending on the branch points present in the molecule. By combining 1) the controlled enzyme treatment, 2) the predictive retention behavior on PGC-material, and 3) the information of online-recorded LC/CE-MS² fragmentation patterns, the structure of two unknown DP 6 arabino-oligosaccharides could be predicted (Chapter 5).

In Chapter 6 four arabino-hydrolases from *Chrysosporium lucknowense* (Abn1, Abn2, Abn4 and Abf3) were characterized in more detail concerning their mode of action using known arabino-oligosaccharides. Linear and branched arabino-oligosaccharides (DP 3-8) as isolated before (chapter 4) were incubated with the different arabino-hydrolases. Concerning the degradation of branched arabino-oligosaccharides, the arabinofuranosidases Abn4 and Abf3 showed different modes of action and linkage specificity. Both enzymes were able to cleave the α -(1,3)-linkages. In contrast to Abn4, Abf3 can hydrolyze a double substitution at O-2 and O-3.

In Chapter 7 the results of the previous chapters are summarized and discussed including possible adjustments of the developed methods and possible future developments in cell wall oligosaccharide analysis.

Samenvatting

Elke cell binnen een plant wordt omgeven door een beschermende celwand die verantwoordelijk is voor de stabiliteit en flexibiliteit van het plantenweefsel. Vooral tijdens de groei moet de plantencelwand zich voortdurend aanpassen om deze functies uit te kunnen voeren. De belangrijkste polysaccharide componenten in de celwand zijn cellulose, hemicelluloses en pectines. Hoofdstuk 1 geeft een algemene inleiding over het vóórkomen, chemische fijnstructuren en biologische variaties in deze plantencelwand polysacchariden. Verder komen de belangrijkste modellen voor de de celwandarchitectuur aan bod. Bovendien wordt een overzicht gegeven van de celwand afbrekende enzymen, waaronder cellulases, hemicellulases en pectinases. De gangbare scheidings- en detectie-technieken voor de analyse van mono-, oligo- en polysacchariden uit de celwand worden kort besproken. De analyse van polysacchariden wordt vooral gekenmerkt door tijdrovende fractionerings- en opzuiveringsstappen, gevolgd door bijvoorbeeld suiker (bindings) analyse en structuuranalyse met behulp van NMR. Echter de analyse van intacte polysacchariden levert slechts beperkte informatie over de chemische fijnstructuur. Daarom concentreert onderzoek naar de fijnstructuur van polysacchariden zich op de scheiding en detectie van karakteristieke oligosacchariden na gecontroleerde enzymatische of chemische afbraak.

Dit AIO-project richt zich op 1) de ontwikkeling van screening methoden voor zowel neutrale als zure celwand oligosacchariden en 2) de ontwikkeling van analytische methoden die zowel neutrale en zure oligosacchariden moeten kunnen scheiden en zelfs de mogelijkheid bieden om structurele kenmerken te voorspellen binnen het te bestuderen molecuul, gebaseerd op retentietijden en online opgenomen MSⁿ data.

Hoofdstuk 2 beschrijft een multi-enzym screening methode voor mutant *Arabidopsis* planten die verschillende structuren van celwandpolysacchariden bevatten. Zuivere en goed gedefinieerde cellulases, hemicellulases en pectinases werden toegevoegd aan geïsoleerd materiaal van de *Arabidopsis* plant. Het doel hiervan was de afbraak van alle plantencelwand polysacchariden, beschikbaar voor de enzymen. Matrix-Assisted Desorption/Ionization Time-of-Flight Mass Spectrometry (MALDI-TOF MS) leverde een snel overzicht van de vrijgemaakte neutrale en zure oligosacchariden (m/z 500-2000, ongeveer DP 3-12) wat resulteert in een karakteristieke vingerafdruk in één enkel MALDI-

TOF massa spectrum. Capillary Electrophoresis-Laser Induced Fluorescence (CE-LIF) detectie bleek aanvullende informatie op te leveren, waaronder de kwantificering van vrijgemaakte oligosacchariden in een op molen gebaseerd detectie principe. De methoden werden gevalideerd met bladweefsel van bekende *Arabidopsis* mutanten. Later werd de methode aangepast voor kleinere hoeveelheden zoals nodig is voor de analyse voor hypocotylen, ook al bemoeilijkt dit de analyse.

In hoofdstuk 3 werd Porous-Graphitized-Carbon (PGC)-HPLC analyse met Evaporative Light Scattering (ELS) en MSⁿ detectie opgezet voor een breed scala van plantencelwand oligosacchariden. Een water-acetonitril gradiënt gedurende de eerste 15 minuten leverde een goede scheiding van bijna alle neutrale oligosacchariden, inclusief α -(1,5)-L-arabino-, β -(1,4)-D-xylo- α -(1,4)-D-gluc-, β -(1,4)-D-gluc-, β -(1,4)-D-galacto- en β -(1,4)-D-manno-oligosacchariden. Binnen homologe series is de scheiding gebaseerd op grootte. Tussen de verschillende series is de scheiding gebaseerd op conformatie van de oligosacchariden: des te vlakker een molecuul, des te later het elueert. Dus, β -(1,4)-D-xylo- en β -(1,4)-D-gluc-oligosacchariden elueren significant later dan de overige neutrale oligosacchariden. Met behulp van neutrale geacetylerde β -(1,4)-D-xylo-oligosacchariden kon worden aangetoond dat door acetylering de retentietijd significant toeneemt. Zure α -(1,4)-D-gebonden galacturonzuur oligomeren (DP 2-9) elueren slechts na de toevoeging van trifluoroazijnzuur (TFA) aan het eluens. De scheiding van deze geladen oligomeren is vooral gebaseerd op lading. Dit is ook aangetoond voor andere geladen pectine-achtige oligomeren (xylogalacturonaan en rhamnogalacturonaan-I oligo-sacchariden). Neutrale zijketens lijken slechts invloed te hebben op de retentietijd als ze een grote invloed hebben op de conformatie. De koppeling met de MS vergemakkelijkt de identificatie van de pieken die in de chromatogrammen aanwezig zijn.

Hoofdstuk 4 beschrijft de isolatie en karakterisatie van nieuwe vertakte arabino-oligosacchariden uit suikerbiet arabinaan. Na enzymatische afbraak door pure arabino-hydrolases van *Chrysosporium lucknowense* werden de vrijgemaakte arabino-oligosacchariden op basis van hun grootte gefractioneerd en gekarakteriseerd met HPAEC-PAD en MALDI-TOF MS. NMR-analyse van de gezuiverde fracties toont de aanwezigheid aan van twee series vertakte arabino-oligosacchariden. Eén van de series is alleen gesubstitueerd met (één) enkele α -(1,3)-gebonden L-arabinosyl residue(n), terwijl de andere serie een dubbele substitutie van α -(1,2) en α -(1,3) L-arabinosyl residuen dragen en wellicht ook een extra enkel α -(1,3)-gebonden L-arabinosyl residu.

HPAEC-PAD bleek niet in staat om alle lineaire en vertakte arabino-oligosacchariden te scheiden, hetgeen kan leiden tot een onjuiste benoeming van arabino-oligosacchariden indien deze aanwezig in complexe mengsels. Daarom werden PGC-HPLC-ELS/MS en CE-LIF-MS onderzocht om de scheiding en karakterisatie van alle lineaire en vertakte arabino-oligosacchariden te bewerkstelligen (hoofdstuk 5). Samenhang tussen het retentie- of migratie-gedrag en de polymerisatiegraad werden geëvalueerd. Vooral het retentiegedrag op PGC-materiaal bleek een goede parameter om structuren te kunnen voorspellen. Door 1) een gecontroleerde enzymbehandeling, 2) het voorspellende retentie gedrag op PGC-materiaal en 3) de informatie van online opgenomen LC/CE-MS² fragmentatie patronen te combineren, kon de structuur van twee onbekende DP 6 arabino-oligosacchariden voorspeld worden (hoofdstuk 5).

In hoofdstuk 6 werden vier arabino-hydrolases van *Chrysosporium lucknowense* (Abn1, Abn2, Abn4 en Abf3) in meer detail gekarakteriseerd, voornamelijk hun mechanisme werd bekeken aan de hand van bekende arabino-oligosacchariden. Lineaire en vertakte arabino-oligosacchariden (DP 3-8), zoals eerder geïsoleerd (hoofdstuk 4), werden geïncubeerd met de verschillende arabino-hydrolases. De arabinofuranosidases Abn4 en Abf3 vertoonden verschillende werkingsmechanismen en bindingsspecificiteit tijdens de afbraak van vertakte arabino-oligosacchariden. Beide enzymen waren in staat om α -(1,3)-bindingen te verbreken. In tegenstelling tot Abn4, kan Abf3 een dubbele substitutie aan O-2 en O-3 hydrolyseren.

In hoofdstuk 7 worden de resultaten van de eerdere hoofdstukken samengevat en bediscussieerd, waaronder mogelijke verdere aanpassingen van de ontwikkelde methoden en mogelijke toekomstige ontwikkelingen in de analyse van celwand oligosacchariden.

Zusammenfassung

Jede einzelne Zelle innerhalb einer Pflanze wird von einer Zellwand umgeben, die sie schützt und zusätzlich sowohl für die Stabilität als auch Flexibilität des Pflanzengewebes verantwortlich ist. Besonders während des Wachstums müssen sich die Zellwände kontinuierlich anpassen, um all diese Funktionen aufrecht erhalten zu können. Die wichtigsten Komponenten in der Zellwand sind die Kohlenhydrate Cellulose, Hemicellulose und Pektin. Kapitel 1 gibt eine allgemeine Einleitung in die chemischen Feinstrukturen der Zellwandpolysaccharide, sowie deren Vorkommen und biologische Variationen. Des Weiteren werden die wichtigsten Modelle bezüglich der Bindungen der verschiedenen Polysaccharide untereinander diskutiert. Zusätzlich werden einige Enzyme wie Cellulasen, Hemicellulasen und Pektinasen, die die Polysaccharide in der Zellwand abbauen können, beschrieben. Auch die am häufigsten genutzten Trennungs- und Detektionsverfahren zur Bestimmung von Mono-, Di-, Oligo- und Polysacchariden aus Zellwänden werden erläutert. Die Analyse von intakten Zellwandpolysacchariden wird häufig erst nach zeitaufwendigen Fraktionierungs- und Aufreinigungsschritten durchgeführt. Die Bestimmung der Zuckerbausteine und deren Bindungstypen (sugar linkage analysis, NMR) liefert jedoch bei der Analyse von intakten Polysacchariden nur bedingt Information über die chemische Feinstruktur der Polysaccharide. Daher konzentriert sich die Kohlenhydratforschung auf die Trennung und Detektion von charakteristischen Oligosacchariden, die entweder nach enzymatischem oder chemischem Abbau der intakten Kohlenhydrate erhalten werden.

Die vorliegende Doktorarbeit legt den Schwerpunkt auf 1) die Entwicklung von schnellen Screening-Methoden für neutrale und saure Oligosaccharide, und 2) die Entwicklung von analytischen Verfahren zur detaillierten Charakterisierung dieser neutralen und sauren Oligosacchariden, die zugleich, basierend auf Retentionszeit und MSⁿ-Daten, Voraussagen bezüglich struktureller Elemente innerhalb der Oligosaccharide zulassen.

Kapitel 2 beschreibt eine Multi-Enzym-Screening-Methode für *Arabidopsis*-Mutanten, deren Zellwandpolysaccharide signifikant von den Wildtyp-Pflanzen variieren. Ein Gemisch von gut charakterisierten Enzymen (Cellulasen, Hemicellulasen und Pektinasen) wurde zu dem aus *Arabidopsis*-Pflanzen isolierten Zellwandmaterial gegeben. Diese Herangehensweise hatte das Ziel, alle enzymatisch abbaubaren Polysaccharide der

Zellwand zu charakteristischen Oligosacchariden zu hydrolysieren. Mithilfe von Matrix-Assisted Desorption/Ionization Time-of-Flight Mass Spectrometry (MALDI-TOF MS) konnten die produzierten neutralen und sauren Oligosaccharide schnell detektiert werden. Dadurch wurde ein charakteristischer Fingerabdruck aller der durch Enzyme zugänglichen Zellwandkohlenhydrate in einem einzigen MALDI-TOF-Massenspektrum (m/z 500-2000, DP 3-12) erhalten. Durch den zusätzlichen Gebrauch von Capillary Electrophoresis-Laser Induced Fluorescence (CE-LIF) konnten ergänzende Informationen wie die Quantifizierung der Oligosaccharide in einem 'mole-based-principle' erhalten werden. Beide Methoden wurden mit Blattmaterial von bekannten *Arabidopsis*-Mutanten validiert und später auf die Nutzung von kleineren Mengen, die z.B. bei der Analyse von *Arabidopsis*-Keimblättern notwendig sind, angepasst.

In Kapitel 3 wird eine Porous-Graphitized-Carbon (PGC)-HPLC-Methode mit Evaporative Light Scattering (ELS)- und MSⁿ-Detektion beschrieben, die für ein breites Spektrum von Oligosacchariden aus der Pflanzenzellwand getestet wurde. Ein Wasser-Acetonitril-Gradient in den ersten 15 Minuten führte zu einer guten Trennung von beinahe allen getesteten neutralen Oligosacchariden, inklusive α -(1,5)-L-Arabino-, β -(1,4)-D-Xylo-, α -(1,4)-D-Gluco-, β -(1,4)-D-Gluco-, β -(1,4)-D-Galacto- und β -(1,4)-D-Mannooligosacchariden. Innerhalb einer homologen Serie von Oligosacchariden basiert die Trennung auf Größe, dagegen basiert sie zwischen verschiedenen Serien auf der Konformation der Oligosaccharide: Je flacher das Molekül ist, desto später eluiert es. Demzufolge eluieren β -(1,4)-D-Xylo- und β -(1,4)-D-Glucooligosaccharide signifikant später als die anderen getesteten neutralen Oligosaccharide. Durch die Analyse von neutralen, acetylierten β -(1,4)-D-xylooligosacchariden konnte gezeigt werden, dass die Acetylierung von neutralen Oligosacchariden die Retentionszeit dieser Oligomere signifikant erhöht. Die geladenen α -(1,4)-gebundenen D-Galakturonsäureoligosaccharide (DP 2-9) eluieren nur nach Zugabe von Trifluoroessigsäure (TFA). Die Trennung dieser Galakturonsäureoligosaccharide sowie auch der Xylogalacturonan- und Rhamnogalacturonan-I-oligosaccharide basiert vor allem auf Ladung. Neutrale Seitenketten haben dann nur Einfluss auf die Retentionszeit des geladenen Oligosaccharides, wenn sie großen Einfluss auf die Konformation dieses Oligosaccharides haben. Die HPLC-MS-Koppelung erleichtert die Identifizierung von Peaks in den Chromatogrammen deutlich.

Kapitel 4 beschreibt die Isolierung und Charakterisierung von neuen, verzweigten Arabinooligosacchariden aus Zuckerrüben-Arabinanen. Nach enzymatischem Abbau des Startmaterials mittels aufgereinigter Arabinohydrolasen aus *Chrysosporium lucknowense*,

wurden die produzierten Arabinoooligosaccharide nach ihrer Größe fraktioniert und anschließend mithilfe von HPAEC-PAD und MALDI-TOF MS charakterisiert. Die NMR-Analyse der isolierten Oligosaccharide konnte zwei unterschiedliche Serien verzweigter Arabinoooligosaccharide identifizieren. Während die Arabinoooligosaccharide einer Serie nur mit α -(1,3)-gebundene L-Arabinosen verzweigt sind, sind die Arabinoooligosaccharide der andere Serie doppelt verzweigt mit α -(1,2)- und α -(1,3)-L-Arabinosen und können zusätzlich noch α -(1,3)-gebundene L-Arabinosen im Molekül enthalten.

Aus verschiedenen Experimenten konnte geschlossen werden, dass HPAEC-PAD nicht in der Lage ist, alle linearen und verzweigten Arabinoooligosaccharide zu trennen. Da die zeitgleiche Elution vieler Arabinoooligosaccharide zur inkorrekten Interpretation der Daten von komplexen Gemischen führen kann, wurden die Methoden PGC-HPLC-ELS/MS- und CE-LIF-MS auf deren Fähigkeit zur Trennung und Charakterisierung von komplexen Arabinoooligosaccharide-Gemischen getestet (Kapitel 5). Der Zusammenhang zwischen Retentions-/Migrationsverhalten und dem Polymerisierungsgrad der Arabinoooligosaccharide wurde ebenfalls evaluiert, wobei sich vor allem das Retentionsverhalten des PGC-Materials als guter Parameter zur Voraussage von Strukturelementen innerhalb der Arabinoooligosaccharide erwies. Durch die Kombination von 1) kontrollierter Enzymbehandlung, 2) dem voraussagenden Retentionsverhalten der Oligosaccharide auf PGC-Material, und 3) der Information aus online-LC/CE-MS²-Fragmentationsprofilen, konnten die Strukturen für zwei noch unbekannte DP6-Arabinooligosaccharide bestimmt werden (Kapitel 5).

In Kapitel 6 wurden vier Arabinohydrolasen aus *Chrysosporium lucknowense* (Abn1, Abn2, Abn4 und Abf3) detailliert beschrieben. Durch die Inkubation von verschiedenen linearen und verzweigten Arabinoooligosacchariden (DP 3-8) mit den Arabinohydrolasen konnten Aussagen getroffen werden bezüglich deren Mechanismus und Bindungsspezifität. Dabei wiesen z.B. die Arabinofuranosidasen Abn4 und Abf3 unterschiedliche Mechanismen und Bindungsspezifitäten auf. Beide Enzyme konnten die α -(1,3)-Bindungen in verzweigten Arabinoooligosacchariden hydrolysieren. Zusätzlich konnte jedoch Abf3 noch die doppelte Substitution an Position O-2 und O-3 hydrolysieren.

In Kapitel 7 werden die Resultate aus allen vorhergehenden Kapiteln zusammengefasst und diskutiert. Mögliche Anpassungen der entwickelten Methoden sowie zukünftige Entwicklungen in der Analyse von Zellwandoligosacchariden werden ebenfalls erörtert.

Acknowledgement

Dankwoord, Danksagung

This is most likely one of the parts mostly read within this thesis. Therefore, it is also the most difficult to write. But it is also a great opportunity to show my great thankfulness to all of you.

During my internship at Unilever R&D in Vlaardingen in 2004/2005, I had the first contact with the Netherlands and ‘the Dutch’. Even though I first had to get acquainted to the (very) direct and open communication of many Dutch friends/colleagues, I have to admit that I really like the open and direct way to communicate.

When I heard from my professor in Hamburg, Prof. Steinhart, that there was vacancy for a PhD position at the Laboratory of Food Chemistry at Wageningen University, I first thought: “Where is Wageningen?”. My answer, after looking it up on the map, was: “In the middle of nowhere!!”, taking into account that I always lived in the direct neighborhood of a big city. Anyway, I decided to come to Wageningen and the adventure ‘PhD student in Wageningen’ could start. And now, after having lived here for more than four years, I have to say that I really appreciate living and working in Wageningen.

An African expression says that you need a whole village to get a child grown up. To my opinion, this is also true for a PhD student finishing his/her thesis. Of course, the main work has to be done by the PhD student, but without good friends, colleagues and family, a thesis is not as successful as it could be. Also in my case, there are many, many people I want to thank and I will devote the following paragraphs to some special persons.

First of all I want to thank my promotor Fons Voragen who gave me the opportunity to start my PhD project in 2006. He accompanied me the whole four years and gave me a lot of advices. Furthermore, I would like to thank my second promotor Harry Gruppen, who joined my PhD project after two years and had very valuable comments to all my publications. Harry, even though your direct comments can be quite direct and confronting, they definitely improved my thesis.

Henk, I am greatly thankful for your supervision in the last four years. Onze ‘tweemanszaak’ heeft alle ups en downs overleefd, ook al heeft het ons beide soms veel energie gekost. Ik hoop echt dat ik zelf ooit zoiets voor een jonge AIO kan betekenen! En ik zal zeker nooit de snack-komkommers of tomaten uit je eigen tuin vergeten, ze waren altijd een leuke afleiding tijdens onze gesprekken. Natuurlijk ook dank aan Anita: je had er altijd begrip voor als Henk weer eens laat naar huis kwam omdat hij met mij nog resultaten doornam of een van de AIO-dips met mij verwerkte!!!

I would like to thank all members of the European project ‘WallNet’. I learned a lot from the scientific discussions with all of you during our project meetings and other international conferences. I found it very interesting and educative to work together with other scientists in a multi-disciplinary project.

The working atmosphere at the food chemistry department was very pleasant and this was mainly due to the great colleagues. Thus, I would like to thank everybody for their ‘gezelligheid’. Especially I want to thank my lab- and office-mates during the years: Gerd-Jan, Joris, Tai, Annemieke, Melliana, Maaïke, Martijn, Lidwien, Lieke, Takao, Evelien, Koen, Jun, Edwin and Peter. Furthermore, I would like to thank Jolanda for her help and kindness. You always made time, no matter how small or big the problem or question was. Dank je wel! And of course I want to thank the technicians, who made the life as PhD student much easier: Edwin, Margaret, Jan, Jolan, Mark, René and Peter, you were always available whenever there was a problem (= challenge) with equipment or there was need for scientific discussion.

I would like to thank my MSc- and BSc students, Yvonne K., Jean-Claude, Fenna and Rianne, for your contribution to my PhD project. I learned a lot by guiding all of you. I wish you all the best for your future.

During one of the first meetings of the organization committee of the PhD trip to China, Koos explained us that there are three phases when working in a group: (1) everybody being nice to each other, (2) arguing a lot after having get acquainted to each other, (3) working together in a nice and efficient way. I think, we came through all three phases and at the end there was a well-organized PhD trip including noodle soup in plastic bags. Even though the organization was tough sometime, I really would not have wanted to miss this experience. Thanks a lot, Yvonne V., Stefan, Rudy and Koos!!

Karin, mijn 'senior-AIO', ik heb heel erg genoten van de wetenschappelijke discussies met een 'niet-suiker-AIO'. En natuurlijk zal ik de gezellige diners op de Marijkeweg en onze Finland-vakantie nooit vergeten!

De laatste vier jaren heb ik ontzettend genoten van het kajakken bij de WKV Bovenste Polder. Tijdens het kajakken kon ik altijd alle problemen en uitdagingen van mijn AIO-project even vergeten en van de natuur genieten. Verder is het ook altijd gezellig om naar de steenfabriek te komen en even bij te kletsen. Petra, Reinoud, Nico, Sonja, Gert, Agnes, Peter M., Tineke, Marianna, Kaat, Theo, Popko, André, René, Carla, Klaas, Erikwim, Bart, Susan en Ernst, bedankt voor jullie gezelligheid!!! En natuurlijk wil ik onze jongste leden, Ingrid en Annika, niet vergeten. Ik hoop dat we eens samen gaan peddelen.

Bijzondere dank aan Annemieke en Edwin, mijn twee paranimfen, en René en Simone. Jullie hadden altijd een luisterend oor voor mij, maakte maar niet uit hoe vaak en hoe laat. Heel erg bedankt! Het voelt goed zulke goede vrienden en collega's te hebben. René, jij hebt heel veel tijd en moeite in de kaft gestoken. Heel erg bedankt. Edwin, soms konden we heel lang over wetenschappelijke dingen discussiëren en soms hadden we aan één woord genoeg. Bedankt voor je gezelligheid. Annemieke en Simone, ik vond ons klarinet-alt-viool-trio echt wel geslaagd en van onze uitstapjes naar Hamburg en Maastricht heb ik echt genoten. Ik hoop dat er nog veel leuke weekendjes zullen volgen.

Hanna, danke, dass ich an Dir schon seit der Schulzeit eine gute Freundin habe. Es ist schön zu wissen, dass wir immer für einander da sind, egal was passiert ist und wo wir sind. Stas und Georg, ich freue mich darauf, Euch noch besser kennenzulernen.

Mama, Papa, ohne Euch wäre ich nie so weit gekommen. Ich möchte Euch von tiefsten Herzen danken für Eure nie endende Liebe und Zuversicht, mit der Ihr mich in jeglicher Situation unterstützt und schon mein ganzes Leben begleitet. Ich habe Euch lieb!

Yvonne

About the author

Curriculum Vitae

Yvonne Westphal was born the 2nd of April 1980 in Reinbek, Germany. She grew up in Glinde, Germany, and finished school at the Gymnasium Glinde in June 1999. In October 1999 Yvonne started studying Food Chemistry at the University of Hamburg. She graduated under Prof. Dr. Dr. Steinhart with the 1st state examination, which included the diploma in Food Chemistry in October 2004. Her diploma thesis was entitled “Determination of the total folate content in vegetables after storage in fridge or freezer, including the identification and quantification of selected folate derivates”. Afterward, Yvonne started her professional training for one year, which she finished with the 2nd state examination in January 2006 to become a certified Food Chemist. During this year she did an internship at Unilever Research and Development Centre (Vlaardingen, The Netherlands) dealing with the determination of the aroma profile of tomato liquids using Twister-GC-MS. Another internship was performed at the Hygiene Institute Hamburg, Germany, dealing with the analysis and legal assessment of food and cosmetics within a governmental food inspection laboratory. The research on the development of analytical techniques for the analysis of plant cell wall polysaccharides described in this thesis was carried out at the Laboratory of Food Chemistry, Wageningen University, from March 2006 until May 2010. The author is now working at the same department on a post-doc project dealing with the foam stability in beer and model systems focusing on protein-protein interactions.

List of publications

Westphal, Y.; Schols, H.A.; Voragen, A.G.J.; Gruppen, H. *J. Chromatogr. A*, Introducing porous graphitized carbon liquid chromatography with evaporative light scattering and mass spectrometry detection into cell wall oligosaccharide analysis, **2010**, *1217*, 689-695.

Westphal, Y.; Schols, H.A.; Voragen, A.G.J.; Gruppen, H. *J. Agric. Food. Chem.*, MALDI-TOF MS and CE-LIF fingerprinting of plant cell wall polysaccharide digests as screening tool for *Arabidopsis* cell wall mutants, **2010**, *58*, 4644-4652.

Westphal, Y.; Kühnel, S.; de Waard, P.; Hinz, S.W.A., H.; Schols, H.A.; Voragen, A.G.J.; Gruppen, H. *Carbohydr. Res.*, Branched arabino-oligosaccharides isolated from sugar beet arabinan, **2010**, *345*, 1180-1189.

Westphal, Y.; Kühnel, S.; Schols, H.A.; Voragen, A.G.J.; Gruppen, H., LC/CE-MS tools for the analysis of complex arabino-oligosaccharides, *accepted for publication*.

Kühnel, S.; Westphal, Y.; Schols, H.A.; Hinz, S.W.A.; Gruppen, H., *Chrysosporium lucknowense* arabinohydrolases: mode of action and molecular mechanism, *submitted for publication*.

Nakai, H.; Baumann, M.J.; Petersen, B.O.; Westphal, Y.; Schols, H.A.; Dilokpimol, A.; Hachem, M.A.; Lahtinen, S.J.; Duus, J.Ø.; Svensson, B. *FEBS Journal*, The maltodextrin transport system and metabolism in *Lactobacillus acidophilus* NCFM and production of novel α -glucosides through reverse phosphorylation by maltose phosphorylase, **2009**, *276* (24), 7353-7365.

Overview of completed training activities

Discipline specific activities

Conferences and meetings

WallNet project meetings, Europe, 2006-2008

Workshop for Production, Functionalization, and Analysis of Hemicelluloses for Sustainable Advanced Products, Hamburg, Germany, 2007

XI. Cell wall meeting, Copenhagen, Denmark, 2007

Pectin & Pectinases, VLAG, Wageningen, The Netherlands, 2008

Gordon-Kenan Seminar, Smithfield, RI, USA, 2009

Gordon Conference, Smithfield, RI, USA, 2009

Courses

Summer School Glycosciences, VLAG, Wageningen, The Netherlands, 2006

Food Enzymology, VLAG, Wageningen, The Netherlands, 2008

VLAG NMR/MRI course, Wageningen, The Netherlands, 2008

General courses

Supervision of Undergraduate Students, Wageningen, 2006

EC Marie Curie training (Antibodies & Genetics), Versailles, France, 2007

Deutscher Lebensmittelchemikertag, Nürnberg-Erlangen, Germany, 2007

EC Marie Curie training (Bioinformatics & Patents), Rome, Italy, 2008

Philosophy and Ethics of Food Science and Technology, VLAG, Wageningen, 2008

Deutscher Lebensmittelchemikertag, Berlin, Germany, 2009

Optionals

Preparation PhD research proposal, Wageningen, The Netherlands, 2006

PhD Study trip, Belgium, France and United Kingdom, 2006

PhD Study trip, China, 2008

Member of the Organization Committee for the PhD study trip to China, 2008

Food Chemistry Seminars, Wageningen, The Netherlands, 2006-2010

Food Chemistry Colloquia, Wageningen, The Netherlands, 2006-2010

The research described in this thesis was performed at the Laboratory of Food Chemistry, Wageningen University, The Netherlands. This study has partly been financed by the Commission of the European Communities (WallNet: “Functional Genomics for Biogenesis of the Plant Cell Wall”, Marie Curie contract number: MRTN-CT-2004-512265). It does not necessarily reflect its views and in no way anticipates the Commission’s future policy in this area.

Cover designed by René Kuijpers, Ede, The Netherlands
Printed by GVO drukkers & vormgevers / Ponsen & Looijen, Ede, The Netherlands